Data Modulation Technique and Modulator/Demodulator Circuit Designs for Ultra Wideband Applications

Presenta:

Gregorio Valdovinos Fierro

Thesis submitted in partial fulfillment of the requirements for the degree of

Doctor of Sciences in Electronics

in the

National Institute of Astrophysics, Optics and Electronics

Advisor:

Dr. Guillermo Espinosa Flores-Verdad
Department of Electronics
INAOE

Data Modulation Technique and Modulator/Demodulator Circuit Designs for Ultra Wideband Applications

By:

Gregorio Valdovinos Fierro

Thesis submitted in partial fulfillment of the requirements for the degree of
Doctor of Sciences in Electronics

in the

National Institute of Astrophysics, Optics and Electronics

Advisor:

Dr. Guillermo Espinosa Flores-Verdad
Department of Electronics
INAOE

Agradecimientos

Al pueblo mexicano que a través de Conacyt me ha apoyado económicamente para realizar este doctorado.

A Conacyt.

A los sinodales: Dra. Teresa Sanz Pascual, Dr. Sergio Solís, Dr. Ignacio Zaldívar, Dr. Alejandro Díaz Méndez y Dr. Rubén Alejos, por sus valiosas aportaciones a este trabajo de tesis.

Dr. Guillermo Espinosa Flores-Verdad.

Dedicatorias

A ti joven hermano, muchacho de mi pueblo, compañero en el fértil compás de los encuentros, brazo fuerte que habrás de sostener a México a ti te envío este mensaje abierto. Trabaja y crea donde quiera que estés sobre los campos o en las mentes, siembra goza tu libertad esa será tu cosecha.

Para México, por que algún día llegue el bienestar real para nuestro pueblo, porque mientras haya desigualdad social, mientras unos trabajan para que otros consuman, mientras hallan políticos sinvergüenzas que siguen engañando al pueblo, y los trabajadores tengan sueldo de hambre y los campesinos no tomen posesión de la madre tierra para hacerla libre, con su trabajo de hombre libre, no habrá una verdadera Paz Social.

Para mis bebés Manuelito y Sebastián con todo mi cariño.

A todas las personas que me han brindado su amistad. Especialmente y sin orden de importancia a la Mosca y al Vic González, Jorge Reyes, Gloria, Martha, Uriel, Carlos Vivas, Ricardo, Góngora y Sergio.

A una persona que no se ha llevado el titulo legal de ser asesor, sin embargo lo agradezco infinitamente que también me haya asesorado, a mi aprendiz de asesor (por el momento) y estimado amigo Edgar López Delgadillo.

Al personal de la dirección de formación académica, especialmente a Cecilia y Guadalupe por toda su amabilidad y atención.

Contents

Chapter 1

Introduction

Recent advances in wireless communications technologies have had a transformative impact on society and have directly contributed to several social aspects of daily life. Increasingly, the exchange of information between devices is becoming a prime requirement for further progress, which is placing an even greater demand on wireless bandwidth. Ultra Wideband (UWB) is a technology that recently opened up to consumer electronics and communications. Historically, UWB systems were developed mainly for radars, sensors and military communications [1]. The technology was first used on ground penetrating radar systems in 1974 [2]. The United States Department of Defense began to use it in wall-transparent images and into the ground. A substantial change in the research and development of UWB systems occurred in February 2002, when the Federal Communications Commission (FCC) opened up UWB for commercial applications [3].

Even though UWB systems have been in use for many years, today, the technology is changing the wireless industry. Nevertheless, UWB technology is different from conventional narrowband wireless transmission technology. For instance, instead of

using two separate frequencies, UWB spreads its signals across a very wide range of frequencies. The sinusoidal radio wave is replaced by trains of pulses at hundreds of millions of pulses per second. Wide bandwidth and very low power spikes make UWB transmissions appear as background noise.

1.1 UWB Physical Layer

UWB communications systems can be defined as a wireless communications system with very large fractional bandwidth. The FCC rules provide the following definitions for UWB signaling (source www.fcc.gov):

- **UWB bandwidth** is the frequency band bounded by the points that are 10 dB below the highest radiated emissions, as based on the complete transmission system including the antenna. The upper boundary is designated as f_h and the lower boundary is designed as f_l.

- **The center frequency** f_c is the average of f_l and f_h, that is:

$$f_c = \frac{f_l + f_h}{2} \tag{1.1}$$

- **Fractional bandwidth (FB)** is defined as:

$$f_B = 2\frac{f_h - f_l}{f_h + f_l} \tag{1.2}$$

On figure 1.1 is depicted the place where UWB is situated on the RF spectrum chart and figure 1.2 shows the usable spectrum permitted under Part 15 of the FCC rules. UWB signal may be transmitted from 3.1GHz to 10.6 GHz at power levels up to -41.3dBm/MHz.

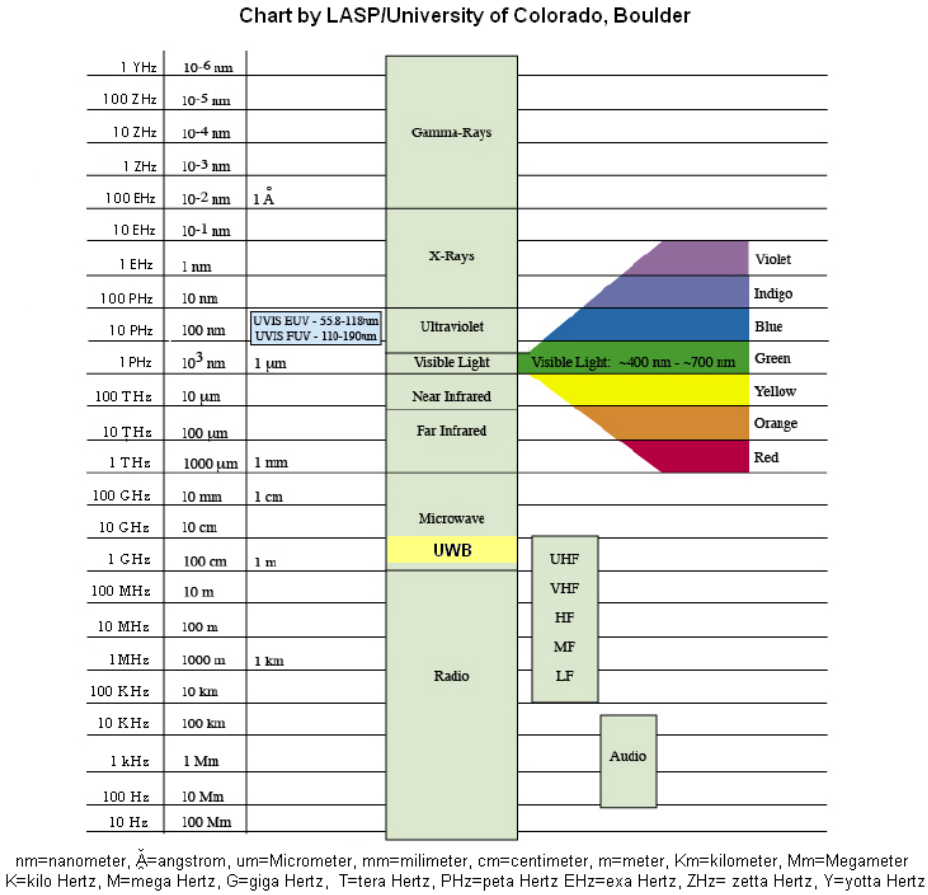

Figure 1.1 RF spectrum chart.

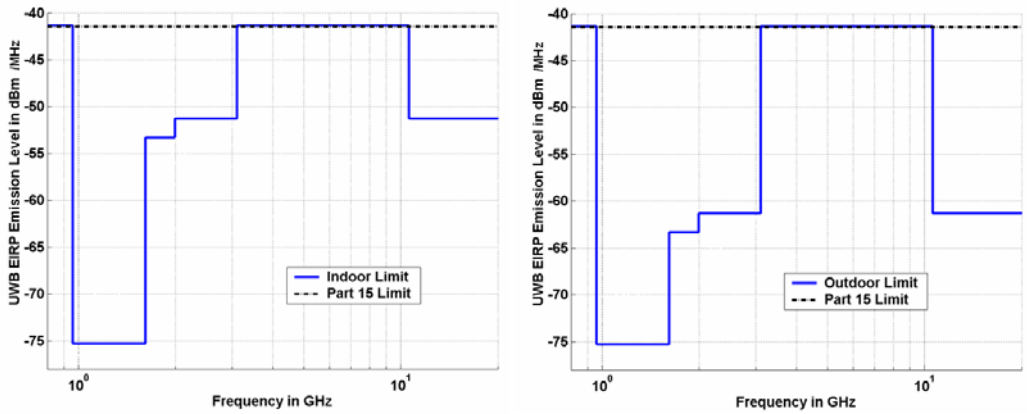

Figure 1.2 UWB emission limits (source www.fcc.gov).

The primary difference between indoor and outdoor operation is the higher degree of attenuation required in the operation band of 1.6 to 3.1 GHz. This will further protect

GPS receivers, centered at 1.6 GHz. If the entire 7.5 GHz band is optimally utilized, the maximum power available to the transmitter is approximately 0.5 mW [4]. This is a tiny fraction available to users of the 2.45 GHz ISM (Industrial Scientific and Medical) bands such as the IEEE 802.11 a/b/g standards (Institute of Electrical and Electronics Engineers).

The UWB generation methods can be grouped in two major categories:

- **Impulse radio (IR) based:** This technique is based on transmitting single pulses (in order of sub nanoseconds) and low power pulses (1 mW). Due to the carrierless characteristic (no sinusoidal carrier to raise the signal to a certain frequency band) these UWB systems are also called free carrier. Other authors called this technique Single Band (SB).

- **Multi Band (MB) based:** This technique employs two or more frequency bands, which can be generated using orthogonal frequency division multiplexing (OFMD). The frequencies have at least 500 MHz bandwidth.

In order to convey the information symbols in UWB communications, several approaches for modulation techniques exist. Most of them are based on the classic band-based modulation types such as on-off keying (OOK), amplitude (PAM), pulse position (PPM), phase (PM), shape (PSM) or any combination therefore.

1.2 Advantages of UWB

New generations of wireless mobile radio systems aim to provide flexible data rates and a wide variety of applications (as video, data ranging etc.) to the mobile users while serving as many users as possible. This goal however, must be achieved under the constraint of the limited available resources as spectrum and power. As more and more devices go wireless, future technologies will face spectral crowding and coexistence of wireless devices will be a major issue. Therefore, considering the

limited bandwidth availability, accommodating the demand for higher capacity and data rates are a challenging task, requiring innovate technologies that can coexist with devices operating at various frequency bands.

UWB has become a suitable candidate for indoor wireless communications; in particular, a multiuser access scheme for UWB because of the following benefits and characteristics [5, 6]; extremely low Power Spectral Density (PSD), spectrum reuse, robust performance under multipath conditions. The basic properties of UWB signals and systems are outlined.

1.2.1 Power Spectral Density

The Power Spectral Density (PSD) of UWB systems is generally considered to be extremely low, especially for communications applications. The PSD is defined as [4]

$$PSD = \frac{P}{B} \tag{1.3}$$

where P is the power transmitted in watts, B is the bandwidth of the signal in Hertz, and the unit of PSD is watts/hertz. For UWB systems, the pulses have a short width and very wide bandwidth B. It is helpful to review some traditional wireless broadcast and communications applications as shown in table 1.1

System	Transmission power	Bandwidth	PSD (W/MHz)	Classification
Radio	50 kW	75kHz	666600	Narrowband
Television	100kW	6MHz	16700	Narrowband
2G Cellular	500mW	8.33kHz	60	Narrowband
802.11a	1mW	20MHz	0.05	Narrowband
UWB	0.5mW	7.5GHz	6.670×10^{-8}	Ultra Wideband

Table 1.1 PSD of some common wireless broadcasts and communications systems [4].

The energy used to transmit a wireless signal is finite and, in general, should be as low as possible, especially for new electronics devices. The communications systems have a fixed amount of energy they can either transmit efficiently large amount of energy density over small bandwidth or very small amount of energy density over a large bandwidth.

For UWB a system, the energy is spread out over very large bandwidth hence they have very low PSD. One of benefits of low PSD is a low probability of detection, which is of particular interest for military applications, such as communications and radar [7].

1.2.2 Multipath

Multipath is the name given to the phenomenon at the receiver whereby after transmission an electromagnetic signal travels by various paths to the receiver. The figure 1.2 shows an example of multipath propagation within a room.

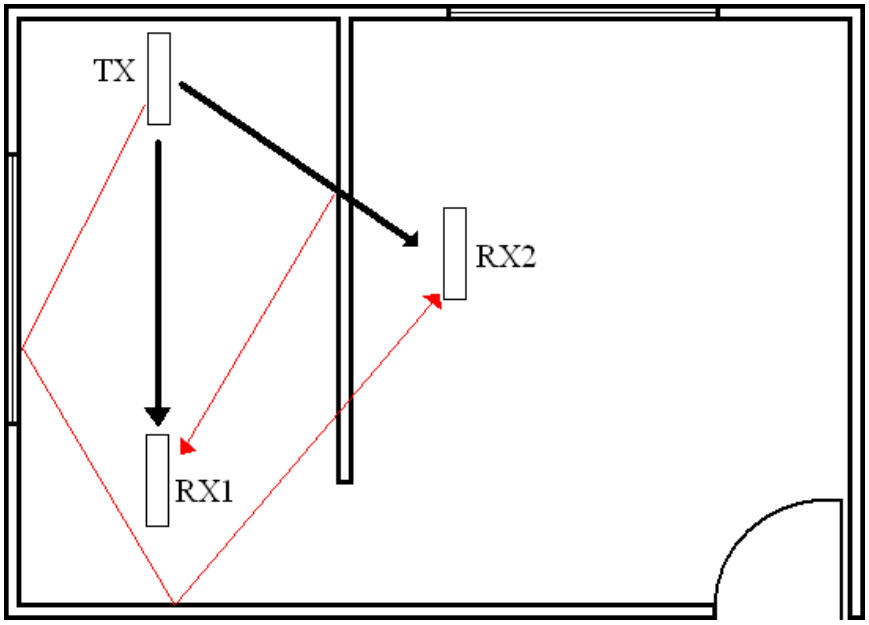

Figure 1.3 Multipath rays, Two Line of Sight (LOS) rays and two single reflected rays in an indoor propagation.

This effect is caused by the absorption, reflection, diffraction, and scattering of the electromagnetic energy [8] by objects in between the transmitter and receiver. If there were no objects to absorb or reflect the energy, this effect would not take place and the energy would propagate outward from the transmitter, dependent only on the transmit antenna characteristics. However, in the real world the signal transmitted will give rise to multiple paths. Due to the different length of the paths, pulses will arrive at the receiver at different times, with the delay proportional to the path length.

UWB systems are often characterized as multipath immune or multipath resistant. Examining the pulses described previously, it is possible to see that if pulses arrive within one pulse width they will interfere, while if they are separated by at least one pulse width they will not interfere. If pulses do not overlap, then they can be filtered out in the time domain or in other words ignored. Assuming one symbol per pulse, they will not produce interference with the same symbol. Alternatively, the energy can be summed together by a rake receiver [9].

Other method to avoid multipath interference is to lower the duty cycle of the systems. By transmitting pulses with time delays greater that the maximum expected multipath delay, unwanted reflections can be avoided at the receiver. This is inherently inefficient and places limits on the maximum speed of data transmission for a given modulation system. In the limit, if pulses were transmitted continuously, then the system would resemble a sinusoidal system [9] In general, if the pulses can be resolved in the time domain then the effects of multipath, such as Inter-Symbol Interference (ISI) can be mitigated.

1.2.3 Penetration Characteristics

One of the most important benefits of the UWB communications system that has been raised is the ability of pulses to easily penetrate walls, doors, partitions, and other

objects in the home and the office environment. The frequency f and wavelength λ are related by the speed of light c as is shown in the equation 1.4

$$\lambda = \frac{c}{f} \tag{1.4}$$

It is to say, as the frequency increases, the wavelength become shorter, and for lower frequencies the wavelength is longer. In conventional sinusoidal communication, lower frequency waves have the characteristic of being able to pass through walls, doors, and windows because the length of the wave is much longer that the material that it is passing through. On the other hand, higher frequency waves will have more of their energy reflected from walls and doors since wavelength is much shorter.

UWB pulses are composed of a large number of frequencies, as is shown in the table 1.2. The UWB communication systems have the ability to pass trough walls, especially in comparison with IEEE 802.11 systems. The penetration capabilities of UWB come only from the lower frequency components which were, for early systems, mostly centered on 1 GHz.

1.2.4 Speed of Data Transmission

One of the advantages of UWB transmission for communications is its high data rate. While current chipset are continually being improved, most UWB communication applications are targeting the range of 100-500 Mbps [10], which is roughly the equivalent of wired Ethernet to USB 2.0. It is significant that this data rate is 100 to 500 times the speed of Bluetooth. As can see in the table 1.2 the current data rate indoor wireless UWB transmission is between 100 Mbps and 500 Mbps. This is compared with current wireless standards. In fact, the speed of the transmission is currently being standardized into three different speeds: 100 Mbps with a minimum transmission distance of 10m; 200 Mbps with a minimum transmission distance of

4m; and 500 Mbps with no fixed minimum distance due to low power transmission that it does not allow to reach more distances.

Technology	Data rate (Mbits/s)	Output Power (mW)	Range (meters)	Freq. Band
Bluetooth	1-2	100	100	2.4 GHz
IEEE 802.11a	54	40-800	20	5 GHz
IEEE 802.11b (Wi-Fi)	11	200	100	2.4GHz
IEEE 802.11g	54	65	50	2.4 GHz
UWB	100-500	1	10	3.1-10.6 GHz

Table 1.2 Comparison of the Mbps in various indoor wireless systems [4].

The reason for these particular distances lies mostly on the different applications. For example, 10m will cover an average room and may be suitable for wireless connectivity for home theater. A distance of less that 4m will cover the distance such as a home server and television. A distance of less than 1m will cover the appliances around a personal computer.

1.2.5 Cost and Size

Among the most important advantages of UWB technology are those of low systems complexity and low cost. UWB systems can be made nearly “all digital”, with minimal radio frequency (RF) or microwave electronics. The low component count, and smaller chip sizes invariable lead to low cost systems. The simplest UWB transmitter could be assumed to be a pulse generator, a timing circuit, and an antenna.

However, as higher data rates are required, more complex timing circuitry is needed. To provide a multiple access system, additional complexity is required. To reduce the cost, more functionality products are implemented on fewer chips, reducing die area and thus manufacturing cost.

The small size of UWB transmitters is a requirement for inclusion in today's consumer electronics. In the 802.1 working groups, consumer electronics companies have targeted the size on the wireless circuit to be small enough to fit into a Memory stick or secure digital (SD) card [10] chipset by Xtreme Spectrum has a small size which enables compact flash implementation [11]. The main arguments for the small size of UWB transmitters and receivers are due to reduction of passive components. However, antenna size and shape is another factor that needs to be considered.

1.2.6 Power Consumption

With proper engineering design the resultant power consumption of UWB can be quiet low. As with any technology, power consumption is expected to decrease as more efficient circuits are designed and more signal processing is done in smaller chips at lower operating voltages. This is not quite truth; modern technologies have of the disadvantage of higher lake currents hence static power consumption increases

The current target for power consumption on UWB chipset is less that 100mW. Table 1.3 shows some figures for power consumption of recent chipset [10]

Applications chipset	Power consumption (mW)
802.11a	15000-2000
400 Mbps 1394 LSI	700
Mobile Telephone RISC 32 bit MUP	200
Digital Camera 12 bit A/D converter	150
UWB (target)	100
Mobile telephone TFT color display panel	75
MPEG-4 decoder LSI	50
Mobile Telephone voice codec LSI	19

Table 1.3 Power consumption of UWB and other mobile communication chipsets [4].

1.3 Challenges

In spite of the advantages of UWB, there are several fundamental and practical issues that need to be carefully addressed to ensure the acceptance of this technology in the wireless communications market. Multi-access code design, multiple access interference (MAI) cancellation, narrowband interference (NBI) detection and cancellation, synchronization of the receiver to extremely narrow pulses, accurate modeling of UWB channels, estimation of multipath channel delays and coefficients, practical, simple, and low power transceiver design, powerful processing capabilities for high performance and coherent digital receiver structures, and adaptive transceiver design are some of the issues that still require a huge investigation or research efforts.

1.4 Objectives

This thesis has the following as objectives:

- Auto synchronization in the receiver to radio impulses (IR).
- Practical, simple and low power transceiver design.
- Signal processing beyond the current state of the art.
- Low cost RF components.

1.5 Goal

To design as a test vehicle, a communication system that complies the established objectives, through characterization of the system design.

1.6 Scope of this Thesis

The basic concepts and regulations are of key importance in the development and design of a communication system. Chapter 2 covers aspects relevant to the transmitter and the receiver, such as: the spectrum, time hopping, FCC rules, direct sequence, match filter, coherent and no coherent reception, pulse shape, and some previous works.

The selection of the signal pulses is a fundamental consideration in the design of UWB circuits and systems because the pulse type sets the level of performance of the new system. Chapter 3 also describes the development and design of a CMOS Transceiver in UWB under the specification IEEE 802.15.4a channel model. In this chapter is presented a low complexity and low power Gaussian pulse generator, and is so versatile that it can be implemented in different modulation schemes. However, the main application is the data modulation focused on the proposed modulation scheme and to get a transceiver as the final product. This modulation scheme allows the receiver to achieve the auto synchronization without an internal clock. The modulation scheme is proposed for 2 bits; however, this technique is not limited to two bits and can be used for M-ary modulation. The four symbols are implemented using one pair of pulses (one positive and one negative), that are shifted in time one from the other. The shifting time will depend on the bit transmitted. The modulation scheme proposal, the different modulation schemes, and some of their characteristics will be considered in detail.

Chapter 4 describes the testing of the modulator and demodulator circuits designed for the proposed modulation scheme. The results are shown in a probability of error vs. Signal to Noise Ratio (SNR) graph.

The conclusion and the future work related to this thesis project are provided in chapter 5.

Chapter 2

UWB Transceiver Systems

2.1 Introduction

In the world of wireless communication, UWB is considered as an attractive technology for its high capacity, high data rates, low power consumption, low cost and low complexity devices. In spite of all the benefits of UWB, the extremely wide frequency bands and exceptionally narrow pulses make it difficult to apply conventional narrowband modulation techniques into UWB systems. Therefore, a significant amount of research has been conducted to come up with the suitable modulation technique and develop new architectures that perform this modulation scheme.

Essentially, UWB communications come in one of two types: single band (SB or IR) and multiband (MB), as mentioned above. The modulation based in MB is accomplished by using multicarrier or Orthogonal Frequency Division Multiplexing (OFDM) modulation with Hadamard or other spreading code [12].

In radio impulse, the pulse width is very narrow and low power, where the signal that represents a symbol consists of serial pulses with a very low duty cycle. Rather than sending a single pulse per symbol, a number of determined pulses and the processing gain of the system are transmitted by symbol [13]. IR is advantageous in that it eliminates the need for up and down conversion and allows low complexity transceivers. Figure 2.1 shows the difference between SB and MB UWB systems.

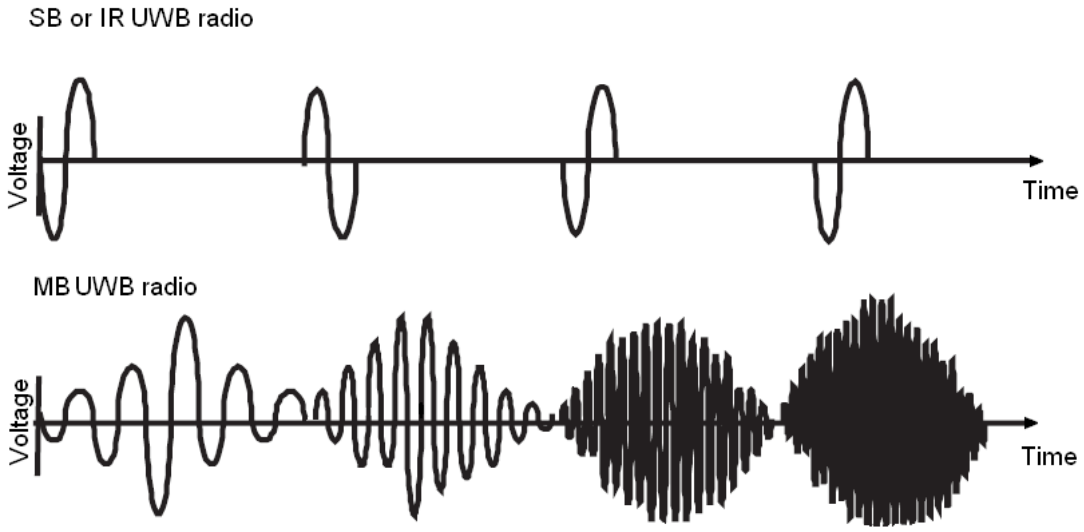

Figure 2.1 SB and MB UWB concept.

This chapter is focused on UWB transceiver concepts, transmission and reception processes, circuit architectures and design considerations.

2.2 Modulation Schemes

A single UWB pulse does not contain information by itself. That is the reason why digital information must be added to the analog pulse by means of modulation. Selecting the appropriate modulation technique in UWB systems still remains a major challenge.

There are several possible modulation options such as: on-off keying (OOK), pulse amplitude modulation (PAM), pulse position modulation (PPM), binary pulse modulation (BPM) etc. and depend on the application, design specifications and constraints, range, transmission and reception power, quality of service requirements, regulatory requirements, hardware complexity, data rate, reliability channel, and capacity. Therefore, it is crucial to choose the right modulation for the right purpose.

2.2.1 PPM

The most common modulation method in UWB reported in the literature is PPM, where each pulse is delayed or sent in advance of a regular time scale. However, the most important parameter in PPM is the delay of the pulse. In this modulation, the shaping pulse can be arbitrarily chosen. The PPM can be written as [14]:

$$S_i = p(t - \tau_i) \tag{2.1}$$

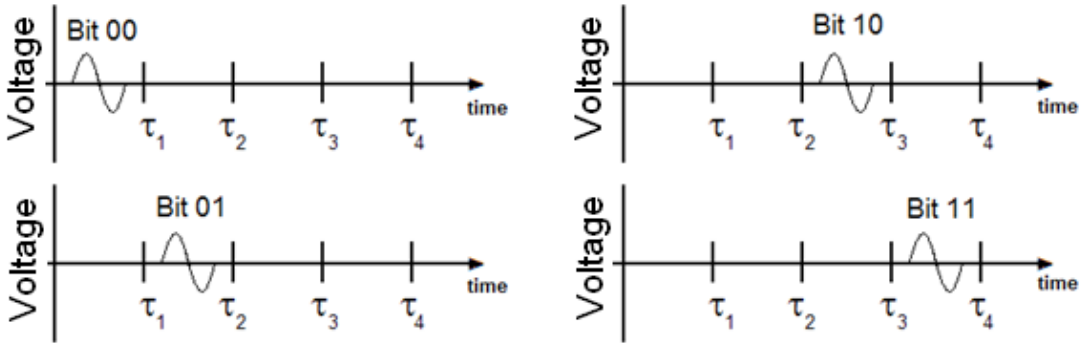

Figure 2.2 4-ary data mapping PPM scheme.

Where S_i is the modulated signal, p is the pulse transmitted, t represents the time, and τ_i is the delaying parameter. The delaying parameter can have two or more values assigned. Figure 2.2 illustrates an example for 4-ary PPM. For this example, the equation 2.1 by the four pulses shapes becomes [14]:

$$
\begin{aligned}
S_0 &= p(t-\tau_0) \\
S_1 &= p(t-\tau_1) \\
S_2 &= p(t-\tau_2) \\
S_3 &= p(t-\tau_3)
\end{aligned}
\tag{2.2}
$$

The advantages of PPM mainly arise from its simplicity and the ease with which the delay is implemented. On the other hand, for the UWB systems, extremely fine time control is necessary to modulate the pulses to sub-nanosecond accuracy.

2.2.2 BPM

The most popular approach used in impulse based UWB systems is BPM, due to its smooth power spectrum and low Bit Error Rate (BER). However, accurate phase detection of the modulated signal in BPM requires accurate channel estimation in the receiver. The information is encoded with the polarity of the pulses. In this case, only one bit per pulse can be encoded because there are only two polarities available to choose from: a positive pulse representing a 1, and a negative pulse representing a 0. Therefore, equation 2.3 is taken [14]:

$$
S_i = \sigma_i p(t) \tag{2.3}
$$

Equation 2.3 represents a binary system based on inversion of the basis pulse p(t). The parameter σ is often known as the pulse weight or shaped parameter and can be 1 or -1. The results for a binary system are the equations 2.4 [14]:

$$
\begin{aligned}
S_1 &= p(t) \\
S_2 &= -p(t)
\end{aligned}
\tag{2.4}
$$

This is clearly illustrated in figure 2.3, where two symbols (S_1 and S_2) are used, which represent a 0 or 1 logical respectively.

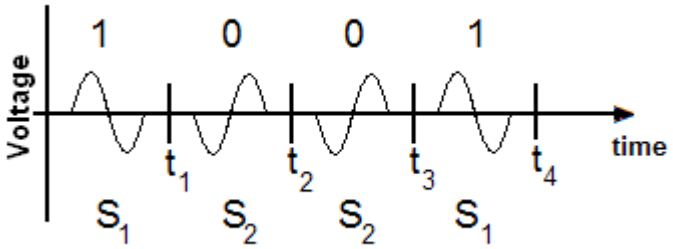

Figure 2.3 Data mapping BPM scheme.

The BPM, in comparison with PPM, has 3 dB in the power efficient gain, as a function of the type of modulation method [14]. Another benefit is the smooth comb lines or spectral peaks that are detailed in the section 2.3.

2.2.3 Other Modulation Schemes

Although PPM and BPM constitute the most significant approaches to modulation in UWB communications systems, there are other modulation schemes depicted in figure 2.4.

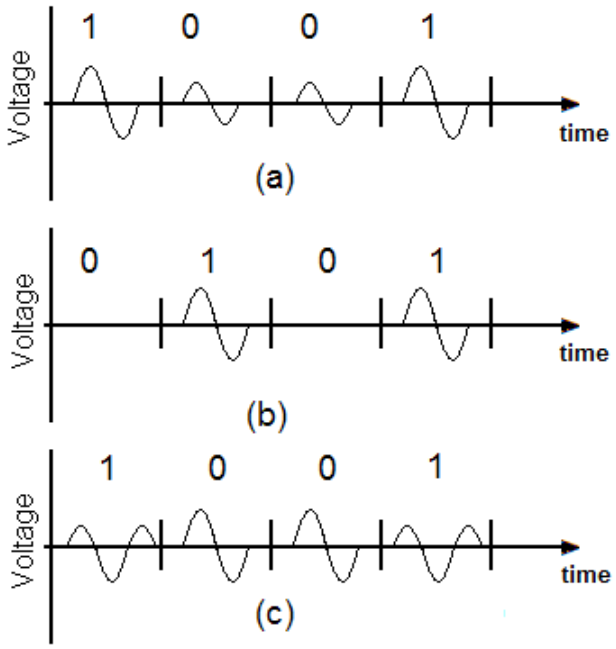

Figure2.4 Binary data mapping schemes (a) PAM, (c) OOK and (c) PSM.

The pulse shaping modulation (PSM), which requires special pulses shapes [15][16]. On-off keying (OOK) is a modulation scheme where the absence or presence of a pulse signifies the digital information of 0 or 1, respectively. Pulse amplitude modulation (PAM) is a technique where the amplitude of the pulse is varied to contain the digital information. Figure 2.4 shows the modulation schemes mentioned above.

All of the modulation schemes mentioned in this section might be combined into one in order to transmit three bits with a single pulse. The pulse shape, position and phase of the pulse could be used simultaneously for increased data rates and to save power. However, the complexity in the transceiver design would be increased.

2.3 Transmitter

One of the essential functions in communications systems is the representation of a message in symbols by an analog waveform for transmission through a channel. In UWB systems, the conventional analog form is a simple pulse that is generally radiated to the air. In UWB systems the pulse shape is not restricted, only its characteristics are restricted. Therefore, any signal obeying the rules is a suitable candidate. This allows the designers to choose the shape of the monocycle according to their particular preference, at least in theory. Today, UWB systems employ nonsinusoidal wave shapes that could have certain properties when they are transmitted from the antenna. Emissions in UWB communication systems are constrained by the FCC regulations 47 CFR section S15.5 (d) [17], which state that:

"Intentional radiators that produce class B emission (damped wave) are prohibited".

Several nondamped waveforms have been proposed in the literature for UWB systems, such as Gaussian [18], Raleigh, Laplacian, cubic waveforms [19], and Hermitian monocycles [20]. In all these waveforms, the goals are to obtain a nearly

flat frequency domain spectrum of the transmitted signal over the bandwidth of the pulse and to avoid a DC component. Therefore, many pulses will typically be combined to carry the information for one bit to irregular intervals. If the transmission of pulses is carried out at regular intervals, several problems emerge. For instance, a comb spectrum would be produced and the peaks in the power spectral density would cause interference to narrow band systems. Figure 2.5 illustrates this comb spectrum problem [21].

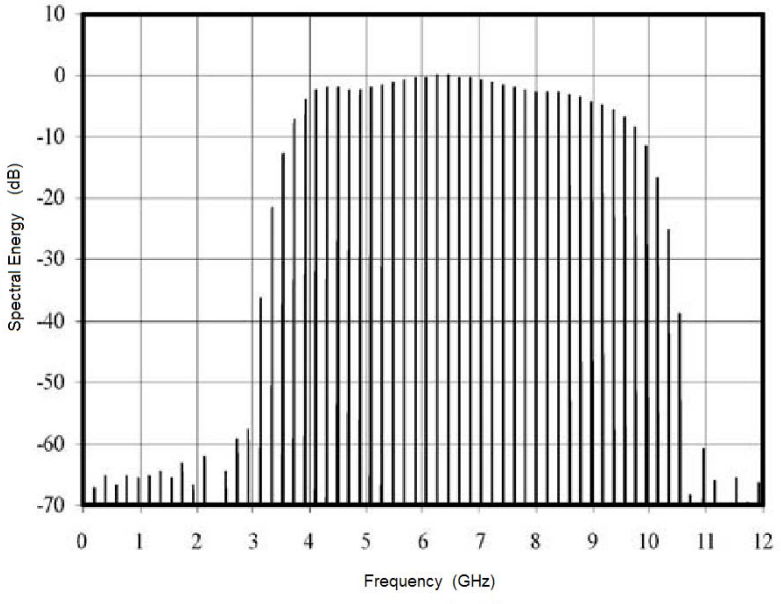

Figure 2.5 Comb spectrum due to regular UWB pulses.

On the other hand, signals from two transmitters may be aligned in time at the receiver, preventing the reception of the data. Several techniques are available for minimizing these problems, some of which are described later in the next section.

2.3.1 Spectrum

A pulses train of the form $w_n r(t-nT_f)$ consist of pulses spaced T_f seconds apart in time. The pulse repetition period T_f must be at least a hundred times [22] that of the pulse width, with its largest value constrained in part by stability of available clocks. If

multiple-access signals were composed only by uniformly spaced pulses, then the collisions from the train of pulses coming from the other user simultaneously using the system could corrupt irreversibly the message. Normally, the receivers already have the code distributed by multiple means (SIM card or other device).

A randomizing technique is applied to break up the spectrum of the train pulses and to protect from collisions within multiple accesses. A typical mathematical description of a multi-access environment is [22]:

$$s^{(j)}(t) = \sum_{n} w\left(t - nT_f - h_n^{(j)}T_h - \delta d_{[n/N_s]}^{(j)} - \beta^{(j)}\right) \tag{2.5}$$

Where $w(t)$ is the pulse waveform and $h_n^{(j)}$ is the pseudorandom code sequence unique to each transmitter. The total shift is given by $h_n^{(j)}T_h$ and the random shift $\beta^{(j)}$ represents the asynchronies between the frame boundaries of the different transmitter units. To encode one bit information, $d_{[n/N_s]}^{(j)}$, N_s pulses are delayed by an additional amount of 0 or δ seconds depending on whether the bit is equal to 0 or 1 respectively (assuming binary signaling).

Each user *j* is assigned a distinct channel code $h_n^{(j)}$. Ideally, a random pattern code is desirable, but in the practice these codes are periodic. The periodic requirements make the codes pseudorandom with period Np, only the receiver with the same sequence code can decode the transmission. Therefore, this code provides an additional time shift to each pulse in the train pulse, with the n-th pulse shifted additionally by $h_n^{(j)}$ T_h seconds. Hence, the added time shifts caused by the code are discrete times between 0 and δ seconds. Also, the greatest shift generated by the code is required to be less than the length of the basic train pulses period T_f.

One effect of the random code is to reduce the power spectral density from line spectral density (1/Tf apart) of the uniformly spaced pulse train down to a spectral density with finer line spacing 1/Tp apart (Tp=NpTf, where Np is the period of the Tf sequence).

Figure 2.6 shows the difference between the spectrum of a simple pulse train (figure 2.6a) and the spectrum of a pulse train that includes a randomizing technique (figure 2.6b). The spurious tones are considerably reduced using a randomizing technique.

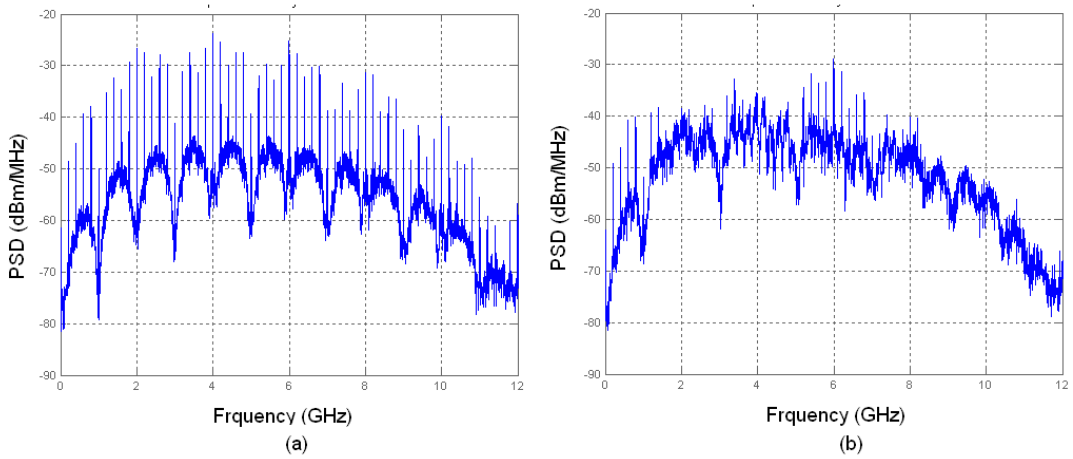

Figure 2.6 Spectrum of pulse train without (a) and with (b) randomizing technique.

A number of randomizing techniques can be found in the literature [23]-[29], but in the practice, two main techniques are used for randomizing the pulse trains: Time Hopping (TH) and Direct Sequence Spread Spectrum (DSSS).

2.3.2 Time Hopping UWB

A simple TH multi access model of the UWB communication systems is shown in figure 2.7. In UWB systems, the pulses are often transmitted with a low duty cycle to represent a bit, where the number of pulses in a symbol is a design criterion which determines the processing gain system. The off time between two consecutive pulses

implies a second type of processing may transmit in the gaps between these pulses. Note that, rather than a constant pulse to pulse interval, a user specific TH code can be used to help the channelization of the system, while smoothing the power spectral density and allowing a secure transmission.

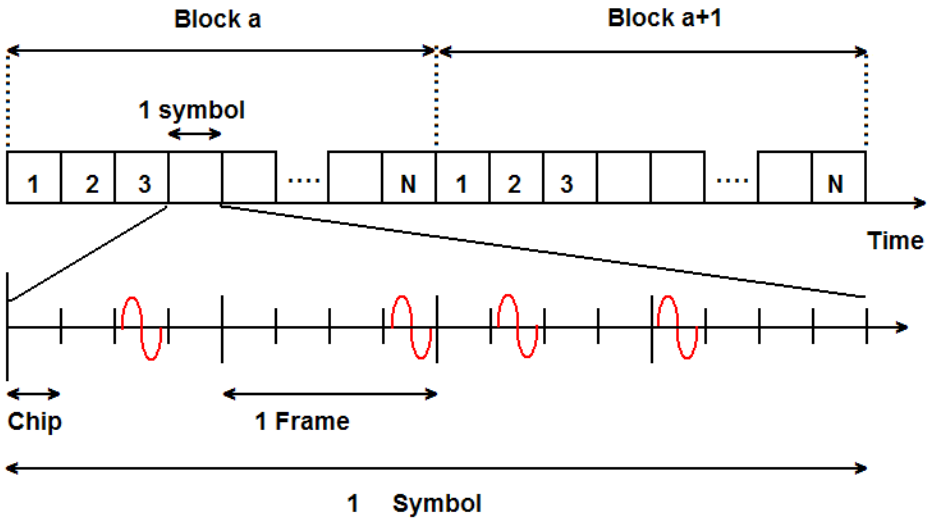

Figure 2.7 A simple TH-UWB signal structures each symbol carrying the information transmitted with a number of pulses.

When a pseudo random (PR) code is used to determine the transmission time within a large time frame, the spectra of the transmitted pulses become much more white-noise-like. On the other hand, the PR code randomizes the signal at time or frequency or both [27]. Pseudo random also minimizes the collision between users in multiple access systems, where each user has a distinct pulse shift pattern [30]. However, a consequence of PR time modulation is that the receiver needs accurate knowledge of PR code phase for each user.

2.3.3 Direct Sequence Spread Spectrum (DSSS) UWB

Direct-sequence spread spectrum (DSSS) [31] is a modulation technique whereby the transmitted signal takes up more bandwidth than the data signal being modulated.

Under this scheme carrier signals are needed to up-convert the full signal spectrum to an appropriate frequency band. A continuous string of Pseudo Noise (PN) code symbols, known as “chips”, are used for modulation. The PN code having a pseudorandom sequence of 1 and -1 values is multiplied with the data signal. Since PN code sequence has a much faster rate than the data signal, the energy of the resultant signal is spread over a much wider band. On the receiver side, de-spreading is done to reconstruct the transmitted data. The PN sequence on the receiver is the same as the transmitted one but needs synchronization for de-spreading to work correctly. Figure 2.8 shows the bit structure for a DS signal for three users.

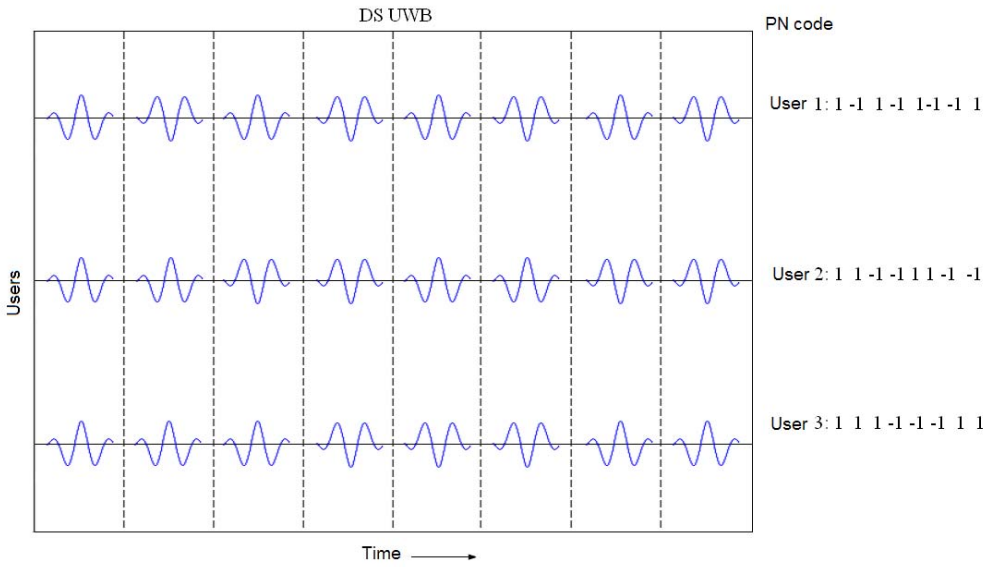

Figure 2.8 The DS-UWB IR signaling structure.

Correlation of the synchronized PN sequence with the received signal enables reconstruction of the transmitted data. The synchronization, being challenging, adds to the receiver complexity. By utilizing different PN sequences, multiple accesses are made possible. This is the basis for the code division multiple access (CDMA) property for DSSS. It allows multiple transmitters to share the same channel so long as it is within the limits of cross-correlation of the PN sequences used for different users.

2.4 Receiver Structures

The receiver performs the opposite operation of the transmitter to recover the data and pass the data to whatever "backend" applications may require. As mentioned earlier, synchronization is one of the main problems in telecommunications, as is in navigation and radar applications. Different synchronization levels operate for carrier, code, symbol, word, frame, and network synchronization. When the synchronization is optimal, the receiver will perform the functions of detection or acquisition to locate the required pulses amongst the other signals and then to continue tracking these pulses to compensate for any mismatch between the clocks of the transmitter and the receiver.

There are several receivers proposed for UWB communications [30]-[36]. In order to implement an efficient UWB system for high rate communication, it is critical to understand the characteristics of the propagation channel. The multipaths have spans of several nanoseconds which could result in inter symbol interference (ISI). This ISI would need to be mitigated through proper waveform design, signal processing, and equalization algorithms. The very wide bandwidth of the transmitted pulse allows resolution of several multipath components. On one hand, the multipath arrivals undergo less amplitude fluctuations (fading) since there would be fewer reflections that cause destructive/constructive interference within the resolution time on the received pulse. On the other hand, the average of the total received energy is distributed between a large numbers of multipath arrivals. In order to take advantage of the energy, the receivers need to be designed with multipath energy capture.

2.4.1 Coherent Receivers

There are several proposed receivers in UWB communications such as fully coherent receivers. Optimal matched filtering for example, typically employed by rake reception, perform well but at the expense of extremely high computational and

hardware complexity. In general, a coherent receiver requires several parameters (side information) concerned with the receiver's signal. Multipath delays, channel coefficients for each delay multipath component, and distortion of the pulse shape need to be estimated for optimal coherent reception.

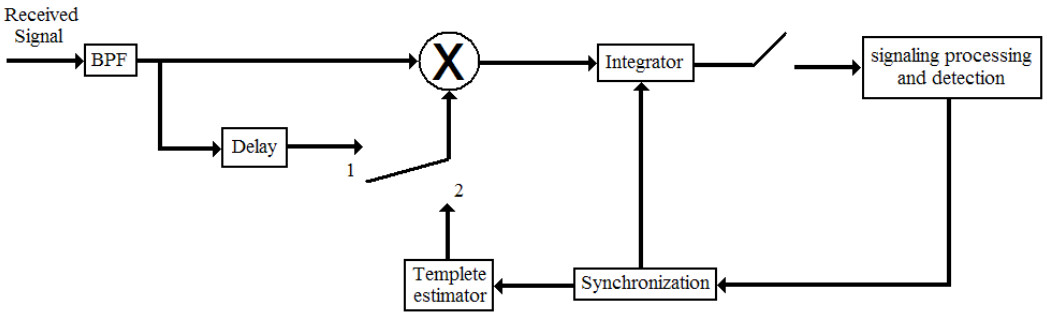

Figure 2.9 A generic layout of typical UWB receiver structure.

A general UWB receiver structure is shown in the figure 2.9. The optimal matched filtering (and simplified version implemented as rake and simple single correlator receivers) correlates the received signal with a local template. The local template can be a pulse template, a frame template, or a template that includes multiple pulses with relative delays between pulses based on the Time Hopping (TH) code. In either cases, the template needs to be estimated locally based on the received signal by transmitting some training sequences, or blindly. This type of receiver, which correlates the receiver signal with a template, is often referred to as "locally generated reference" systems [37] or simply as "correlation" receivers [38].

2.4.2 Optimal Matched Filter

In matched filtering, the basic principle is to estimate to noiseless replica of the receiver waveform and to use this estimate as filter to maximize the SNR at the output of the matched filter. The detection of the transmitted bits is achieved by correlating the received signal, $r(t)$ with the estimation of the noiseless replica of the

receiver waveform for a duration bit, i. e., for N_s pulses. The template waveform used in the correlation of the q^{th} bit, $v_q(t)$, is given by [22]:

$$v_q(t) = w_q(t) - w_q(t-\delta) \tag{2.6}$$

$$w_q(t) = \sum_{n=qN_s}^{(q+1)N_s-1} w\left(t - nT_f - h_n T_h - \beta\right) \tag{2.7}$$

A decision as to whether the *q-th* data bit, d_q, is 0 or 1 in a binary modulation is made depending on whether the correlator output is greater than or less than zero, respectively. Received pulses from other users, delayed and faded replicas of the desired signal and thermal noise degrades the detection process. The interval $[-t_d/2, t_d/2]$ is defined around the received pulse, $w(t)$, such that the correlator output for a single pulse becomes negligible when correlation is performed outside this interval. Thus we have [22]:

$$m_p = \int_{-\infty}^{\infty} w(t)v(t)dt = \int_{-t_d/2}^{t_d/2} w(t)v(t)dt \tag{2.8}$$

The matched filter can be implemented in multiple parallel correlator structures called rake receivers as shown in figure 2.10. The local templates are estimated in each parallel branch. The template used in each branch just matches the received pulse shape with estimated delays and TH codes. The estimated tap coefficients are then used for combining different branches optimally by maximal ratio combining (MRC).

The correlation is followed by weight combining. In the correlation, each parallel branch is tuned to a different multipath location. The local templates in each branch require the knowledge of the received pulse shape. The outputs of the correlators are sampled in frame or symbol-space depending on whether the template is a single

pulse or a train of pulses. Various implementations are possible depending on the desired sampling rate at the output of the correlator.

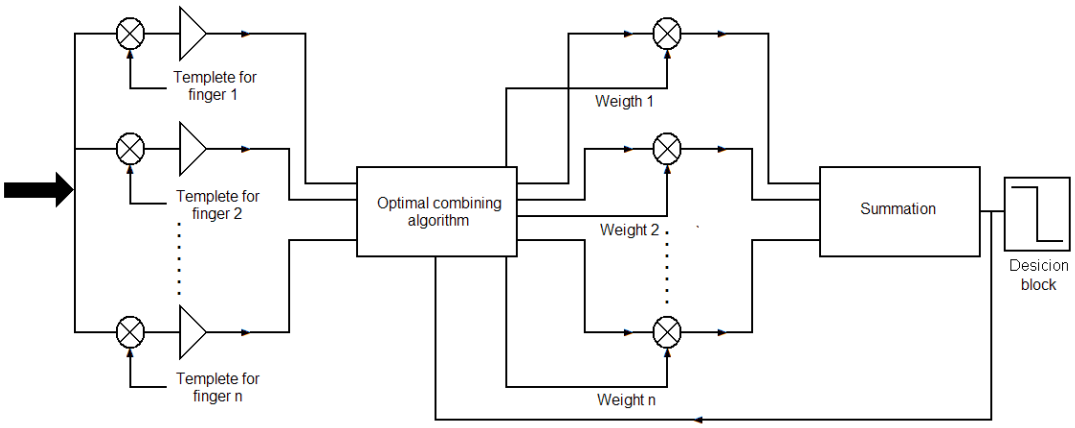

Figure 2.10 A basic rake receiver structure.

2.4.3 Noncoherent Receivers

Noncoherent (or lightly coherent) receiver designs relax the amount of information that need to be estimated accurately for the detection of transmitted bits in UWB receivers [4]. In other words, the synchronization, channel estimation, and pulse shape estimation is not stringent as is the case of the fully coherent receivers. Some of the Noncoherent transceiver designs include Transmitted Reference (TR) based UWB, energy detector, and differential detector. Commonly, the channel and receiver pulse estimation are not necessary. Also, the timing estimation is easier and the receiver performance is more immune to the timing mismatch [4].

2.4.3.1 TR Based Scheme

The basic principle in TR based scheme is to transmit a reference (unmodulated) pulse along with the data pulse (modulated). The reference pulse and the data pulses are transmitted with delay between them. When the delay is less than the coherent time of the channel, the reference and data pulses can be assumed to be affected

similarly due to the channel. The TR scheme uses the reference pulses as the template for correlating the data pulse, and for the demodulation of the transmitted information. Figure 2.11 shows a basic TR receiver structure.

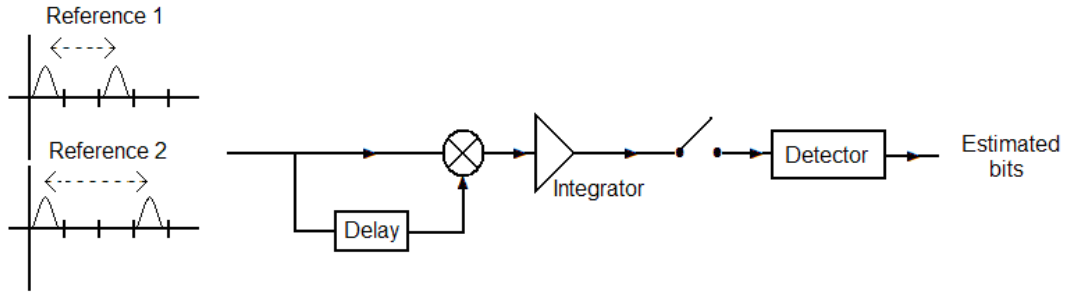

Figure 2.11 A simple TR receiver structure.

The TR based scheme has the ability to capture the energy from multipath components of the received signal with a simple receiver structure. However, in TR scheme, there is no need for a fine timing estimate of all the multipath components. This has both advantages and disadvantages. The advantage is more simple timing and more immunity to timing errors [38]. The disadvantage is that, without the fine timing, both the noise and signal over the window (whether there is a multipath component or not) are absorbed.

The TR scheme assumes that everything is useful over the integration window. In reality, some samples contain energy, and some contain noise. If one integrates all of them, then the integrator is not collecting the energy optimally. One way to solve this problem is to control the integrator [37][39]-[43]. If the locations of multipath components are known, then the energy of only these multipath components samples would be collected. Then, this will end up being a rake reception. The averaging window size should be chosen carefully to make sure that the channel is constant over the averaging window.

2.4.3.2 Differential Detector

The differential detector is similar to the TR scheme. The reference data pulses correspond to the previous symbol and are used as the template. [44]-[46], so that the information is in the difference of two consecutive symbols. Figure 2.12 shows the modulation by differential scheme.

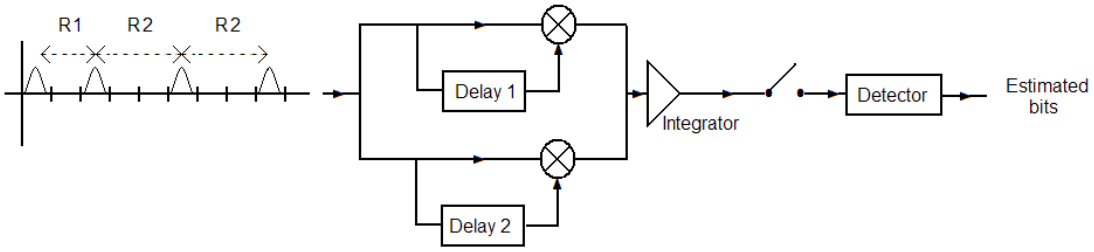

Figure 2.12 Block diagram for a simple differential receiver.

The differential detector does not provide the flexibility of TR scheme in terms of adjusting the power, position, and number of the reference signal. Averaging the reference information in a differential detector is not possible.

2.4.3.3 Energy Detector

Noncoherent energy detection based receiver for both communications and ranging have in recent times received the most attention for low power and low cost applications for sensor network. An energy detector is a simple suboptimal Noncoherent UWB IR receiver scheme. Similar to TR scheme, the energy detector receiver requires only coarse synchronization, which makes the systems robust against clock jitter and triggering inaccuracy [47][48]. It is also not sensitive to distortion and phase nonlinearity of devices like antennas, amplifiers or filters [47]. Figure 2.13 shows a simple energy detector.

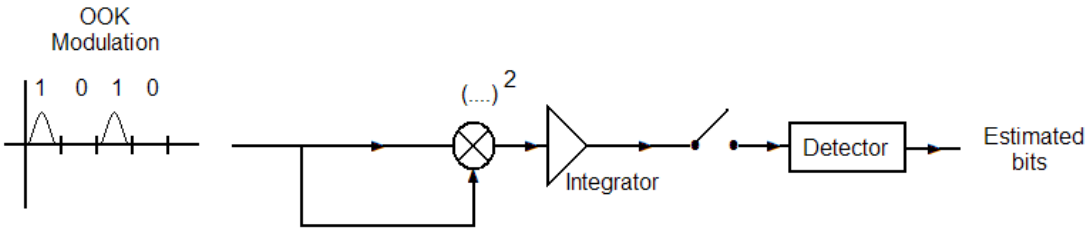

Figure 2.13 Block diagram for a simple energy detector.

2.5 Generation of Gaussian UWB Waveforms

The selection of the pulse signal types is one of the fundamental considerations in the design of UWB circuits and systems because it sets the level of performance of the new UWB systems. There have been many attempts to choose a signal waveform suitable for UWB applications and yet, it has had minimal interference with proximity systems [5] [6]. However the optimal selection depends on application of system.

2.5.1 Damped Sine Wave

According to [52] a damped sine wave is of the form

$$y(t) = Ae^{\lambda t}\sin(2\pi f_0 t) \tag{2.9}$$

where A is an arbitrary amplitude, λ is the exponential decay coefficient, f_0 is the frequency of oscillation of the sine wave, and t≥0 is the time. Figure 2.14(a) demonstrates this waveform, and any wave of this general form can be considered as being a damped sine wave, or class B emission.

Figure 2.14(b) clearly indicates that the damping oscillations of the waveform lead to a small effective bandwidth and sharp peak in the spectrum. This is in contradiction

with the required flatness of the spectrum of permitted waveforms by FCC [17]. Waveforms with damped oscillatory tails can not be used in UWB communication systems that are available in the area.

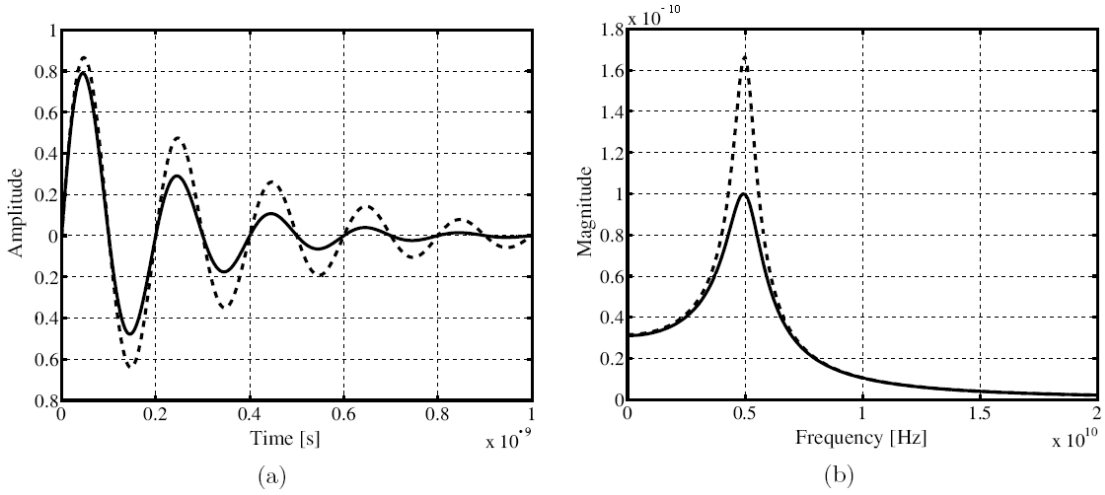

Figure 2.14 (a) Damped sine wave and their (b) Fourier transform [4].

The basic theoretical model for pulse radio uses a waveform knows as "Gaussian waveform" [50]. Gaussian pulses offer an excellent time frequency product [51] and provide better BER and Multipath performance then other pulse signals [52]. The transferring rate and wide operation are some desirable characteristics and have a direct relation with the selected waveform [53].

2.5.2 The Gaussian Pulse

A Gaussian pulse has the shape and the PSD shown in figure 2.15. The mathematical expression for a Gaussian pulse is:

$$v(t, f_c, A) = Ae^{-2(\pi t f_c)^2} \tag{2.10}$$

Where A is the amplitude of the Gaussian pulse, and f_c is the center frequency [54].

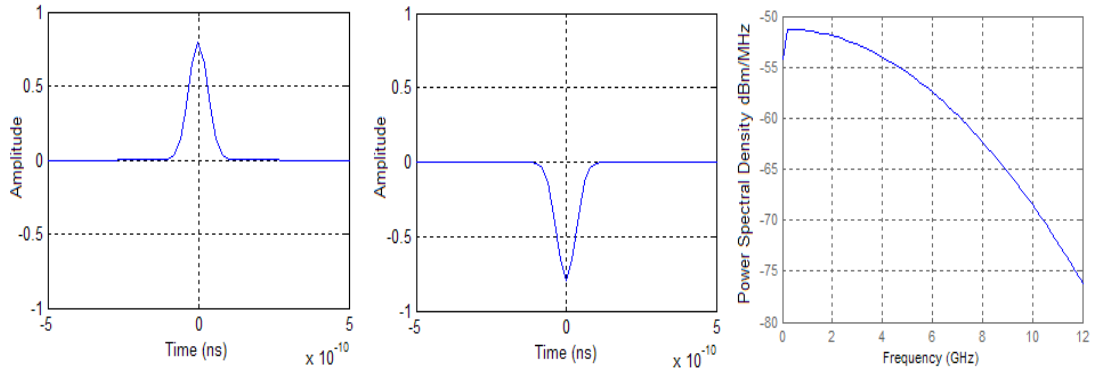

Figure 2.15 Positive and Negative Gaussian pulses and their PSD.

2.5.3 Gaussian Monocycle Pulse

Taking the derivative of the equation 2.10, we can obtain the equation for a Gaussian monocycle pulse, as follows:

$$v(t, f_c, A) = 2\sqrt{e}A\pi t f_c e^{-2(\pi t f_c)^2} \tag{2.11}$$

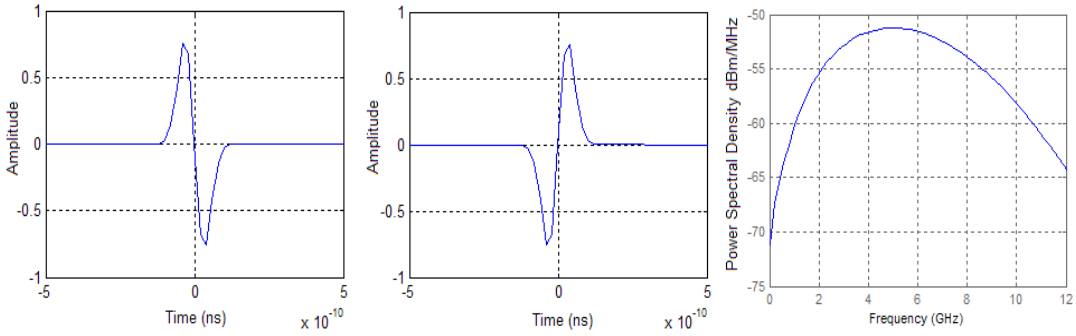

Figure 2.16 Positive and Negative Monocycle Gaussian pulses and their PSD.

The center frequency of the monocycle pulse is usually defined as $(\pi\tau_0)^{-1}$ Hz, where τ_0 is defined as the time between the maximum and minimum points of the monocycle pulse [55]. Figure 2.16 shows the Monocycle Gaussian pulse and its

frequency spectrum. Again, note that the frequency spectrum does not meet the FCC regulations due to the bandwidth being too large as it is shown in the PSD.

2.5.4 Gaussian Doublet Pulse

The Gaussian doublet is often used in UWB systems because its shape is easily generated. It is a simply a square pulse which has been shaped by the limited rise and fall times of the pulse and the filtering effects from the transmitter and receiver antennas. This idealized pulse shape received can be written as [56]:

$$v(t, f_c, A) = \left[1 - 4\pi(tf_c)^2\right] A e^{-2\pi(tf_c)^2} \tag{2.12}$$

Figure 2.17 shows the Doublet Gaussian pulse and its frequency spectrum. Again, note that the frequency spectrum does not meet the FCC regulations due to the bandwidth being too large as it is shown in the PSD.

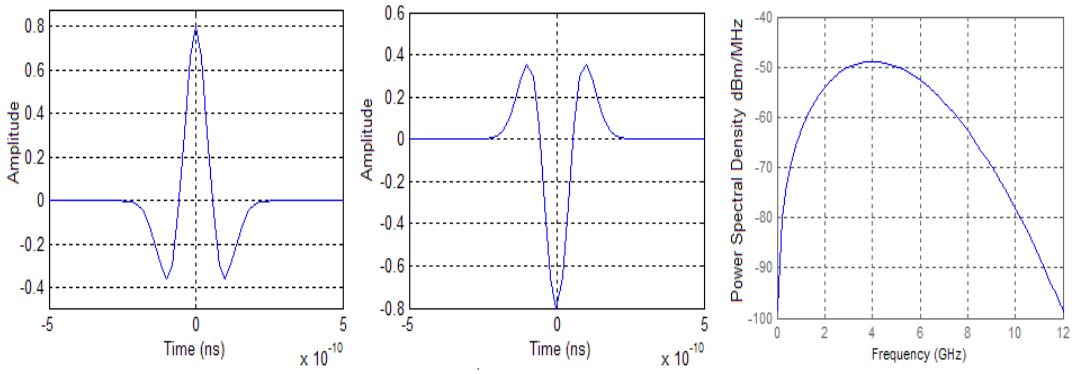

Figure 2.17 Positive and Negative Doublet Gaussian pulses and their PSD.

2.6 Previous Work

There are several methods to generate subnanosecond pulses. Some implementations require large circuits, which result in increased cost. These existing pulse generators

are often not evaluated in terms of power consumption and the feasibility to be integrated into a wireless device. Multi Spectral Solution Company introduces three schemes to generate pulses to burst of pulses in their patent [57]. The first class consists of two pulse generation schemes. The first pulse generation scheme, presented in figure 2.18, utilizes an impulse generator and a mixer (switch) to chop the signal coming from an oscillator, thereby providing a burst train to the subsequent circuit.

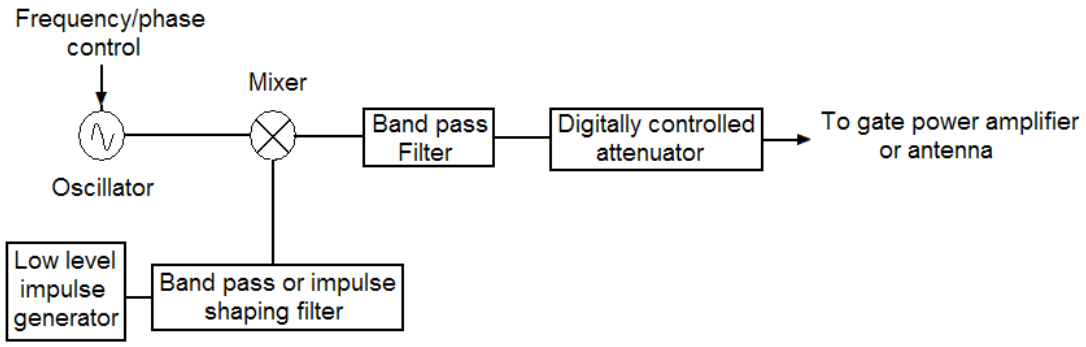

Figure 2.18 First class of transmitter.

The second pulse generator scheme in the first class is shown in figure 2.19. A band pass or pulse shaping filter is directly exited by a low level impulse, so that a mixer and oscillator are not needed.

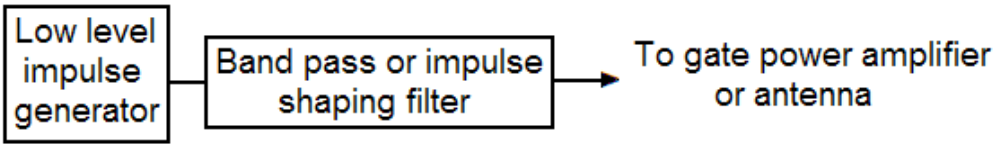

Figure 2.19 Special case of the first class of transmitter.

The transceiver is less complex since there is no need to generate the derivative. The trade off is that the circuit is relatively more expensive, since very short impulse requires fast switches and digital signal processors deal with the fast calculations.

Xtreme Spectrum transceiver architecture is covered in a 2001 patent [58]. The idea is to produce two short pulses, which are half the length of the desired monocycle pulse. These short pulses, S1 and S2 shown in figure 2.20, are combined by a Gilbert cell, which is used as a differential mixer. As a result, the mixer produces the monocycle.

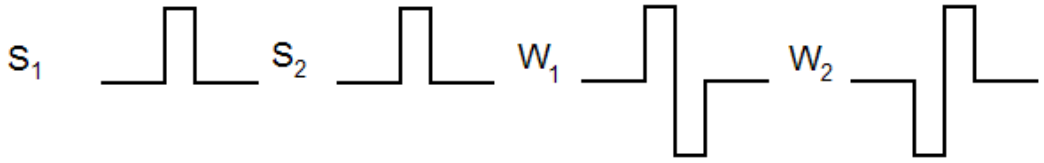

Figure 2.20 Ideal pulses and waveforms.

In the reference [59], an avalanche transistor is used to generate a monocycle pulse. The pulse generation is based on operating the transistor in avalanche mode, which requires high voltage; however, high voltage solutions are not covered in this thesis, therefore this method is introduced the high voltage applications..

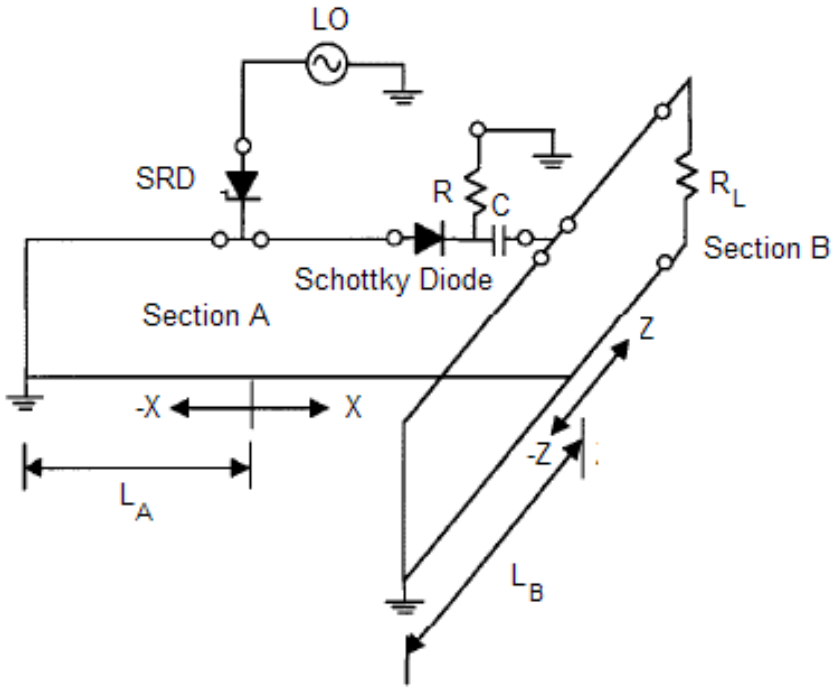

Figure 2.21 Pulse generator developed in [60].

Another method of generating sub nanosecond monocycle pulses involves the use of a schottky diode, a step recovery diode (SRD), and a coplanar waveguide [60]. The pulse generator developed in using a step recovering diode (SRD) is shown in figure 2.21.

In order to examine how a pulse is generated, the pulse generator is broken into two sections, A and B. First, the LO provides a 10 MHz square wave to the SRD, which generates a step-like pulse. Once a step-like pulse arrives at transmission line A, it is divided into two other step pulses that propagate in the +x and -x direction. The step function traveling to the short circuit is reflected back along the transmission line and combines with the other step pulse to form a Gaussian pulse. This Gaussian-like pulse then travels to the schottky diode, turns the diode on and charges the capacitor C. This pulse is then high-pass filtered by the capacitance, C, and resistance, R, which allows only the positive and negative edges of the pulse to continue to section B and into the +z and -z directions. Just as in section A, the pulse propagating in the -z direction is reflected back at the short circuit and travels to the load. This negative pulse arrives at the load and combines with the positive pulse to form a monocycle pulse.

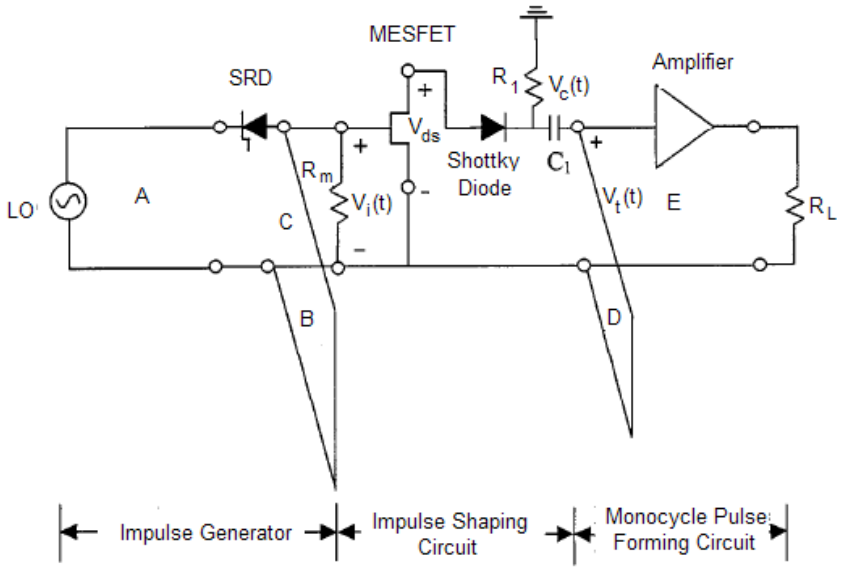

Figure 2.22 Pulse Generator Developed in [61].

Another embodiment of this development has been introduced by incorporating an impulse-shaping network using a MESFET [61]. A depiction of this improved circuit is shown in 2.22. The basic idea is the same as in figure 2.21, except that there is an additional MESFET as amplifying unit.

Two short pulses are presented in [62] with digital pulse generation circuit. The first method is presented in figure 2.23. The delay between the two pulses is realized by a simple delay element consisting of two inverters and PMOS varactor, which provides the opportunity to tune the length of delay.

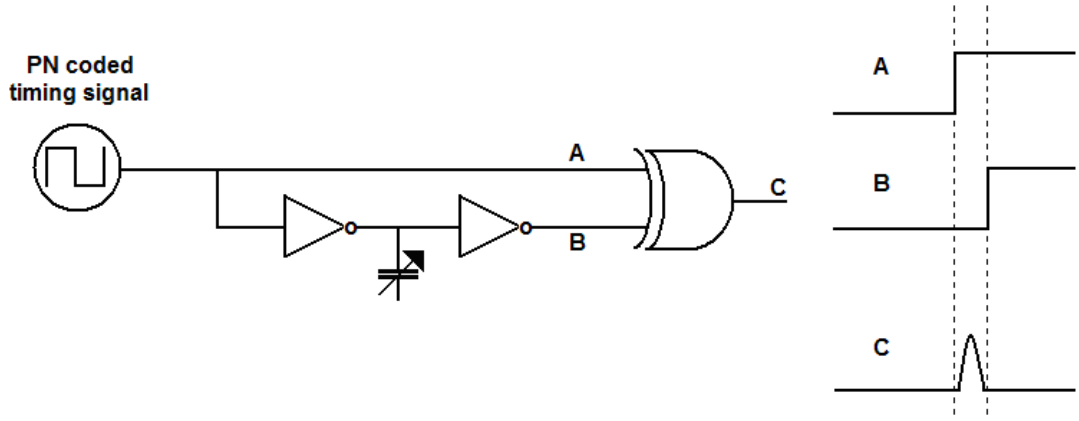

Figure 2.23 Digital pulse generator by a XOR gate.

The XOR operates so that whenever both input signals are at different logical levels, the output is at high level, i.e. logical 1, and when both input signals have the same logical levels, the output is at low level, i. e. logical 0 [63]. The length of the high level output can be adjusted by the phase difference between the inputs. This is also provided by a simple delay element.

The second method presented in [63] is shown in figure 2.24. The AND gate operates so that whenever both inputs are at high level, the output is at high level [41]. An inverter is connected to one of the inputs of the AND gate, and a clock signal is connected to both, the inverter and the AND gate.

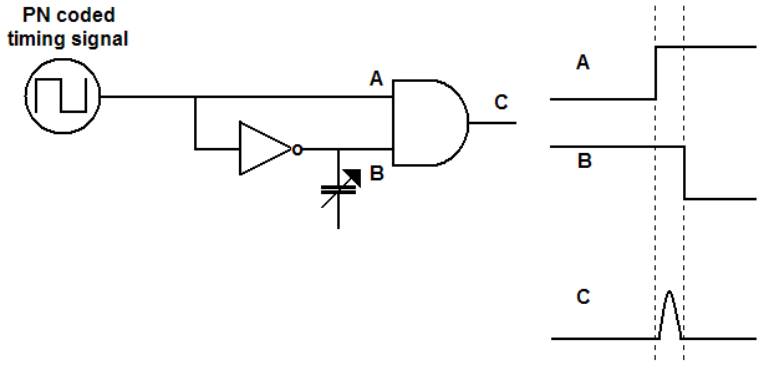

Figure 2.24 Digital pulse generator by an AND gate.

The output of the AND gate is now at low level at all times, but the output still reacts to the rising edge of the clock. This is because the inverter has a delay during which it is still at zero while the clock has already risen. This effect is called a glitch, or hazard, which results in a short pulse with length corresponding to the length of the inverter delay. The delay can be adjusted by connecting a varactor at output of the inverter. If the delay is very short, the resulting pulse might not have time to rise all the way up to the logical 1, but is still useful for generating short pulses. When using this circuit, the pulse repetition frequency (PRF) decreases to half that when using the XOR circuit, since the short pulse will occur only on the rising edge clock. The XOR reacts to both the rising and falling edge of the clock.

The gate AND shown in figure 2.24 can be replaced by a NAND gate where the operation is the same as in the case of an AND gate, the difference being that the pulse will occur on the falling edge of the clock and the pulse is from high to low levels. The NAND gate is faster than the AND gate and is therefore used in the implementation of the transceiver.

The shape of the pulse is defined by the RC time constant of the used gate in all three circuits. Reference [63] presents a Gaussian pulse generator that is based on ten complex first order system (CFOS) stages that need to be cascaded to achieve a reasonable approximation of the Gaussian envelope. The block scheme for the

resulting UWB pulse generator is depicted in figure 2.25, and figure 2.26 shows the CFOS stage used in the pulse shaping network.

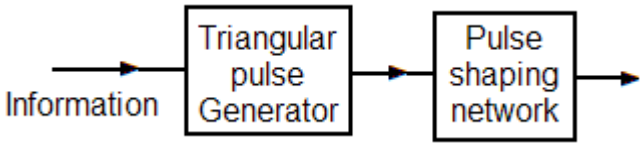

Figure 2.25 CFO Pulse Generator.

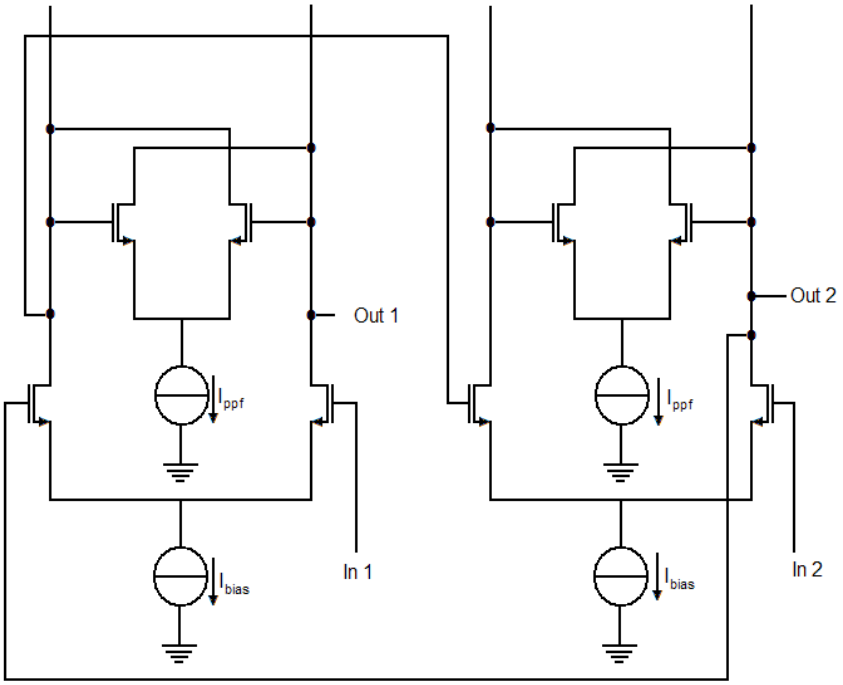

Figure 2.26 Differential pair with gain enhancement single stage CFOS.

The triangular pulse generator is made up of a single ended to differential converter, followed by an even symmetry function as shown in figure 2.27. The even symmetric function is able to evoke the impulse response of the succeeding pulse shaper.

Reference [64] presents a Gaussian pulse generator. The basic idea is the same as in figures 2.23 and 2.24, except that there is not a PMOS varactor. The pulse generator consists of a delay line and a XOR block. Figure 2.28 shows a block diagram.

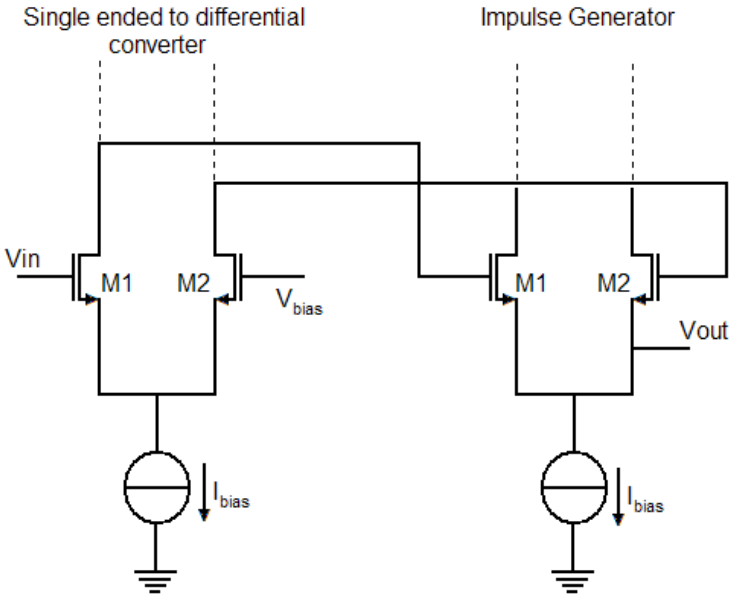

Figure 2.27 Triangular pulse generator.

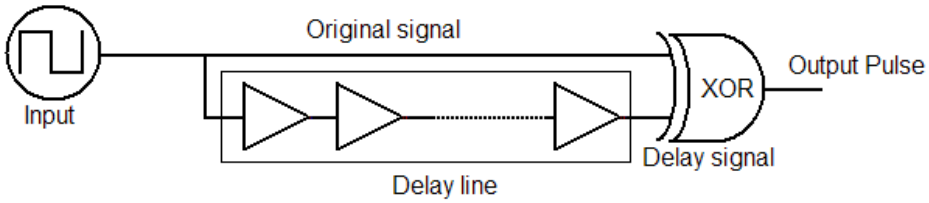

Figure 2.28 Pulse Generation Block Diagram.

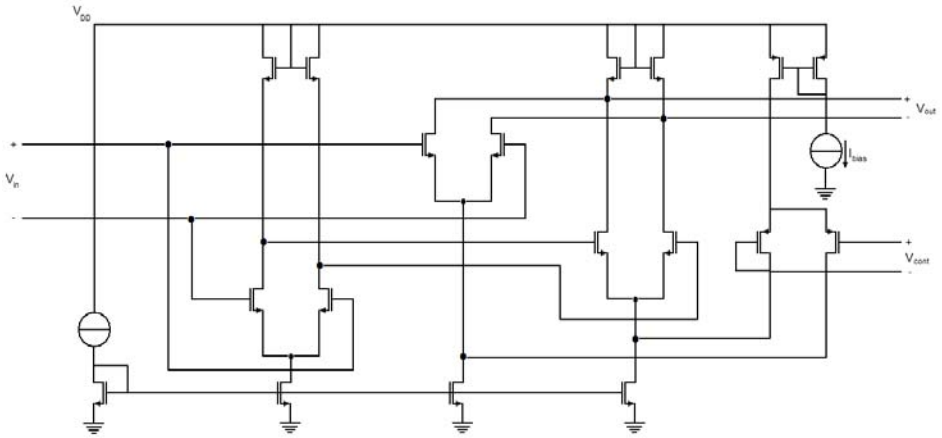

Figure 2.29 Interpolation delay cell.

The delay block consists of a fast path with a single differential pair and a slow path with two differential pairs. As shown 2.29, the control voltage, V_{cont}, adjusts the delay time by controlling the gain of each path. The Gilbert cell in figure 2.30 serves as XOR and creates pulses when the two different input signals have opposite levels at the same time. The generated short pulses become the input signal of the impulse shaping circuit.

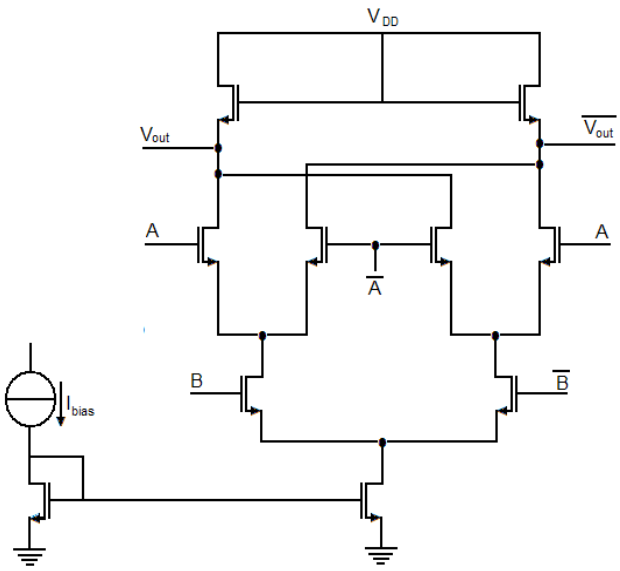

Figure 2.30 Gilbert cell with NMOS load.

The rectangular pulses obtained are shaped using the circuit shown in figure 2.31. The components are implemented using the on-chip substrate RF instead of the off-chip or active components.

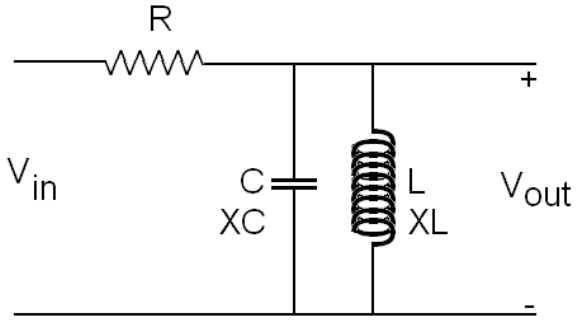

Figure 2.31 RLC 2nd order BPF (impulse shaping).

An alternative approach is to use a single stage CMOS amplifier [65]. The basic CMOS amplifier is shown below in figure 2.32.

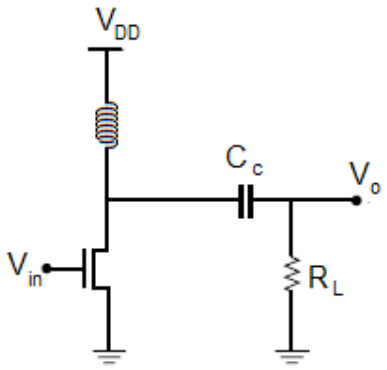

Figure 2.32 Single stage basic amplifier.

The amplifier generates pulses at the output by switching the input of the single transistor. By toggling the input of the transistor, the direction of the current is controlled, and a pulse is generated through the charging and discharging of the capacitor. This approach can be implemented onto a single chip, at a low cost compared to existing pulse generation methods. The pulse repetition frequency and shape can be controlled by control logic applied to V_{in}. The basic structure of this design involves a power amplifier with four control taps, A through D, as shown in figure 2.33 [66]. The desired pulse is broken into specific transitions in time. The pulse generator generates the desired pulse through a combination of specific input transitions on the control taps.

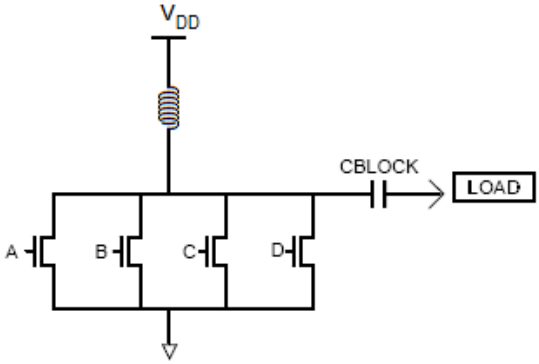

Figure 2.33 Pulse generator basic structure.

The circuit involves an off-chip RF Choke, which provides a constant current source over a large range of frequencies. A blocking capacitance is used, as in most circuits, to eliminate the amount of DC at the output of the amplifier.

In figure 2.33, suppose that control taps A, B, C, and D are set to V_{DD}, GND, GND, and V_{DD}, respectively. The power amplifier is in an idle state with no current flowing to the load. Note that the current flows through the RF choke and the two conducting transistors. Here is exposed the generation of a positive Gaussian monocycle pulse as an example. From the idle state, suppose that the control tap B switches to GND, turning transistor B off. The current flowing through transistor B starts to flow through the capacitor to the load, generating the first positive slope of a pulse. After a certain delay, the control taps A and D are turned on. Then the current starts to flow in the opposite direction, generating the negative slope of the pulse. Lastly, the tap control C is turned off, and the direction of the current changes again, generating a positive slope of the pulse. Figure 2.34 shows a waveform illustrating the switching sequence of the four control taps and the resulting Gaussian monocycle pulse.

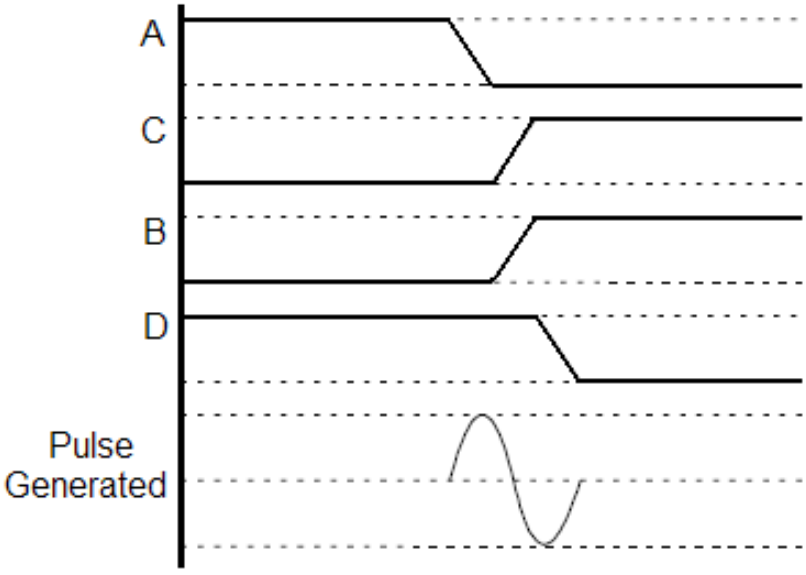

Figure 2.34 Monocycle pulse generator.

In addition to generating a positive monocycle pulse as described above, this four tap power amplifier can also generate both positive and negative Gaussian pulses and monocycle pulses through different input switching sequences. An example of the generation of a Gaussian pulse is shown in Figure 2.35

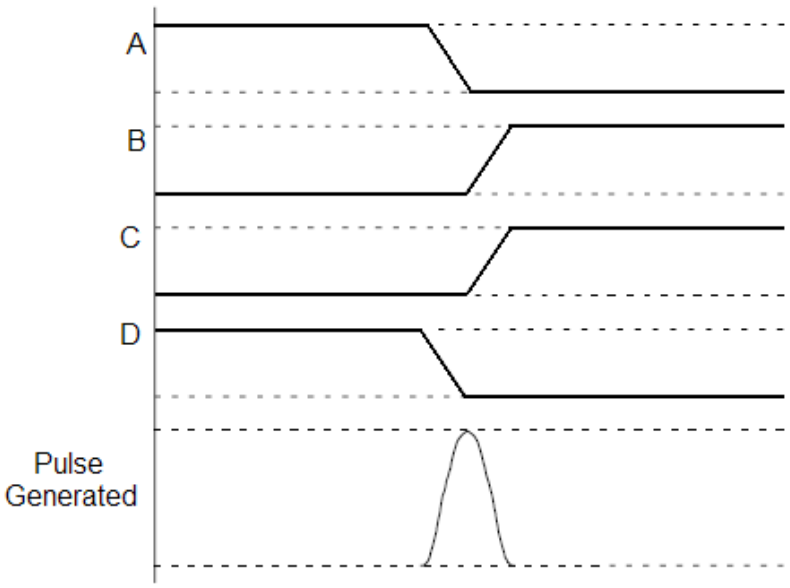

Figure 2.35 The Gaussian pulse generator.

The generation of the pulses shown above is possible using a CMOS power amplifier with only four taps. However, this approach can be extended to generate additional pulses such as a Gaussian doublet, or further derivatives of the Gaussian pulse, by adding additional control taps. The number of pulses that are possible using this approach is limited only by the complexity of the control circuitry, which is directly related to the number of control taps.

The methods described in references [57] [58] [59] [60] [61] all have a problem in common: large area requirements and hence, high cost. The other approaches presented in references [62] [63] [64] [65] [66], but the problems are the complexity and the process variations. This thesis project proposes a low complexity and area Gaussian pulse generator as seen with more detail in chapter 3**.**

2.7 Pulse Design Consideration

Single short pulse (or impulse) generation is the traditional and fundamental approach for generating waveforms. By varying the pulse characteristics, the characteristics of the energy in the frequency spectrum may be defined based on the desired design criteria. Generally, there are three parameters of interest when defining the properties of energy which is filling a specified frequency spectrum:

Pulse duration in the time domain determines the bandwidth in the frequency domain. As a rule of thumb it may be written:

$$\frac{1}{Duration} \approx \text{Bandwidth} \tag{2.13}$$

Pulse repetition is a characteristic that may determine the center frequency of a band of transmitted energy if the repetition is regular.

Pulse shape determines the characteristics of how the energy occupies the frequency domain.

Essentially, the design pulse shapers with desirable spectral properties can be of two types: SB analog/digital and MB t. In radio impulse, the pulse width is very narrow and low power, where the signal that represents a symbol consists of serial pulses with a very low duty cycle. Rather than sending a single pulse per symbol, a number of determined pulses and the processing gain of the system are transmitted by symbol [13].

As mentioned before single pulse architectures offer relatively simple radio designs, reduce the implementation cost and architecture complexity. However, they provide

little flexibility in the cases where the spectrum management is an objective. Examples of scenarios where managing the spectrum might be desirable are:

- matching different regulatory requirements in different international regions;
- dynamically sensing interfering technologies and suspending use of contending frequencies;
- choosing to use narrower bands of spectrum to either share spectrum in a local area or to enable devices that require a large bandwidth for a specific application.

An alternative is to use multi band UWB waveforms. Which have been proposed for wireless personal area network (WPAN) under IEEE 802.15 [67]. In a multiband system, multiple bands of bandwidth greater that or equal to 500 MHz are employed, with each band being occupied by distinct pulse. With the entire bandwidth divided into several non overlapping sub bands, multi band UWB systems provide flexibility in efficiently “filling up” the spectral mask, and facilitate co existence with legacy systems. It also allows for world wide deployment by enabling some sub bands to be turned off in order to avoid interference and comply with different regulatory requirements. In addition, MB systems provide another dimension for multiple accesses, and frequency hopping can also be easily implemented by switching among those base band pulses to acquire greater frequency diversity.

As mentioned before, OFDM has become a very popular technique due to its special features, such as: robustness against multipath interference, ability to allow frequency diversity with the use of the efficient forward error correction (FEC) coding, capability of capturing the multipath energy efficiently, and the ability to provide high bandwidth efficiency through the use of sub band adaptive modulation and coding technique [68]. OFDM can overcome many problems with high bit rate communication, where the most serious is time dispersion [69].

2.8 Conclusions

UWB systems can be primarily divided into impulse radio (IR) systems and multiband systems. Multiband systems offer the advantages of potentially efficient utilization of spectrum. On the other hand, IR is essentially a base band technique.

As already shown, the PPM performance degrades in multipath and multi-user environments because the symbols occupy large time durations. Compared with other modulations, OOK and M-ary PAM are more susceptible to modulations and to jitter-especially in high frequency. In summary, BPSK is preferred for its high power efficiency and smooth spectrum, OOK for its simple transceiver structure, M-ary PPM for its improved power efficiency, and M-ary PAM for higher data rates.

This chapter has explored some fundamental issues that need to be addressed when attempting to implement an UWB transceiver. The chapter is also focuses on the main aspects of the UWB transceivers; the pulse generation and key aspects of the transceivers architectures.

Several receiver options in UWB systems have been discussed. Each receiver option has several trade-offs in terms of performance, cost, hardware, and computational complexity. Depending on the applications and the transceiver requirements, different receivers might be preferable. Currently, the implementation of fully digital and fully coherent reception is not feasible for UWB radio yet. There have been efforts to reduce the complexity of the coherent matched filtering-based receiver. These efforts include reducing the number of fingers in a rake reception while trying to keep the performance as close as possible to “All rake” receivers, avoiding the intensive estimation of the time varying channel parameters, developing simple and computationally efficient channel parameters estimation techniques. In parallel, there are also recent efforts to improve the performance of noncoherent receivers to close the performance gap with respect to fully coherent receivers. Mainly, the approaches

for improving the performance of the noncoherent receivers are based on estimating some additional parameters regarding the channel parameters, and making these receivers more coherent.

Several pulse generation techniques were explored, including a digital generation technique. Some problems have been considered in these techniques with respect to the design and implementation on chip.

Chapter 3

Scheme Modulation, and Modulator/ Demodulator Circuits

3.1 Introduction

In all wireless communication systems, it is very important that the receiver and the transmitter be aligned in time. In other words, the synchronization among them must be perfect. The synchronization can be roughly described as the process of providing the same time reference for the receiver as used by the transmitter [5]. Fast and accurate acquisition with low overhead is desired. Without a correct timing synchronization, demodulation and data detection are not possible.

In principle, the reception of a UWB signal is very simple. The signal is amplified and sampled at the time the pulse is expected and then the energy captured is measured. The difficulty is in acquiring a signal and maintaining the time synchronization since the sampling point must be aligned to better than 50 ps [4]. Any errors in the local frequency reference will rapidly cause timing accuracy to be lost. The problem is mainly due to the following two reasons: 1) The received signal

power is low, which forces the acquisition system to have a large time delay in order to improve the signal to noise ratio of the static decision (stationary random process). 2) The large system band that results in a very fine time resolution of the ambiguity region, which increases the number of phases in the search space on the acquisition system. Thus, the acquisition system is forced to process the signal over long periods of time before it gets a reliable estimate on the timing of the signal. Here there is a need to develop more efficient acquisition schemes by taking into account the signal and channel characteristics [5]. Therefore, clock synchronization is an integral part on the receiver. The clock difference at the transmitter and the receiver needs to be estimated and compensated continuously.

Recently, a family of blind synchronization techniques was developed [70], which take advantages of so called “cycle stationary” of UWB signaling, that is, the fact that every information symbol is made up of UWB pulses that are periodically transmitted (one per frame) over multiple frames. While such an approach relies on frame rate rather than Nyquist rate sampling, it requires relative large data sets in order to achieve good synchronization performance.

Another challenge arises from the fact that the design of an optimal UWB receiver must take into account certain frequency dependent effects on the received waveform. That is, due to the broadband nature of UWB signals, the components propagating along different paths typically undergo different frequency selective distortion [71]. As a result, a received signal is made up of pulses with different pulse shapes, which makes the problem of optimal receiver design a much more delicate task than in other wideband systems [72]. In [73] an array of sensors is used spatially separate the multipath components, which are then followed by identification of each path using and adaptive method, the so called Sensor CLEAN algorithm. However, due to the complexity of the method, and the need for an antenna array, it has been used primarily for UWB propagation experiments. In recent work [74], the authors present a data aided Maximum Likelihood (ML) estimation approach, which uses symbol rate

samples of the correlator output, assuming that the received signal is correlated with a received noisy template. In particular, the term noisy template comes from the fact that each received segment is noisy, distorted by the same, unknown channel and subject to the same time offset (corresponding to the time delay of an "aggregate" channel). A similar technique is discussed in [75] where, at the receiver, integrating and dumping operations are carried out on products of such segments, and the timing offset is found from symbol rate samples. While such an approach significantly reduces the sampling rate primarily for timing acquisition in UWB impulse radios, but cannot be directly extended for estimating channel response.

In less coherent (TR, differential detector, and energy detector), the receiver does not require to lock into individual multipath components. Instead, the receiver locks into where clusters of multipath components are gathered (the start and end point for integration region). More important than this, it is less sensitive to timing jitters.

3.2 Proposed Modulation Scheme

In UWB channels the large bandwidth can raise new effects compared to conventional wireless channel modeling. For example, only few multipath components overlap within each resolvable delay bin, so that the central limit theorem is no longer applicable, and the amplitude fading statistic are not longer Rayleigh. This project proposes a modulation scheme following the characteristics of the IEEE 802.15.3a standard model.

The IEEE 802.15.3a channel model encompasses the main features of the Saleh-Valenzuela channel model (SV) [76]. The SV model thus distinguishes between "cluster arrival rate" and "ray arrival rates". The first cluster starts by definition at time t=0 and the following rays arrive at rate given by the Poisson process with rate λ. The power of those rays decays exponentially with increasing delay from the first ray. The "cluster arrival rate" which is smaller than the "ray arrival rate", in turn

determines when the next cluster has its origin. The rays within that cluster are again a Poisson process with rate λ. Mathematically, the impulse response is described as

$$h_i(t) = X_i \sum_{l=0}^{L} \sum_{k=0}^{K} \alpha_{k,l}^{i} \delta\left(t - T_l^i - \tau_{k,l}^i\right) \tag{3.1}$$

where $\alpha_{k,l}^{i}$ are the multipath coefficients, T_l^i is the delay of the l^{th} cluster, $\tau_{k,l}^i$ is the delay of the k^{th} multipath component relative to the l^{th} cluster arrival time (T_l^i), X_i represents the log-normal shadowing, and *i* refers to the i^{th} realization. By definition, $\tau_{o,l} = 0$. The distribution of cluster arrival time and the ray arrival are given by:

$$p\left(T_l \mid T_{l-1}\right) = \Lambda \exp\left[-\Lambda\left(T_l - T_{l-1}\right)\right], \quad l > 0 \tag{3.2}$$

$$p\left(T_{k,l} \mid T_{(K-1),l}\right) = \lambda \exp\left[-\lambda\left(\tau_{k,l} - \tau_{(k-1),l}\right)\right], \quad k > 0 \tag{3.3}$$

The channel coefficients are defined as a product of small scale and large fading coefficients, i. e.,

$$\alpha_{k,l} = p_{k,l}\xi_l\beta_{k,l} \tag{3.4}$$

The amplitude static of the measurements were found to best fit the log normal distribution rather than the Rayleigh that was used in the original SV model. In addition, the large scale fading is also log normally distributed.

$$20\log 10\left(\xi_l\beta_{k,l}\right) \propto Normal\left(\mu_{k,l}, \sigma_1^2 + \sigma_2^2\right) \tag{3.5}$$

or

$$\left|\xi_l \beta_{k,l}\right| = 10^{\left(\mu_{k,l}+n_1+n_2\right)/20} \tag{3.6}$$

where

$$n_1 \propto \text{Normal}\left(0,\sigma_1^2\right) \tag{3.7}$$

and

$$n_2 \propto \text{Normal}\left(0,\sigma_2^2\right) \tag{3.8}$$

are independent and correspond to fading on each cluster and ray, respectively. The behavior of the average power profile is

$$E\left[\left|\xi_l \beta_{k,l}\right|^2\right] = \Omega_0 e^{-T_l/\Gamma_e - \tau_{k,l}/\gamma} \tag{3.9}$$

which reflects the exponential decay of each cluster as well as the decay of the total cluster power with delay. $p_{k,l}$ is equiprobable +/-1 to account for signal inversion due to reflection. The $\mu_{k,l}$ is given by

$$\mu_{k,l} = \frac{10\ln\left(\Omega_0\right) - 10T_l/\Gamma - 10\tau_{k,l}/\gamma}{\ln(10)} - \frac{\left(\sigma_1^2+\sigma_2^2\right)\ln(10)}{20} \tag{3.10}$$

In the equation 3.10, ξ_l reflects the fading associated with the l^{th} cluster, and $\beta_{k,l}$ corresponds to the fading associated with the k^{th} ray of the l^{th} cluster. A complex tap model was not adopted by IEEE 802.15.3a.

Finally, since the log normal shadowing of the total multipath energy is captured by term, X_i, the total energy contained in the terms $\{\alpha_{k,l}^{i}\}$ is normalized to unity for each realization. This shadowing term is characterized by following:

$$20\log 10\left(X_i\right) \propto Normal\left(0,\sigma_x^2\right) \tag{3.11}$$

The IEEE 802.15.3a channel model is composed of four different channel scenarios defined according to seven key parameters:

- Λ: cluster arrival rate;
- λ: ray arrival rate, i.e. the arrival rate of path within each cluster;
- Γ: cluster decay factor
- γ: ray decay factor
- σ_1: standard deviation of cluster log normal fading term (dB)
- σ_2: standard deviation of ray log normal fading term (dB)
- σ_x: standard deviation of log normal shadowing term for total multipath realization (dB)

These parameters are obtained by the group IEEE 802.15.3a as the best effort to match the most important characteristics of the channel such as:

- the mean and rms excess delay;
- the number of multipath components;
- the power decay profile.

Four different channel characteristics have been obtained based on many experiments and much measurement data. These channel characteristics depend on the average distance between the transmitter and receiver, and the type of transmission, i.e. either line of sight (LOS) or Non line of sight (NLOS) transmissions. The first model

channel called channel model type 1 (CM1) corresponds to very short distances, i.e. 0 to 4m and LOS transmission. The channel model type 2 (CM2) scenario is defined for the same range, but with a NLOS antenna configuration. CM3 and CM4 are defined for a NLOS antenna configuration and greater transmission distances, i.e. 4 to 10 m for CM3 and over 10 m for CM4.

Target Channel Characteristics	**CM1**	**CM2**	**CM3**	**CM4**
Mean excess delay [ns]	5.05	10.38	14.18	
rms delay spread [ns]	5.28	8.03	14.28	25
NP_{10dB}			35	
NP (85%)	24	36	84	
Model Parameters				
Λ [1/ns]	0.0233	0.4	0.0667	0.0667
λ [1/ns]	2.5	0.5	2.1	2.1
Γ	7.1	5.5	14	24
Γ	4.3	6.7	7.9	12
σ_1	0.3907	0.3907	0.3907	0.3907
σ_2	0.3907	0.3907	0.3907	0.3907
σ_x	0.3454	0.3454	0.3454	0.3454
Model Characteristics				
Mean excess delay [ns]	5.1	9.6	15.3	28.5
rms delay [ns]	5	8	15	25
NP_{10dB}	17.7	17.7	34.3	53.4
NP(85%)	23.4	34.3	80.6	191.3
Channel energy mean [dB]	0.0	-0.3	-0.1	0.2
Channel energy Standard [dB]	3	3.1	3.1	3.0

Table 3.1 Multipath channel target characteristics and model parameters [76].

The main parameters of the four channel scenarios are listed in table 3.1, where NP_{10dB} represents the number of the paths within 10 dB of the peak; NP (85%) stands for the numbers of paths capturing 85% of the energy. These parameters have been

obtained by this group using the Matlab program, generating 1000 independent channel realizations of the continuous time channel impulse response, and collecting the average result for each parameter.

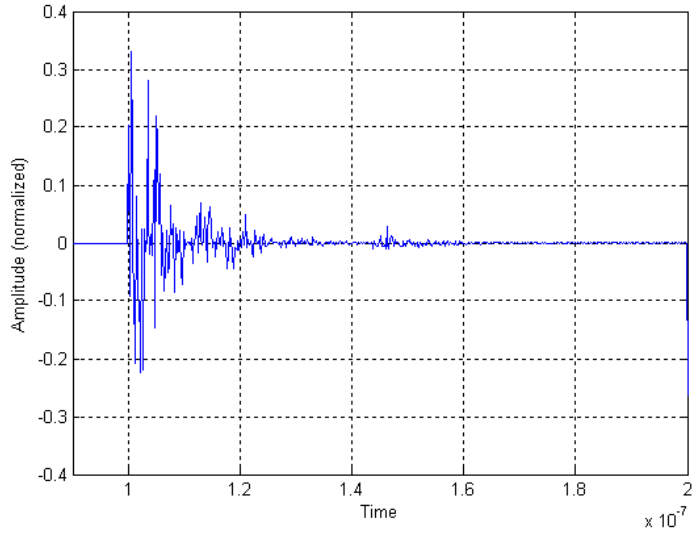

(a)

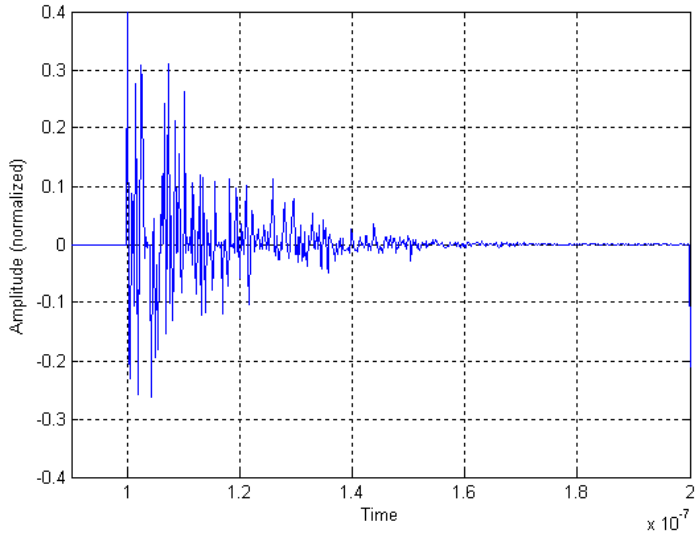

(b)

Figure 3.1 Impulse responses based on (a) CM1 and (b) CM2 respectively.

In the first instance, the thesis is focused on applications shorter than 4m of distance between the transmitter and receiver; it is to say, in CM1 and CM2 scenarios.

Nevertheless, the technique can be employed in CM3 and CM4 considering the behavior of the impulse response for these scenarios. Using Matlab program and the IEEE 802.15.13a channel model programmed by [77] in this platform, the impulse response is simulated for CM1 and CM2. The figures 3.1(a) and 3.1(b) show impulse response for CM1 and CM2 channel respectively.

The figures 3.1 (a) and (b) are simulation results which show great amounts of multipath that exist in a time interval are shown. For example in rake receivers, these multipaths can be collected for a better performance and have a good symbol estimation of BIT transmitted. In the same figure, we can observe that the multipath decrease in amplitude with respect to time; in this case the pulse width is 300 ps. For a simulation where the pulse width is 150 ps the result is presented in the figure 3.2.

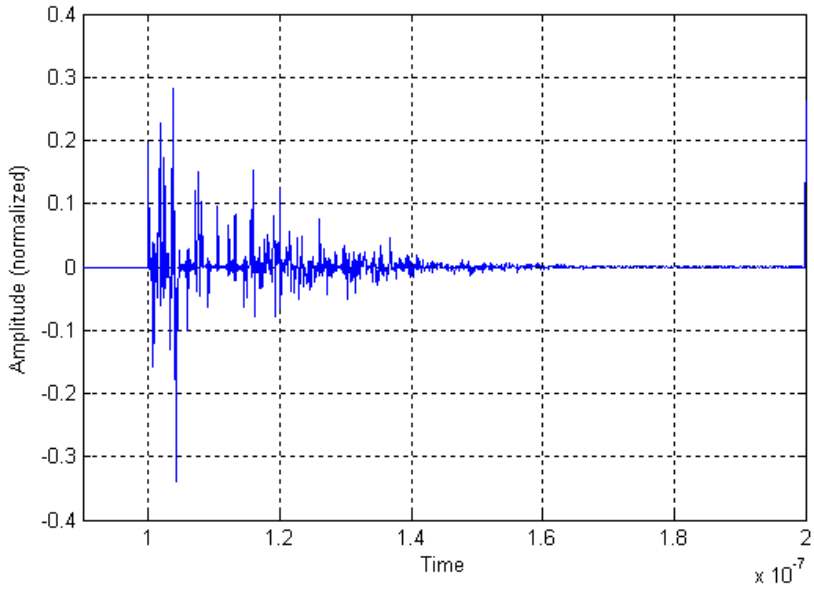

Figure 3.2 Impulse responses based on CM2 for a width pulse of 150 ps.

The difference between figure 3.1b and 3.2 is the time interval where the multipaths have a considerable presence it is to say the difference between the "rms delay spread". In this case the difference of rms delay spread between figure 3.1b and 3.2 is approximately 20ps. This is one reason why a narrow pulse is preferred. For example, values for the rms delay spread for indoor channels have been reported to be between

19 ns and 47 ns in [78], and mean values between 20 ns and 30 ns for 5 to 30 m antenna separation were reported in [79]. In addition, the multipath delay spread increases with increasing separation distance between receiving and transmitting antennas.

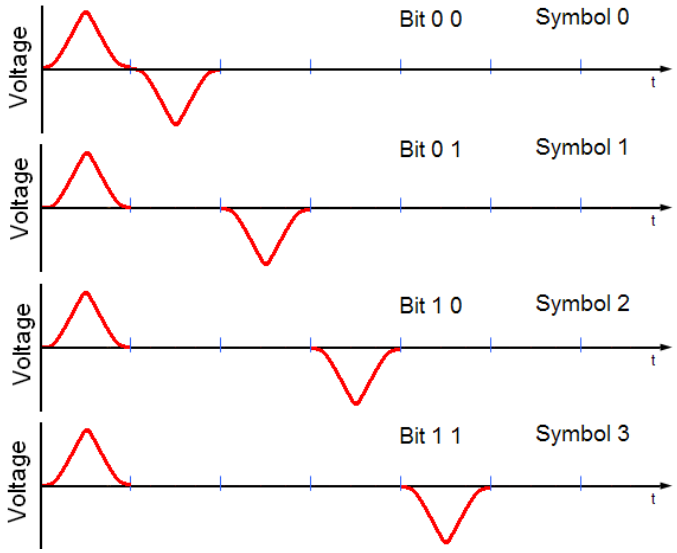

Figure 3.3 Proposed Symbols.

A UWB receiver that waits a determined "rms delay spread" to transmit other symbol, result to be a receiver with very low duty cycle and therefore with a low data rate. On the other hand, high data rate UWB systems present a dense multipath profile where many components can be distinguish from the received signal introducing more than one correct synchronization cell. The perspective of code synchronization, this phenomenon causes problems, such as the following: the energy of the signal is spread over many components and the energy of each path is very low. Therefore, the paths are difficult to acquire and, depending on the receiver structure, a number of paths should be acquired.

Base on exposed before, in this thesis is proposed a modulation scheme that consists in transmitting four symbols, where all the symbols are represented by a pair of positive and negative Gaussian pulses shifted in time among them. Figure 3.3 shows the four symbols for this proposal. This modulation can be expressed as:

$$S_k = \sum_{i=0}^{1} (-1)^{i} \varpi (t - \tau_k \alpha_i) \tag{3.12}$$

α can be $\alpha_0 = 0$ or $\alpha_1 = 1$ and S_k is the transmitted signal, ω is Gaussian pulse shape, and τ_k is the delay parameter.

In a duty cycle, the receiver initializes opening a positive window that is exclusive only for the first positive pulse; it is to say that the next positive pulses are discarded by the receiver. The positive window is closed when the first positive Gaussian pulse is detected and a negative window that is exclusive only for the first negative pulse is opened. When the first negative Gaussian pulse is detected, immediately, the negative window is closed and the receiver will not process any pulses until a TDX time (determined by the designer) has elapsed. TDX is the time, when other positive window is opened and a new cycle begins. Figure 3.4 shows the general concept of how this process works, where the control windows will be determined by the signal.

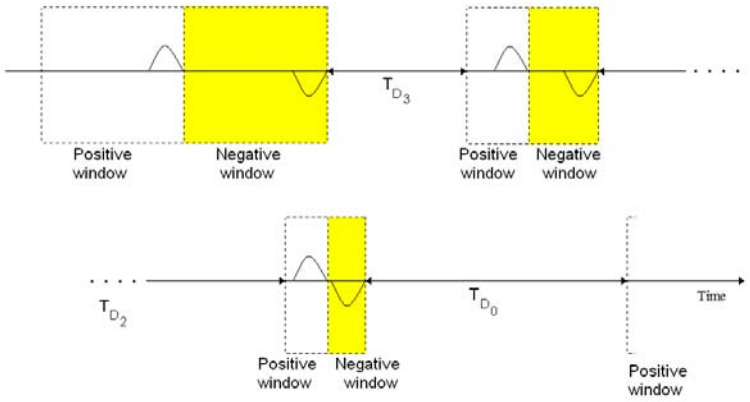

Figure 3.4 Synchronization process by the transmitted signal.

The sequence signal (positive and negative) allows that the receiver controls the reception and at the same time allows auto synchronization without the need of an internal clock. On other hand, the clock difference between the transmitter and the

receiver does not need to be either estimated or compensated continuously because the receiver knows when a duty cycle is initiated and finalized due to the order in which the pulses arrive. The synchronization and estimation of the bit is carried out in digital domain, therefore, the Gaussian pulses are represented by digital pulses. In this case, D1 represents the conversion of the positive pulse and D2 represents the conversion of the negative pulse, as shown in figure 3.5.

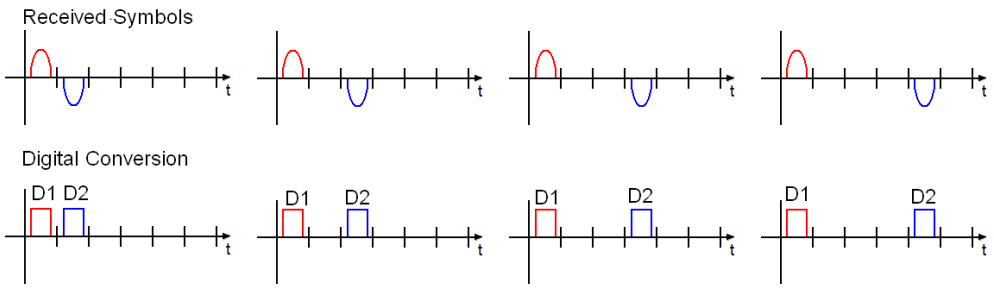

Figure 3.5 Conversion of the analog to digital pulses.

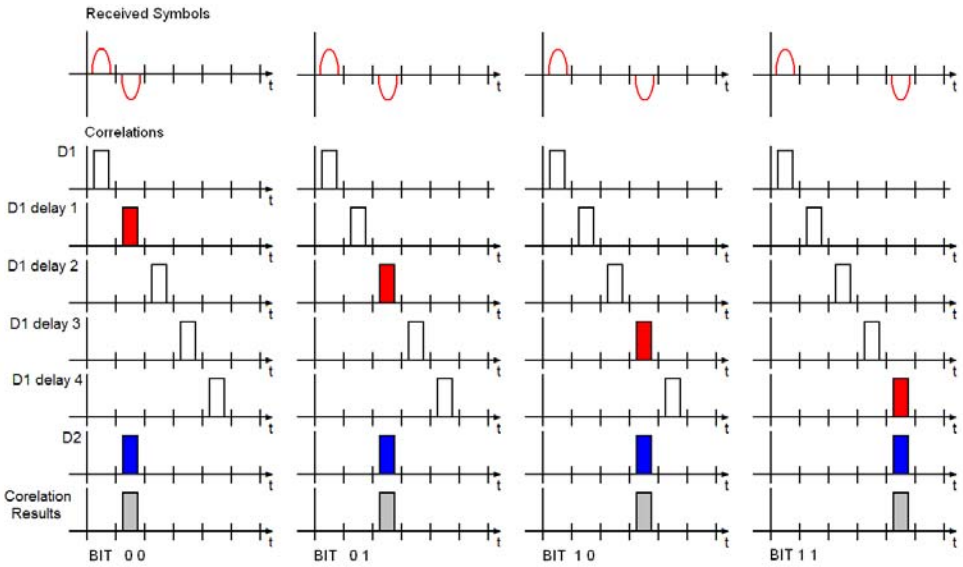

Figure 3.6 Four possible correlation points.

The bit estimation is determined by the correlation in time between negative and positive Gaussian pulses as is shown in the figure 3.6, where it can see that the correlation process is carried out when the D1 and D2 are present at the same time;

therefore, D1 is delayed to align in time with respect to D2 and achieve the correlation. There are four points to estimate the correlations and depending on the symbol transmitted a 00, 01, 10 or 11 will be detected.

The bits estimation process will be affected by intrinsic noise present in all the communication systems. It is important to know how the noise affects in the detection probability of this communication system. In practice, the noise will result in performance degradation in terms of SNR and BER, and in this thesis, it will be illustrated by numerical result in the next chapter.

In principle, this modulation scheme by simplicity can be seen as a binary system represented by:

$$s_0(t) = A\varpi_0(t) \tag{3.13}$$

and

$$s_1(t) = A\varpi_1(t) \tag{3.14}$$

Where ω_0 is a positive Gaussian pulse and ω_1 is a negative Gaussian pulse. Here, ω_0 and ω_1 are finite energy [80], time limited signal of duration *T*. When a pulse ω_i is transmitted, the received signal is:

$$s_i = \varpi_i(t) * h(t) + n(t) \tag{3.15}$$

where *i=0* or 1, *h(t)* is the impulse response of the channel and *n(t)* is the noise added to the transmitted signal. *n(t)* is an additive Gaussian noise (AGN) channel, not necessarily white. Figure 3.7 presents a general binary base band system model for the physics based signal.

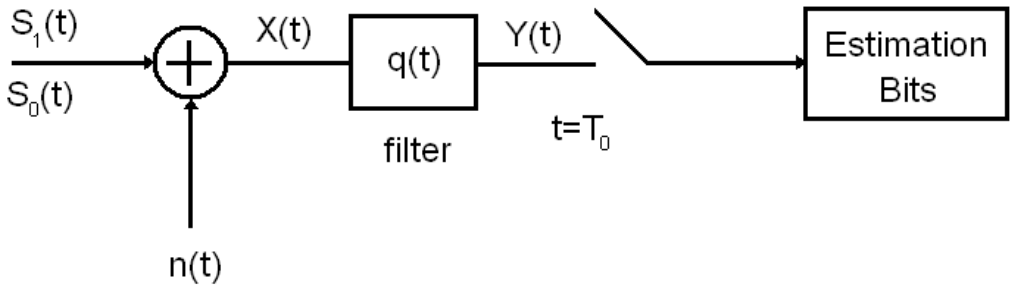

Figure 3.7 General model for binary base band data transmission.

The channel noise is stationary with zero mean and is independent of the receiver input. The filter *q(t)* is not necessarily matched to the signal $s_i(t)$. Following the steps of [81, 82], the probability of error can be obtained. The probability of error when a positive or negative Gaussian pulse sent is respectively given by:

$$P_{e,0} = q\left(\left[\mu_0(T_0) - \gamma\right]/\sigma\right) \tag{3.16}$$

and

$$P_{e,1} = q\left(\left[\gamma - \mu_0(T_0)\right]/\sigma\right) \tag{3.17}$$

where

$$\mu_i(t) = s_i(t) * q(t),\ i = 0, 1, \tag{3.18}$$

and

$$\sigma^2 = \left(q(t) * q(-t) * R_X(t)\right)|_{t=0} \tag{3.19}$$

Q(x) is defined as:

$$Q(x) = \int_{x}^{\infty} \frac{1}{\sqrt{2\pi}} \exp\left(-y^2/2\right) dy \tag{3.20}$$

$R_X(t)$ is the autocorrelation of the AGN *n(t)*. For AWGN:

$$\sigma^2 = \frac{1}{2} N_0 \int_{-\infty}^{\infty} q^2(t) dt \tag{3.21}$$

where $1/2N_0$ is the spectral density for the white noise process *n(t)*. In the equations 3.17 and 3.18, γ is arbitrary. When the Bayes decision criterion is used, the threshold is given by [81]:

$$\overline{\gamma} = \frac{\mu_0(T_0) + \mu_1(T_0)}{2} + \frac{\sigma^2 \ln\left(\pi_1/\pi_0\right)}{\mu_0(T_0) - \mu_1(T_1)} \tag{3.22}$$

where π_0 and π_1 are the probabilities that a positive or a negative pulse is sent, respectively. The average probability is given by:

$$\begin{aligned} \overline{P}_e &= \pi_0 P_{e,0}(\overline{\gamma}) + \pi_1 P_{e,1}(\overline{\gamma}) \\ &= \pi_0 Q\left[SNR - \left(2SNR\right)^{-1} \ln\left(\pi_1/\pi_0\right)\right] + \pi_1 Q\left[SNR + \left(2SNR\right)^{-1} \ln\left(\pi_1/\pi_0\right)\right] \end{aligned} \tag{3.23}$$

where SNR is the signal to noise ratio at the input to the threshold device given by:

$$SNR = \frac{\mu_0\left(T_0\right) - \mu_1(T_0)}{2} \tag{3.24}$$

When a positive or negative Gaussian pulse is sent with equal probability, then $\pi_0=\pi_1=1/2$. As a result, the average probability is reduced to:

$$\overline{P_e} = Q(SNR) \tag{3.25}$$

Now it is possible to optimize *q(t)* in terms of SNR defined by:

$$SNR = \frac{\left(s_0(t) * q(t)\right)|_{t=T_0} - \left(s_1(t) * q(t)\right)|_{t=T_0}}{\sqrt{2N_0}\,\|q\|} \tag{3.26}$$

where:

$$\|q\| = \left(\int_{-\infty}^{\infty} q^2(t)\,dt \right)^{1/2} \tag{3.27}$$

$\|q\|$ is the norm of q(t). Equations (3.24) and (3.26) are valid when the filter impulse response, *q(t)*, is arbitrary. There is a relation between the SNR and the average error probability determined in the equation 3.24, where, depending on the SNR the system will detect or not the correct symbol. There are four possibilities where the process detection can be raised:

When the reception is optimal:

$$y = \int \omega^2(t)_{p,n}\,dt \tag{3.28}$$

When the positive pulse is detected, but the negative sample is noise:

$$y = \int \omega_p(t)\,n_2(t)dt \tag{3.29}$$

When the negative pulse is detected, but the positive sample is noise:

$$y = \int n_1(t)\omega_n(t)\,dt \tag{3.30}$$

When the positive and negative samples are noise:

$$y = \int n_1(t)n_2(t)dt \tag{3.31}$$

Other possible considerations that will depend on internal troubles at the receiver or transmitter for example when the negative pulse is not detected:

$$y = \int \omega_p(t)dt = 0 \tag{3.32}$$

When the positive pulse is not detected:

$$y = \int \omega_n(t)\,dt = 0 \tag{3.33}$$

The noise is an important component that affects the transceiver performance, but it is not unique, UWB antennas usually distort the transmitted pulse. The transmitter and receiver antennas as a whole can be modelled as a linear filter with impulse response $h_a(t)$ and their impact can be absorbed in the new transceiver. This thesis is not focused in this kind of distortion; hence the antenna's impact is ignored.

3.3 Demodulator Design

The proposed modulation scheme is implemented in a non coherent or light coherent receiver design. Therefore, the receiver design does not need to generate either a template to detect the pulses or a clock signal related to transmission. In other words, the synchronization, channel estimation and pulse shape estimation are not as stringent as in the case of a fully coherent receiver. The Antenna, the Band Pass Filter

(BPF,) and the Low Noise Amplifier (LNA) are not part of the receiver design. The processing begins when the received signal has passed through the previous stages. A block diagram of the proposed receiver is presented in figure 3.8.

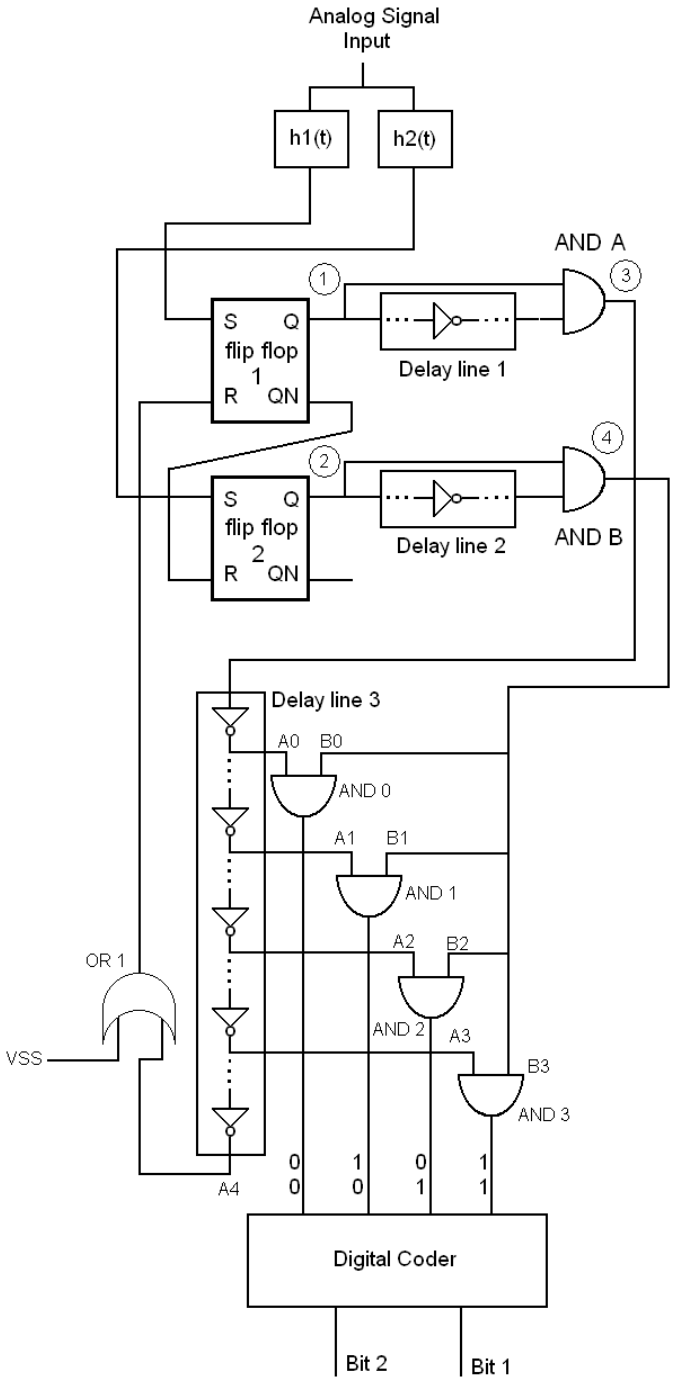

Figure 3.8 Block diagram for the proposed modulator.

Figure 3.8 shows that the transmitted signal is received by the blocks $h_1(t)$ and $h_2(t)$, where, the block $h_1(t)$ only processes positive Gaussian pulses and the block $h_2(t)$ is exclusive for negative Gaussian pulses. Each block is implemented by two differential amplifier stages connected in a cascade as shown in figure 3.9.

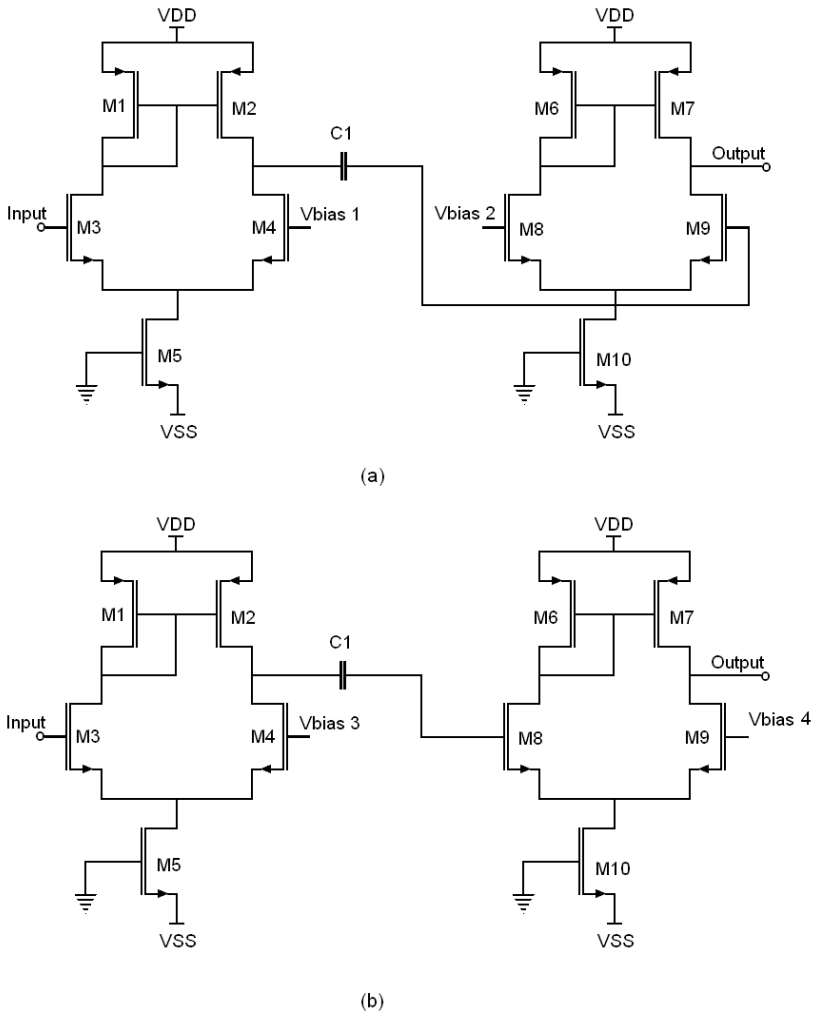

Figure 3.9 Pulse detector circuits (a) $h_1(t)$ positive and (b) $h_2(t)$negative.

In the $h_1(t)$ circuit, the first stage pre-amplifies the positive Gaussian pulses and attenuates the pulses with opposite polarity. The second stage amplifies the positive pulses and almost eliminates the negative pulses. On the other hand, a similar operation is achieved in $h_2(t)$ for the negative pulses. The V_{bias} (1, 2, 3 and 4) are

determined by the design requirements. The figure 3.10 a and b show this process with $h_1(t)$ and $h_2(t)$ respectively. M5 and M10 are working in the liner region thus the current control is determined only by its gate voltage or V_{bias} the capacitance C is used to eliminate the amount of DC at the output of the amplifier.

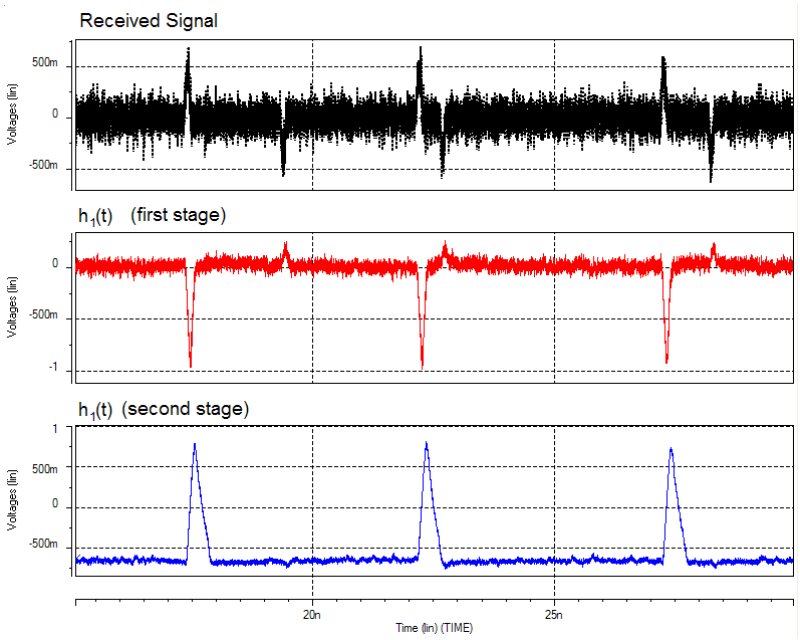

(a)

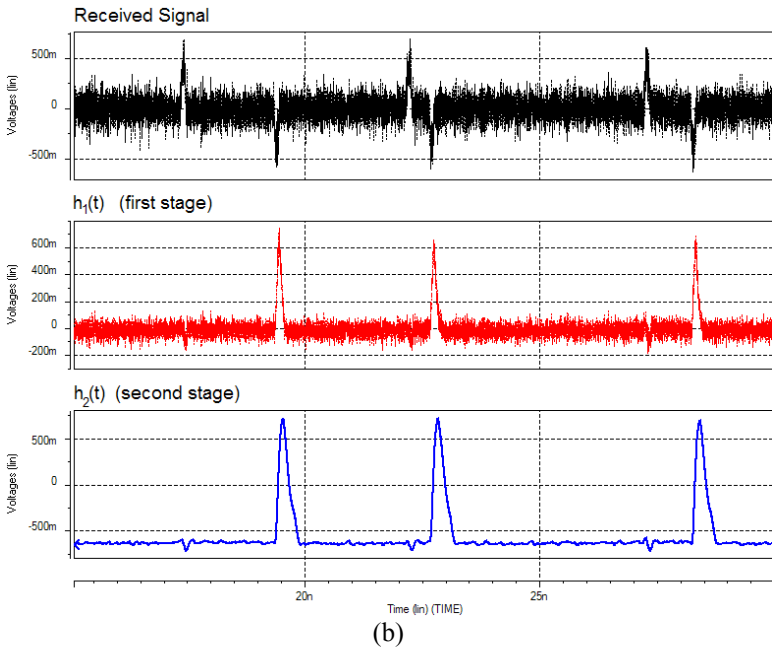

(b)

Figure 3.10 Impulse response of (a) $h_1(t)$ and (b) $h_2(t)$ with AWGN.

The amplifier outputs are connected to a digital buffer that converts the analog pulses to digital. The buffers are simply two NOT gate connected in cascade that convert the Gaussian pulses to digital pulses as is showed in the figure 3.11.

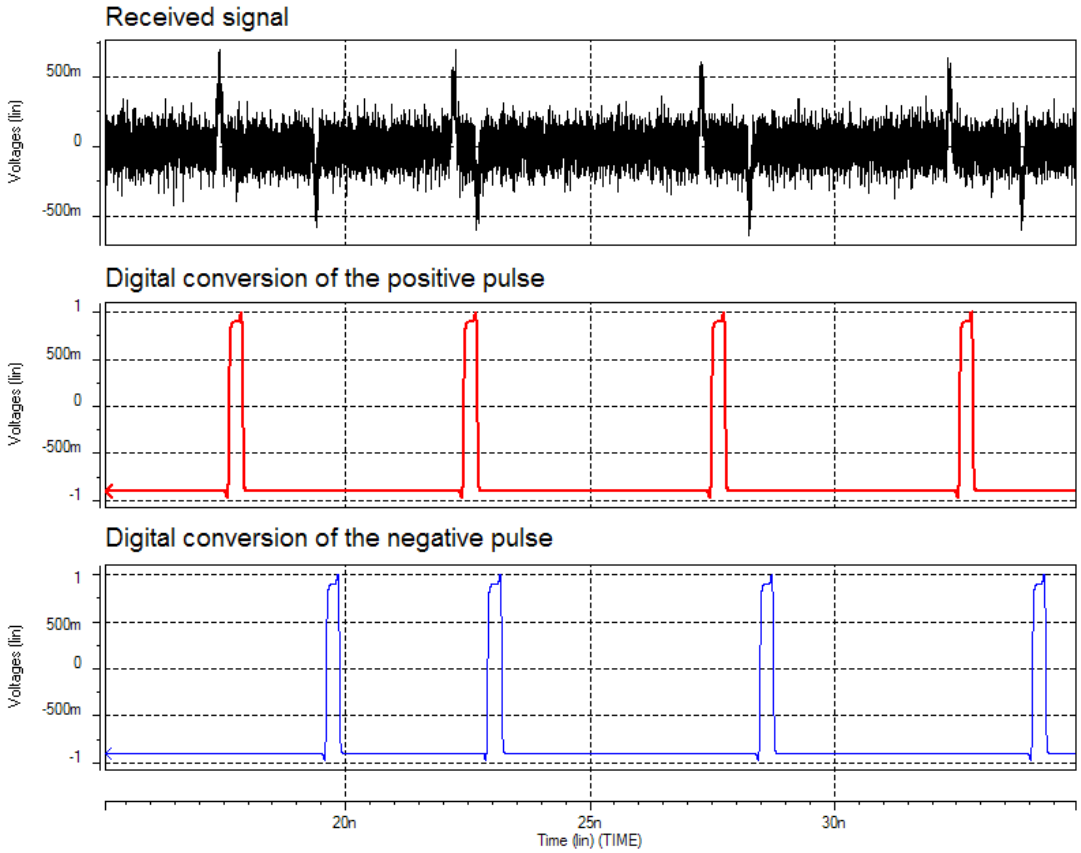

Figure 3.11 Analog to digital representation pulses.

The presence of the digital pulses is detected by theirs corresponding flip flop and as is shown in the figure 3.8.

In a duty cycle, the detection pulses can be divided in two steps: 1) the first positive pulse detection by the flip-flop 1 and 2) first negative pulse detection by the flip-flop 2. In the initial conditions, the Q1 output will be in high level until that the positive pulse arrives at the flip-flop 1(1 step). Therefore, QN1 output will change from high level to low level. This low level enables the flip-flop 2 so that the negative pulse is

detected. When such pulse arrives at the flip-flop 2, the Q2 output change from low to high level and the detection process is ended (2 step).In this step booth flip-flops´s are disable, and so that, other detection cycle begins, booths the flip-flop´s must be RESET. The first flip flop that is RESET is the 1, it is enabling until the duty cycle has been finished. The duty cycle time will be determined by the design requirements. The flip flop 2 will keep enabled until the first positive pulse has been received.

The pulses at Q1 and Q2 outputs only give the time information in which the pulses were detected, nevertheless, it very import to know the elapsed time between two pulses, because it will give the transmitted bit information. In order to obtain this information, the widths of such pulses are reduced to more narrow pulses widths and delayed in time.

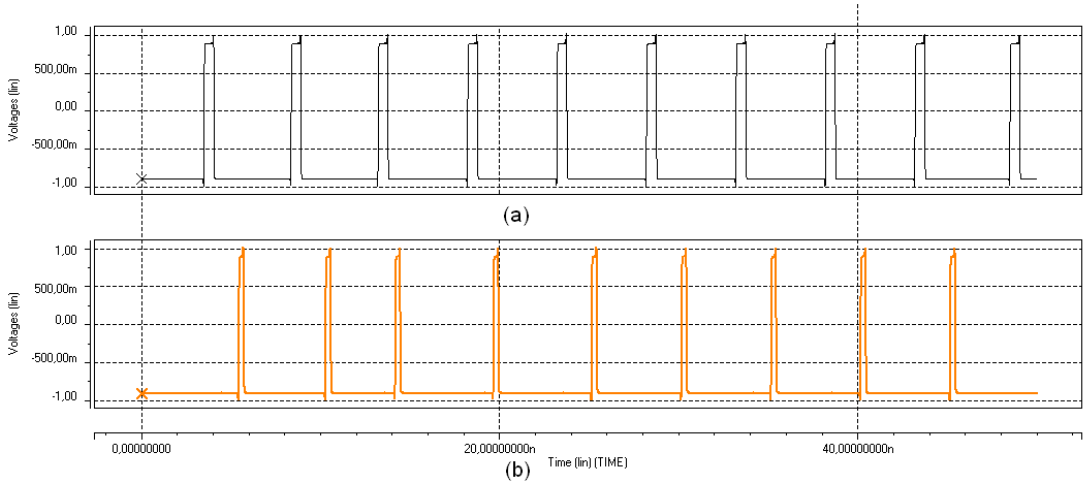

Figure 3.12 PD1 and PD2 simulation result from the circuit illustrated in figure 3.8.

To implement this process, two inverter lines are connected between Q1 and one ANDA gate input, and Q2 and one ANDB gate input respectively, the other AND inputs are connected to Q1 and Q2 respectively as shown in figure 3.8. The AND gate outputs will be normally in a low level until that the AND gate inputs are in high level at the same time. The pulse width will be determined by the design requirements and the variation process compensation as will be able in the chapter 4. The pulses

from AND A gate output are called PD1 as shown in figure 3.12a and the pulses from AND B gate output are called PD2 is shown in the figure 3.12b. In fact, PD1 and PD2 are the digital representation of the Gaussian pulses negative and positive. In a duty cycle, the correlation process is carried out when the PD1 and PD2 are presented at the same time, so that, PD1 needs to be delayed in time and to keep until PD2 is detected. PD1 is delayed through the delay line 3 shown in figure 3.8. The demodulator has been designed for to achieve four output correlations points that correspond to A0, A1, A2, and A3 delay line 3 outputs (in figure 3.8). Where each point is connected to AND gate input and the rest AND gate inputs are connected to Q2. When A0, A1, A2 or A3 output is aligned in time with respect to PD2, then one word will be detected. For example, if the PD2 is aligned in time with respect to A1 the symbol detected will be 01 and only the AND 1 output will be in high level while the rest of the AND gates will be in low level in other words:

$$y_0 = \int_0^{t1} A0(t) * PD2(t)\,dt = 0 \qquad PD2(t)\big|_0^{t_1} = 0 \tag{3.34}$$

$$y_1 = \int_{t1}^{t2} A1(t) * PD2(t)\,dt = 1 \qquad PD2(t)\big|_{t_1}^{t_2} = 1 \tag{3.35}$$

$$y_2 = \int_{t2}^{t3} A2(t) * PD2(t)\,dt = 0 \qquad PD2(t)\big|_{t_2}^{t_3} = 0 \tag{3.36}$$

$$y_3 = \int_{t3}^{t4} A3(t) * PD2(t)\,dt = 0 \qquad PD2(t)\big|_{t_3}^{t_4} = 0 \tag{3.37}$$

If PD2 corresponds in time with A2, then the symbol detected will correspond to word 10 and the rest of the AND gates will be in low level as is shown in the next expression:

$$y_0 = \int_0^{t1} A0(t) * PD2(t)\,dt = 0 \qquad PD2(t)\big|_0^{t_1} = 0 \tag{3.38}$$

$$y_1 = \int_{t1}^{t2} A1(t) * PD2(t)\,dt = 0 \qquad PD2(t)\Big|_{t_1}^{t_2} = 0 \tag{3.39}$$

$$y_2 = \int_{t2}^{t3} A2(t) * PD2(t)\,dt = 1 \qquad PD2(t)\Big|_{t_2}^{t_3} = 1 \tag{3.40}$$

$$y_3 = \int_{t3}^{t4} A3(t) * PD2(t)\,dt = 0 \qquad PD2(t)\Big|_{t_3}^{t_4} = 0 \tag{3.41}$$

Figure 3.13 shows the correlation process for these two examples

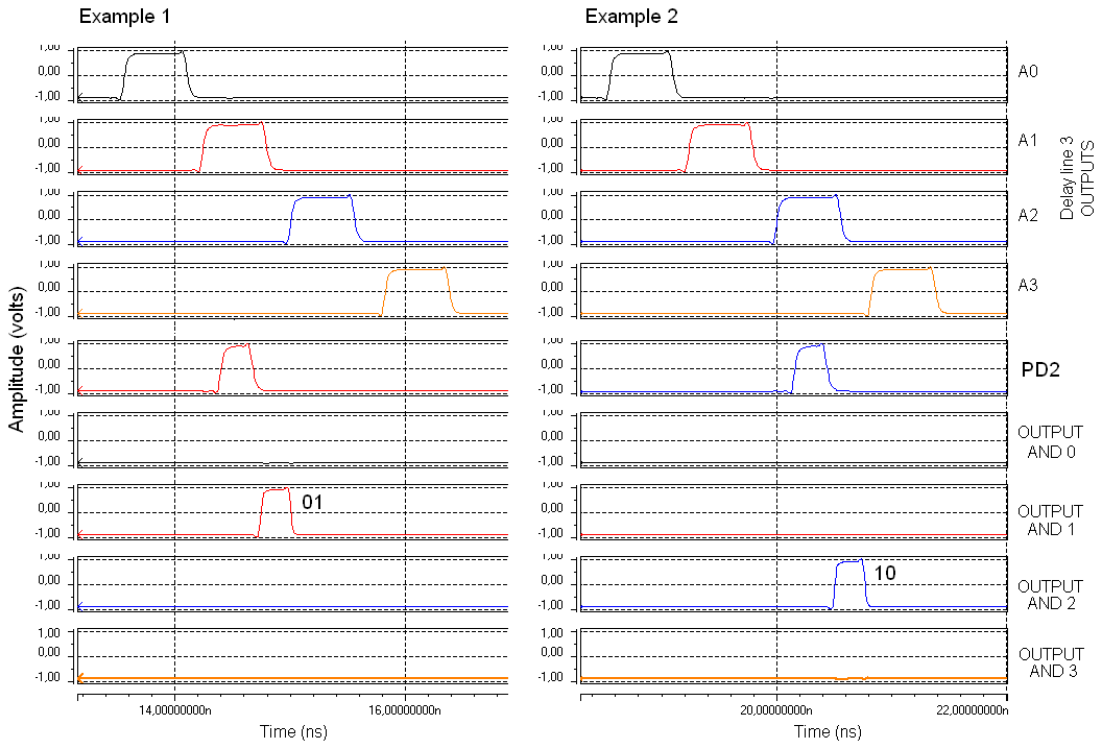

Figure 3.13 Correlation between the digital outputs of delay line 3 and PD2 simulations.

In summary, the correlation process is determined when a pair of pulses is aligned in time; therefore, a symbol is interpreted as a word (00, 01, 10 or 11) where the widths PD1 and PD2 are determined to compensate the process variation. In other words, when the correlation process is achieved the detection process is ended in a duty

cycle. A new duty cycle will be indicated by the output A4; the time between duty cycle and duty cycle will be determined by the design requirements.

Up to here, the symbol detection process step is concluded, however, the codification stage in binary or other codes are the stage that can be resolved to different way. This thesis a possible manner by which the codification process can be implemented and shows that the demodulator can be easily adapted for codify digital processing is presented.

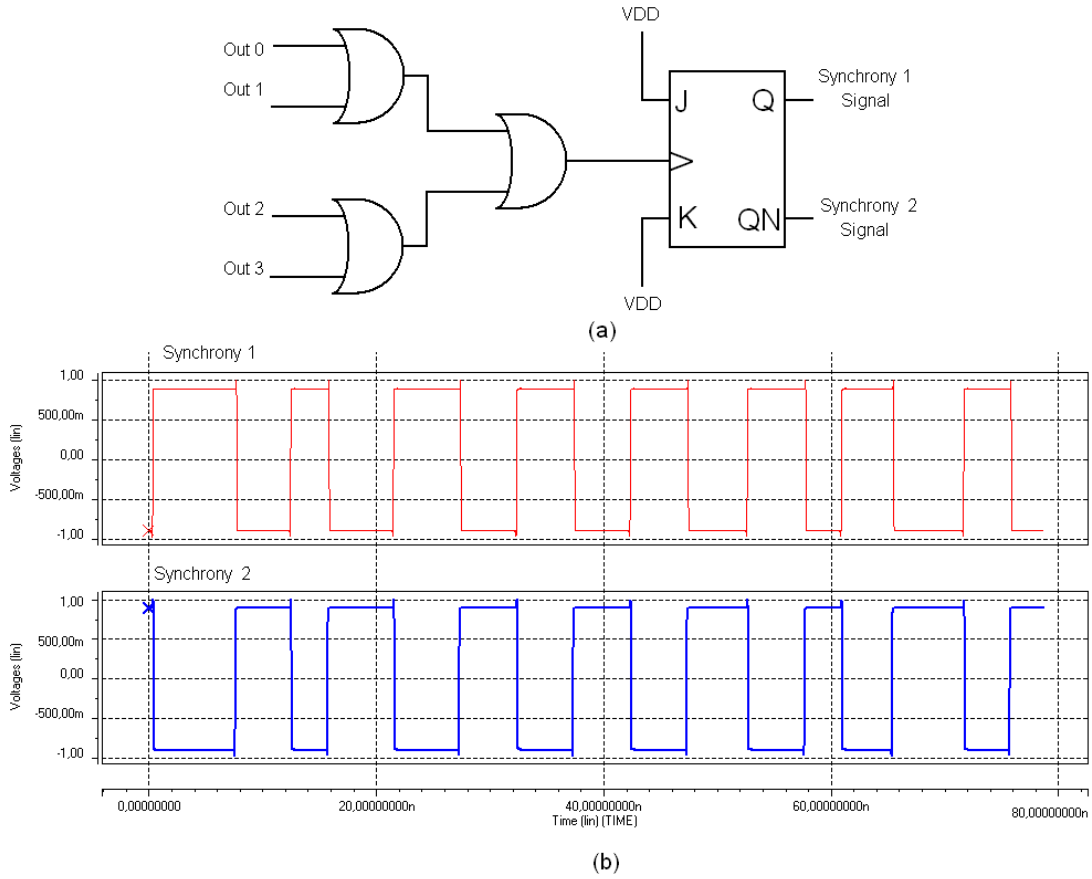

Figure 3.14 Synchrony circuit generator and simulation result.

When a symbol is detected, one output of the AND gates (AND 0, AND 1, AND2, or AND 3) is activated. The outputs are converted to only one output that is connected to a flip-flop JK that has a counter configuration as shown in the figure 3.14a. The circuit shown in the figure 3.14a indicates to the system when a symbol has been

detected and that it needs to be codified in this case to binary code. Figure 3.14b shows a change in the levels in Q and QN, which will be called synchrony 1 and synchrony 2.

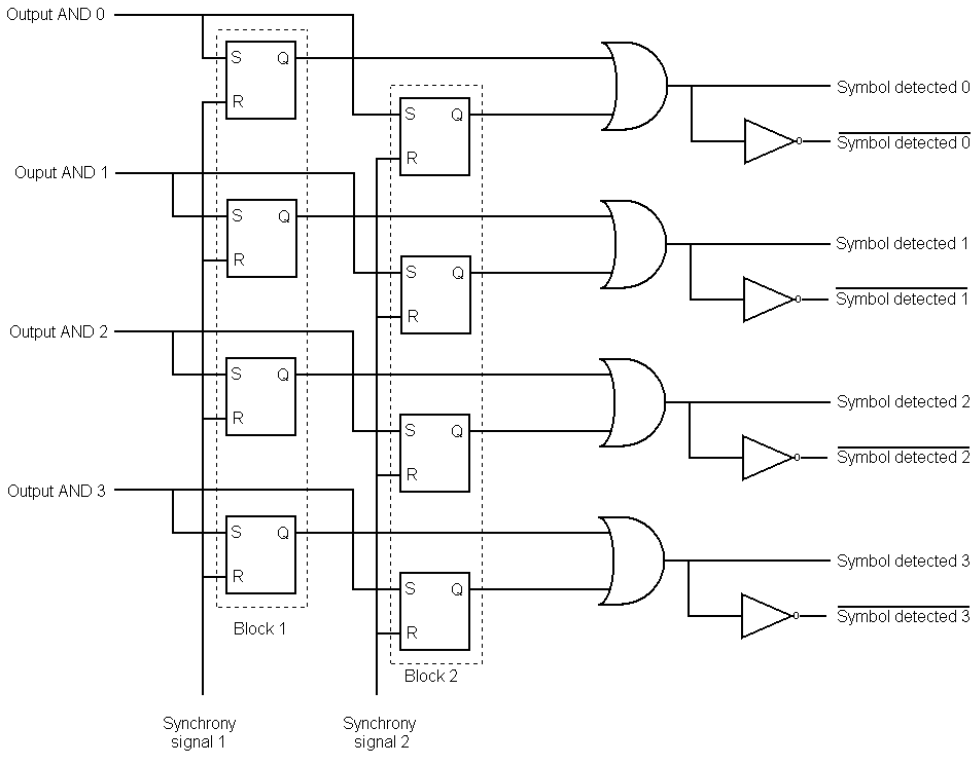

(a)

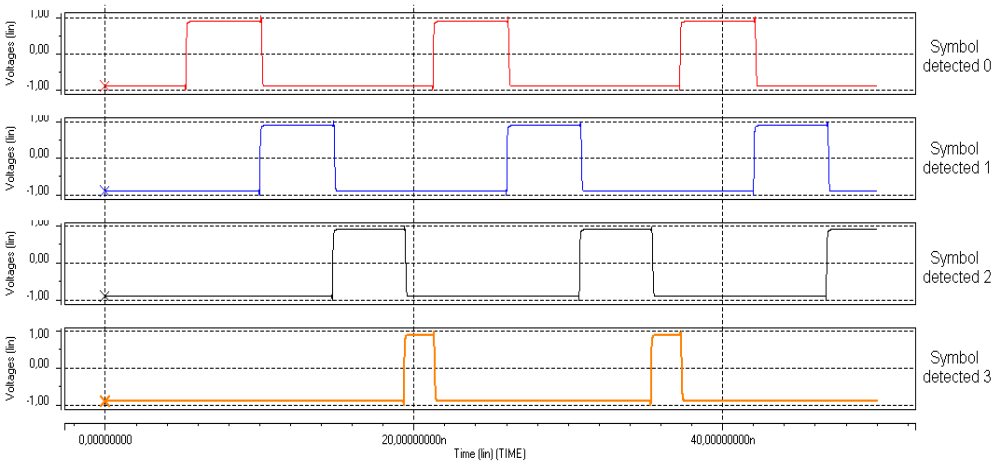

(b)

Figure 3.15 (a) Two memory banks and (b) simulation results.

On the other hand, the outputs A0, A1, A2 and A3 are connected to two memory banks, as shown in the figure 3.15a. The synchrony signals from the circuit shown in figure 3.14 have the access control of memory bank. When synchrony signal 1 is in low level, memory bank 1 will be able to store the pulse A0, A1, A2, or A3, and memory bank 2 will be inactive because it will be in a high level. When the synchrony signals change to logic levels, the bank 1 will be disabled and 2 will be enabled and store the pulse from A0, A1, A2 or A3. For example, in a duty cycle, the memory bank 1 stores a pulse (read mode), whereas the bank 2 only presents the pulse already stored (write mode), this action allows the system to codify a pulse whereas other pulse is read at the same time as shown in figure 3.15b.

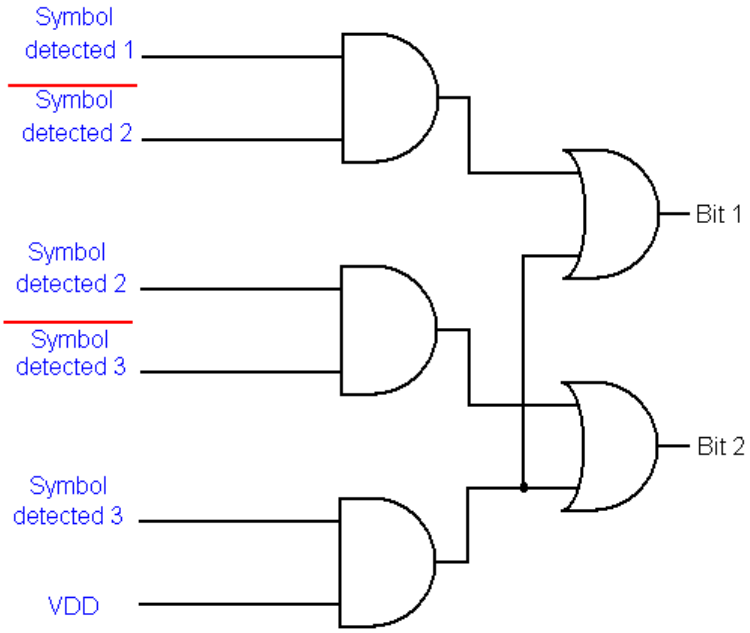

Figure 3.16 Binary Coder.

The OR gate outputs are connected to a binary coder as shown in figure 3.16. The figure 3.17 shows the difference in width between the pulses transmitted and the pulses received due to the way in which the data have been modulated. This difference can be resolved by increasing two stages of memory

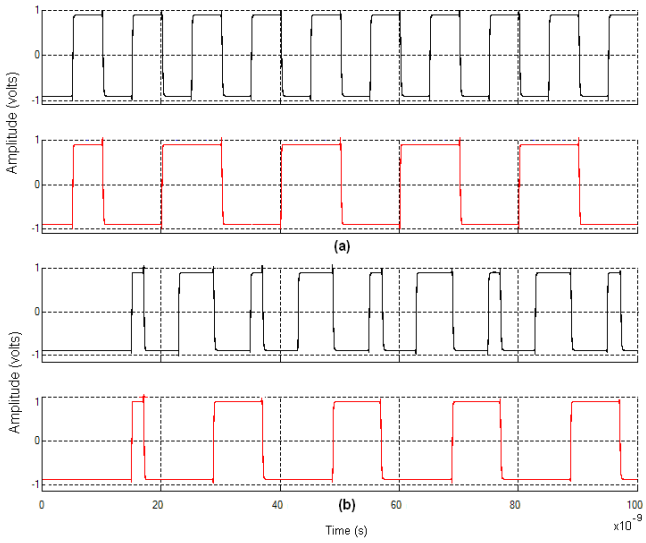

Figure 3.17 Comparison between the (a) transmitted and (b) received bits (simulation results).

Here the modulator system has been designed and finished, but some aspects in the design must be contemplated for to achieve a good performance in the detection process. Thus, it is important to consider that, in the design of circuits $h_1(t)$ and $h_2(t)$, the outputs must as close as possible to V_{DD} and $V_{SS,}$ respectively, without the transistors leaving the saturation region. Circuits $h_1(t)$ and $h_2(t)$ perform as a comparator. V_{bias} in both cases allow that the differential amplifiers not be in current balance. Therefore, their output voltage will be in V_{DD} or V_{SS} and will depend on the V_{bias} voltage applied. Another consideration is that the inputs will be connected to a LNA, and because of that, the circuits $h_1(t)$ and $h_2(t)$ will represent a load that could be not driven if the design is not correct.

On other side, the positive edge flip-flop must have a RESET circuit that can be used by the users. Therefore, one of the inputs of OR 1 gate of figure 3.8 is connected to a RESET circuit that can be controlled by the users. In general, the digital circuits can be designed in minimal dimensions, but, it is very important to consider the load that is connected to digital circuit. The key points in the system that have to drive a relevant load are the correlation points, and the synchrony generator. They must be

designed with a fan out that can drive the load represented by the converter from 4 outputs to 1 with the delay line data and the memory bank respectively.

3.4 Modulator Design

In principle, the transmitter is very simple and consists of a pulse generator and a digital timing circuit that controls the timing transmission. This section is focused on a Gaussian pulse generator and the modulator or timing control that modulate the Gaussian pulses according to scheme modulation proposed.

Mathematically, a Gaussian function is describing as [4]:

$$y = e^{-x^2} \tag{3.42}$$

The circuit proposal that represent a Gaussian function approximation is shown in the figure 3.18 and its equivalent circuit is depicted in figure 3.19. The generator architecture essentially consists of a shaped Gaussian pulses stage, and a power amplifier.

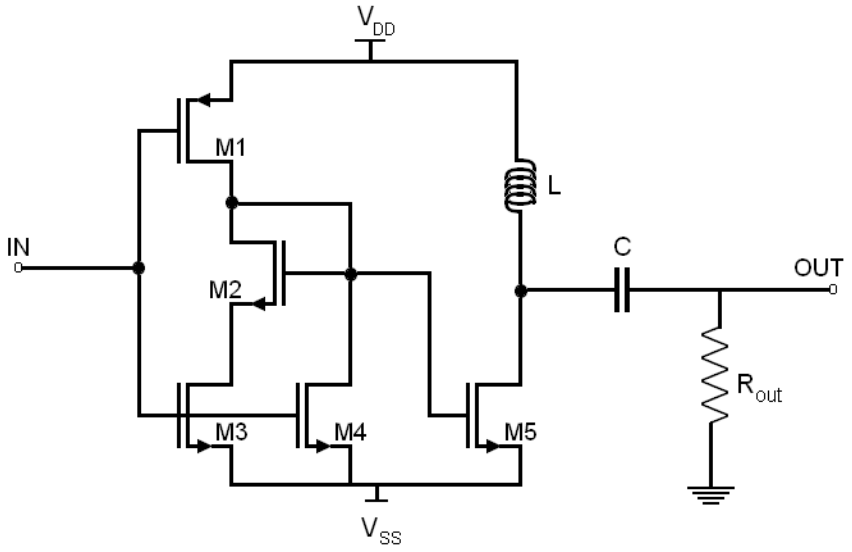

Figure 3.18 Gaussian pulse generator schematic.

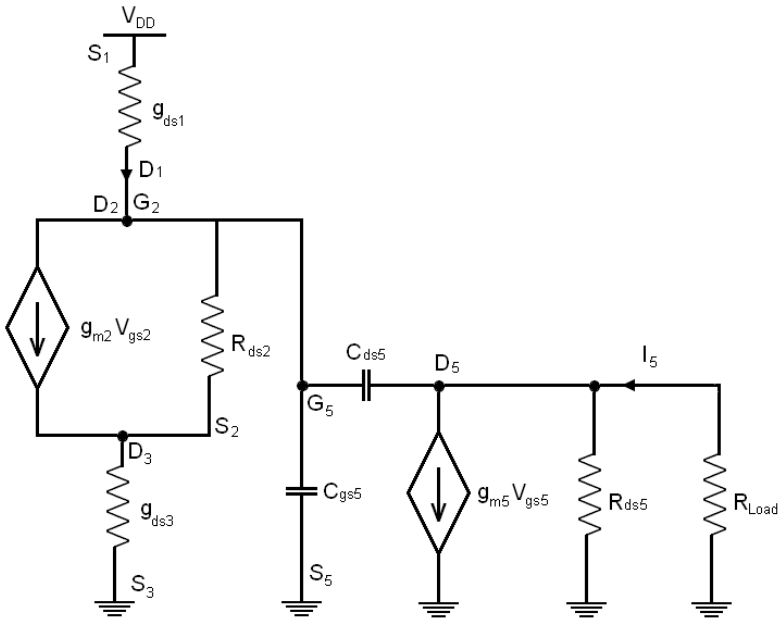

Figure 3.19 Equivalent circuit of the Gaussian pulse generator

Typically $r_{ds2} >> 1/g_{m2}$, therefore the equivalent impedance for M2 transistor is simply $1/g_{m2}$ [9]. The C_{ds5} effect can be divided in two part using Miller theorem. The output resistance $R_{Load} << R_{ds}$ therefore the equivalent resistance is $R_{Load.}$ Thus, the equivalent circuit simplify can be represented as shown in figure 3.20.

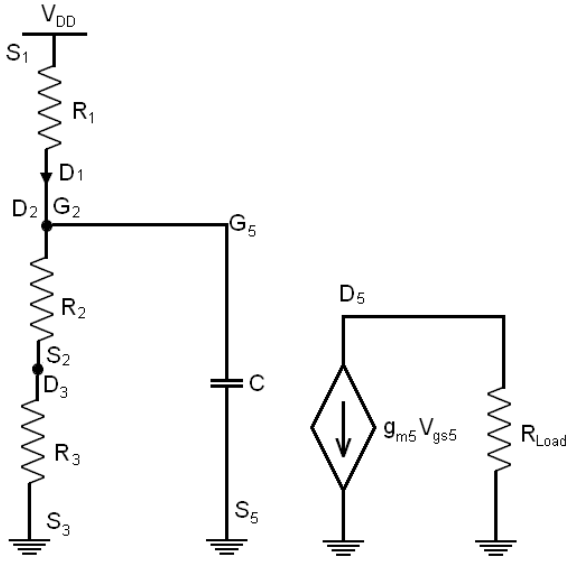

Figure 3.20 Simplify equivalent circuit.

The transfer function of the equivalent circuit is as:

$$\frac{V_{gs}-V_{DD}}{R_1}+\frac{V_{gs}}{R_2+R_3}+SCV_{gs}=0 \tag{3.43}$$

$$V_{gs}\left(\frac{1}{R_1}+\frac{1}{R_2+R_3}+SC\right)=\frac{V_{DD}}{R_1}$$

$$V_{gs}\left(\frac{R_1+R_2+R_3}{CR_1(R_2+R_3)}+S\right)=\frac{V_{DD}}{CR_1}$$

$$\frac{V_{gs}}{V_{DD}}=\frac{1}{\frac{1}{C}\frac{R_1+R_2+R_3}{R_1(R_2+R_3)}+S}\left(\frac{1}{CR}\right) \tag{3.44}$$

The inverse Laplace transform of the equation 3.44

$$L^{-1}\left(\frac{1}{s+z}\right)=e^{zt}$$

$$V_{gs}=V_{DD}\frac{1}{CR_1}e^{-\frac{R_1+R_2+R_3}{R_1(R_2+R_3)}t} \tag{3.45}$$

$$Vout=-g_{m5}\left(V_{DD}\frac{1}{CR_1}e^{-\frac{R_1+R_2+R_3}{R_1(R_2+R_3)}t}\right)R_{Load} \tag{3.46}$$

The circuit operation can be seen as RC circuit where the capacitance is charged through R1 if a falling raising edge is presented, or discharged through R3 if it a raising edge is presented. In the raising edges, the transistor M1 changes from linear to cut region, and the transistor M3 changes from cut to linear region. In falling edge, M1 changes from cut to linear region and M3 from linear to cut region. However, in the transition, from low to high level or vice verse, there is an interval called “active

region", where the transistors M1 and M3 allow that the transistor M2 works in saturation region and that the Gaussian pulses are generated as shown in figure 3.21.

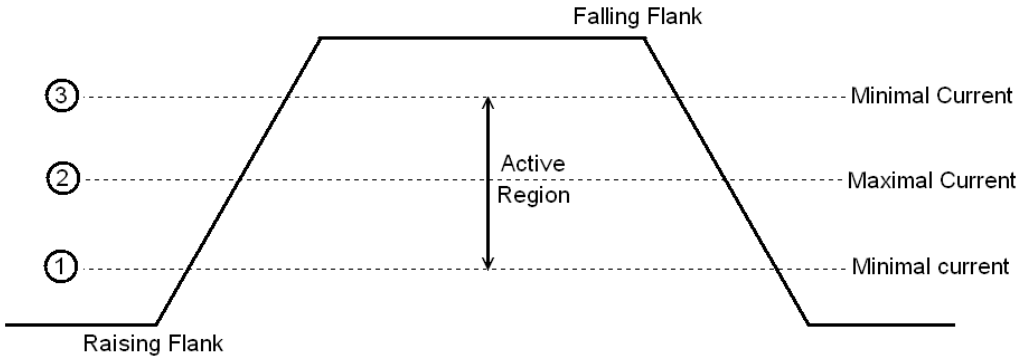

Figure 3.21 Operation points in the Gaussian pulses generator.

In the transition can be divided in two cases, a) between 1 and 2 point; and b) between 2 and 3 point.

a) In the case "a" the M1 is in the lineal region, M2 and M3 are in the saturation region the transfer function is as:

$$V_{out1} = -g_{m5}\left(V_{DD}\frac{1}{CR_1} e^{-\frac{W_1 K_p}{CR_1}t} e^{-\frac{K_n W_3}{2CL_3}\left(V_{gs3}-V_{TN}\right)^2 t} \right) R_{Load} \tag{3.47}$$

a) In the case "b" the M1 and M2 are in the saturation region, M3 is in the linear region, the transfer function is as:

$$V_{out2} = -g_{m5}\left(V_{DD}\frac{1}{CR_1} e^{-\frac{gm_2}{C}t} e^{-\frac{\lambda_1 K_p W_1}{2CL_1}\left(V_{gs1}-V_{TP}\right)^2 t} \right) R_{Load} \tag{3.48}$$

The equation 3.46 and 3.47 are approximations to a Gaussian function and the booth adding is the total behavior of the Gaussian pulse generator circuit. The positive

Gaussian pulse is presented in a raising edge in the contrary case it is generated a negative Gaussian pulse. The pulse polarity is determined by the current flow at the generator output. The simulation results of the Gaussian pulses generators are showed in the figure 3.22.

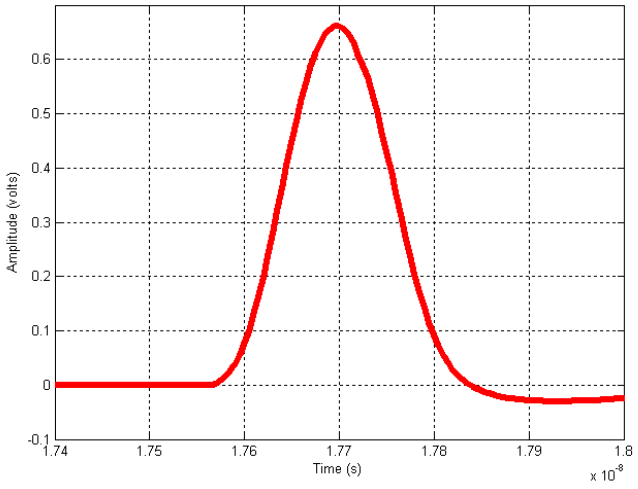

(a)

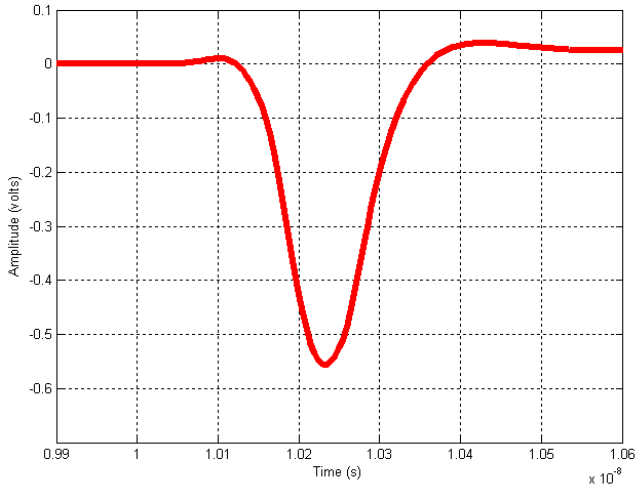

(b)

Figure 3.22 (a) Positive and (b) Negative Gaussian pulse simulation result.

When a high level is present at the generator input, a high impedance node is formed at the M5 gate; this reason by which the transistor M4 has been placed in the

Gaussian pulse generator. The transistor M4 performs as switch that avoids the high impedance node in the M5 gate and connects it directly to V_{SS}. By consequence the charge in the parasitic capacitance C_{gs5} is discharged quickly, such that the Gaussian pulses are narrowed. M4 is not presented in the analysis because when it changes from cut to saturation region the generator is totally turned off. In this case, there is a direct trajectory from V_{SS} at the M5 gate, thus the M5 is in the cut region it could not to amplify.

When a low level is presented at the input of the generator, the transistor M1 is in the active region. Therefore, a direct path from V_{DD} to M5 gate is formed because the drain of the transistor M1 is connected to the drain and gate of the transistor M2, and the M2 gate is connected directly to M5 gate. The V_{DD} voltage at the gate of the transistor M5 implies that it works in the saturation region and, Thus, other direct trajectory from V_{DD} to drain of V_{SS} is formed through L and V_{DS5}. This trajectory implies a static current consumption when the generator is inactive or low level. The proposal is to realize digital pulses with short duration at low level. The generated short pulses become the input signal of the Gaussian pulses generator.

There are different ways to get digital narrow pulses. In this project, this stage consist of an inverted delay line and a NOR block [58] [60]. The reference clock signal is sent to the inverted delay line circuit and its output signal is applied to the NOR gate along with the reference clock signal. Because a shifted delay is used to achieve a certain pulse width, the interpolation scheme is placed in series as delay block.

Figure 3.23a illustrates the digital pulse generator and can generate digital pulses as in the figure 3.23b or 3.23c; the difference is the NOT gate at the output. The short digital pulse (fig 3.23c) allows generating positive monocycle Gaussian pulses, as shown in figure 3.24, and reduces the static power consumption, as the digital pulse will be normally in a high logic level.

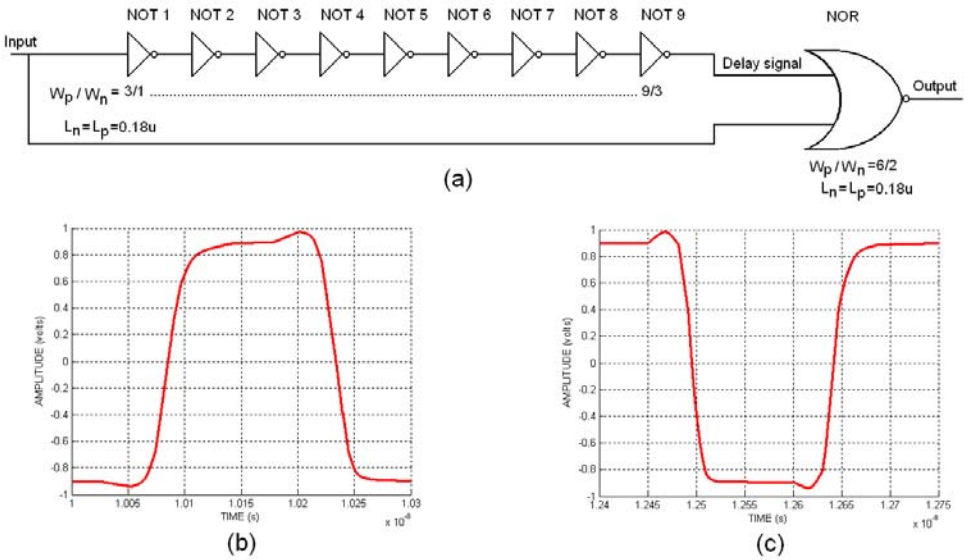

Figure 3.23 Block diagram of the digital pulse generator.

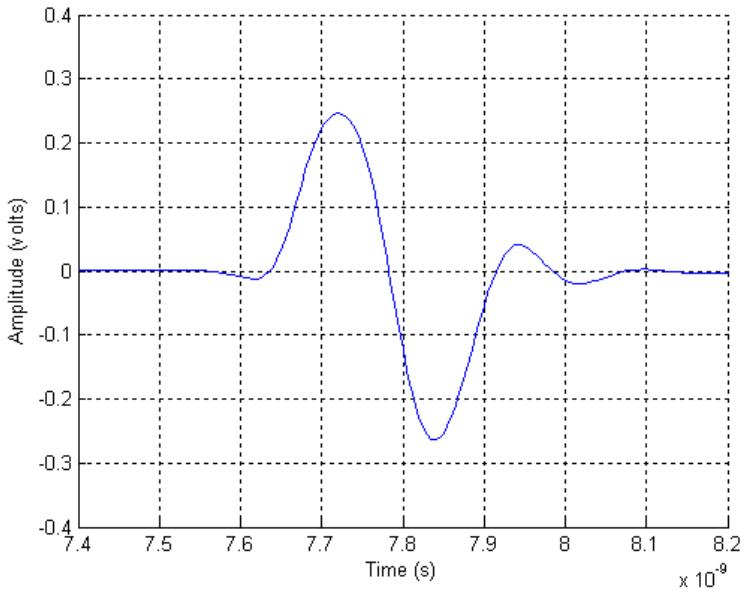

Figure 3.24 Positive monocycle Gaussian pulse simulation result.

The negative monocycle Gaussian pulse can not be generated by the circuit shown in the figure 3.18. Therefore another circuit is necessary generate it. The proposal is illustrated in the figure 3.25 and the simulation results are shown for the monocycle

Gaussian pulses in the figure 3.26. Tis circuit is the complement of the positive Gaussian pulse generator and both have the same operation characteristics.

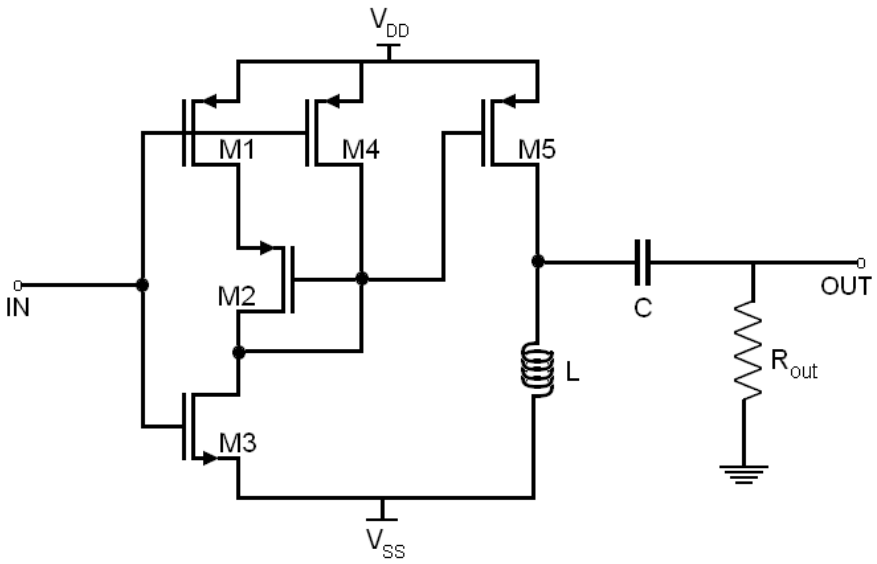

Figure 3.25 Gaussian pulses generator complement.

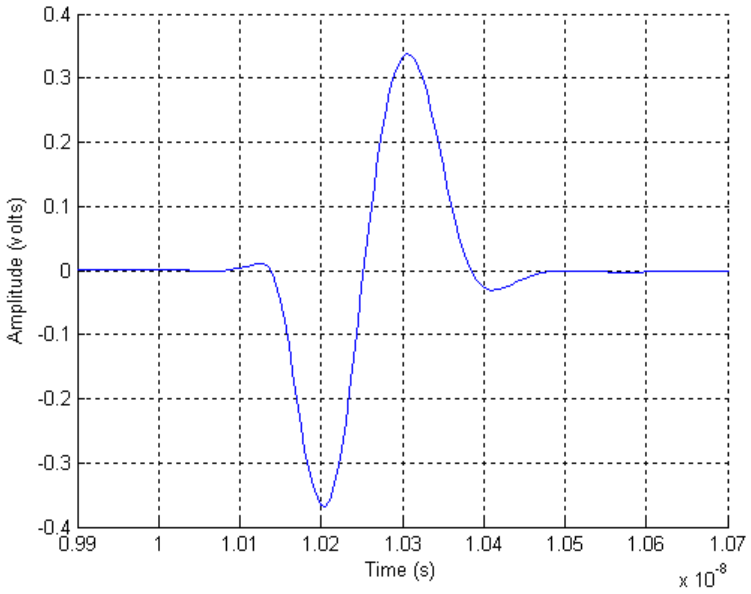

Figure 3.26 Negative monocycle Gaussian pulse post lay out simulation.

The pulse generator is an option with high potential applications and depending on the requirements of the design, can be used the monocycle generator or Gaussian

generator. However, this work focuses on low complexity. Therefore, the Gaussian pulses generator is the chosen option for the modulation proposal.

3.4.1 The Modulator or Timing Control.

As stated before, in the propose modulator the maximal size word in this case is two bits. The input data are received by a coder from two inputs to four outputs, where only one output will change of logic level depending on the information received at the coder inputs in a duty cycle. For example if the word 00 is received by the coder, then the output δ_0 that was in a low level will change to high level and the other outputs (δ_1, δ_2, and δ_3) will keep in low level. Figure 3.27 shows a block diagram of the proposed modulator.

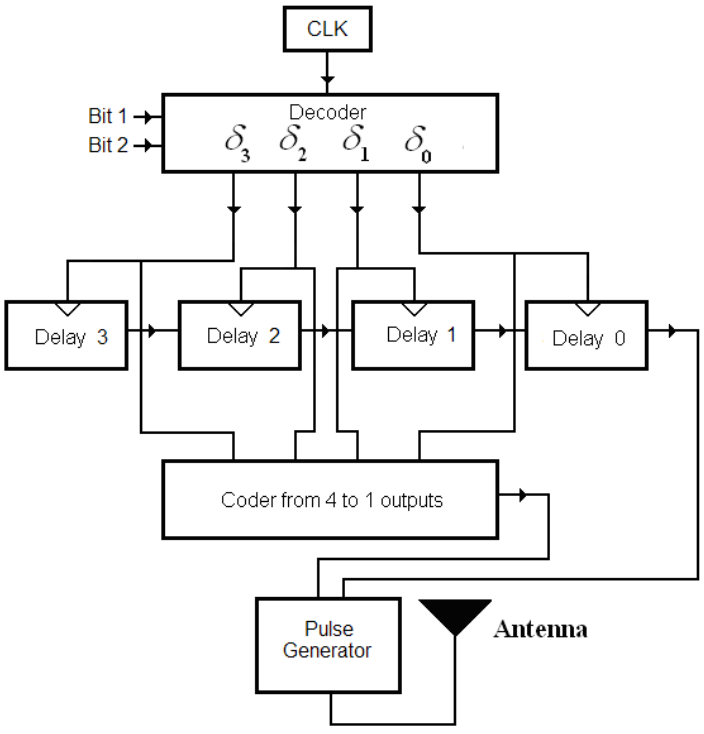

Figure 3.27 Block diagram of a UWB transmitter.

The decoder is in fact a converter as shown in figure 3.28.

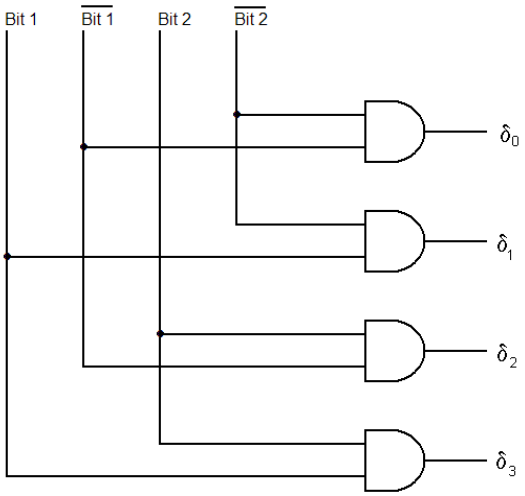

Figure 3.28 Coder from two inputs to four outputs.

The output δ_x is received by two blocks: (1) the inverter delay line as shown in figure 3.29, and (2) a coder from four to one shown in figure 3.30 The δ_x output is sent to the delay line blocks and its output (A1) signal is applied to a Gaussian pulse generator with the coder from four to one output (A2).

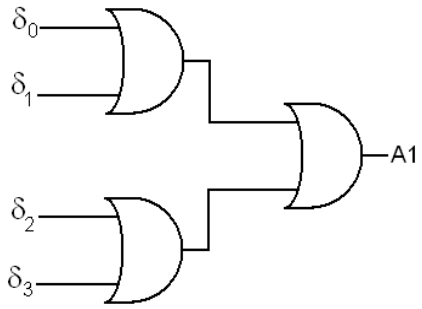

Figure 3.29 Coder from 4 inputs to 1 output.

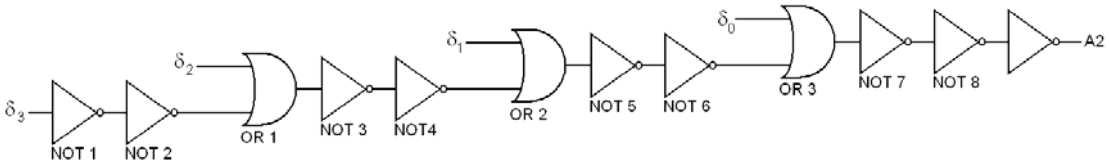

Figure 3.30 Delay line circuit diagram.

The delay between A1 and A2 is used to achieve a certain pulse width (A3) that will depend on the word received and according to modulation scheme proposed; four possible symbols delaying can be generated, as shown in figure 3.31.

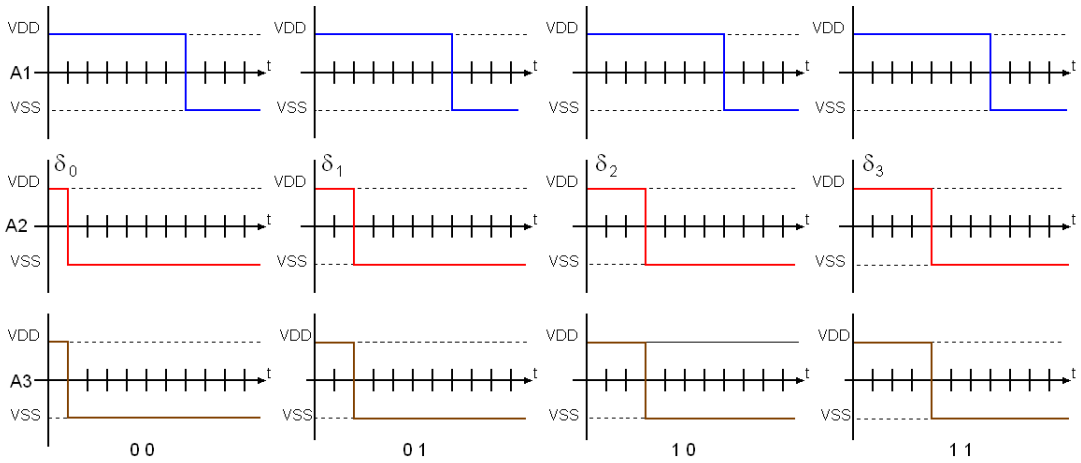

Figure 3.31 Four different widths that correspond to the word to transmit.

As mentioned before, in the raising and falling edges the Gaussian pulses are generated. Therefore, the A3 width pulse will determine the separation between the positive and negative Gaussian pulse. Thus then a symbol has been achieved. Figure 3.32 shows the different symbols that the system can generate.

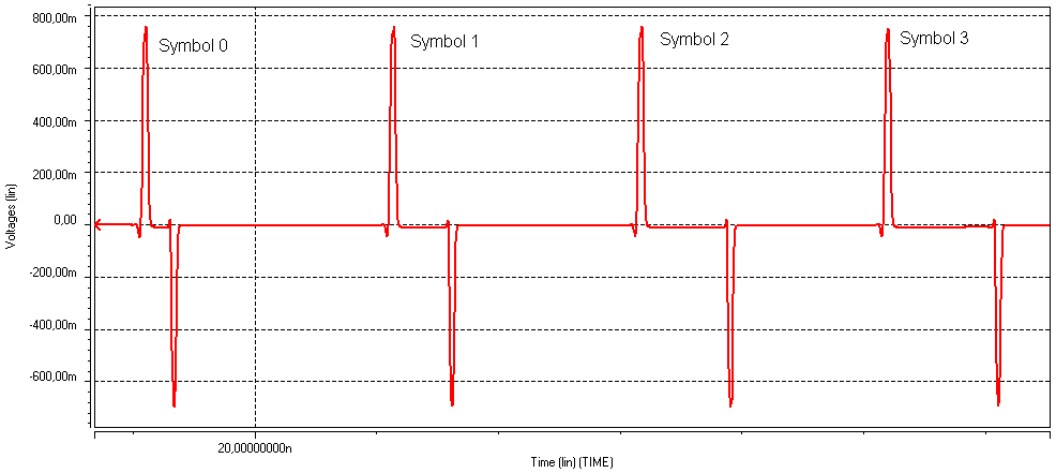

Figure 3.32 Four symbols generated by the proposal.

All the digital blocks can be implemented with minimal dimensions, but it is important to keep in mind that critical point is A3 output that is a AND gate. The raising and falling times will depend on the charge connected to it. If A3 drives a large load, then the raising and falling times will be large, therefore the Gaussian pulse width will be large. On the contrary, if the charge connected to A3 is small, then the raising and falling times will be small and the Gaussian pulses width will be small. In other words, for transistors sizing it must be chosen taking into account the charge connected to the gate.

The delay between a positive pulse and a negative pulse must wide enough for the pulses not to be overlapped and it must be at least one pulse width. The designers have to consider the delays and the dispersion effect that the channel could cause to the pulses [65] [66]. This thesis takes into consideration the following: “when the delay is less than the coherence time of the channel, the pair of pulses can be assumed to be affected similarly due to the channel” [68].

3.5 Conclusions

In this section, Gaussian pulse generators have been presented. They can be used as Gaussian and Monocycle pulse generators. The low complexity in the generator architecture is an advantage with respect to others generator presented in this chapter. The disadvantages are that the pulses generated are not completely Gaussian pulses and they are not completely symmetric, although these advantages, they are not representing degradation in the reception process. The generator input are completely digital, this represents other advantage with respect to other proposal because it can be easily adapted to other modulation schemes. The transmitter delivers the pulses to a 50 ohms load.

On the other hand, the receiver has been implemented for the scheme modulation proposed and the circuits have been designed too. The modulation scheme and the

good impulse response of the circuit allow to the demodulation process achieve the auto synchronization. The demodulator circuit complexity is very low and. almost all processing, is digital domain. The transmitted signal has two functions: the synchronization and the word representation. Therefore it is not necessary complex algorithms for carry out the process reception.

In conclusion the scheme modulation allows relax the specification in the circuit design and in the processing.

Chapter 4

Design and Characterization of the Modulator/Demodulator

4.1 Introduction

This chapter is focused on the characterization of the proposed UWB circuit. The objective of the characterization is to compare the performance with respect to other systems.

Concepts as PSD, TH, BER, etc. that have been seen in previous chapters are measured in the characterization of the transceiver. The main objective is to demonstrate that the proposed circuit design and the modulation scheme have a good performance and are a strong candidate with respect to other architectures and modulation schemes. Also they can be used in practical conditions.

In this thesis all the circuits have been designed and simulated using Mentor Graphics and the technology TSMC 0.18um MMRF CMOS process with a power supply of +/- 0.9v.

4.2 Modulator

For the spectrum overlay control, the FCC regulations imposes spectral mask that strictly constrain the power transmission of a UWB signal to be well below the noise floor in all bands. The spectrum of the transmitted signal is influenced by the modulation format, the multiples access scheme and, most critically, by the spectral shape of the underlying UWB pulse. The shape of the pulse is thus a key design decision in UWB systems, with the following points to fulfill:

Efficient Spectral Utilization– the transmission reliability of a UWB system is determined by the SNR. Given the stringent transmission power limitations maximization of the received SNR requires efficient utilization of the bandwidth and the power allowed by FCC mask.

Convenient Implementation– the pulse shape design must consider the implementation technique challenges imposed by ultra wide bandwidth, and the extent to which the design can be readily implemented using off the shelf hardware components

In particular, in this thesis the pulse generator is examined as a critical part of the transmitter. The advantage that offers this Gaussian pulse generator is that it can be easily adapted to other timing control systems in the digital domain. The dimensions of the transistors of the generator depends on the output current, as mentioned in chapter 3, where the equation 3.7 relates the dimension of the transistor M5 with M3. The table 4.1 shows the final dimensions of the transistors in the Gaussian pulse generator.

The layout is shown in the figure 4.1. The circuit can be used as Gaussian pulse generator or a Monocycle Gaussian pulse generator; in other words, the layout implements two Gaussian pulse generators in parallel connection.

	M1(p)	M2(p)	M3(p)	M4(p)	M5(p)	M1(n)	M2(n)	M3(n)	M4(n)	M5(n)
W(µm)	60	44	44	44	44	60	60	30	60	60
L(µm)	0.18	0.18	0.18	0.18	0.18	0.18	0.18	0.18	0.18	0.18

Table 4.1 Transistor dimensions of the positive and negative Gaussian pulse generator

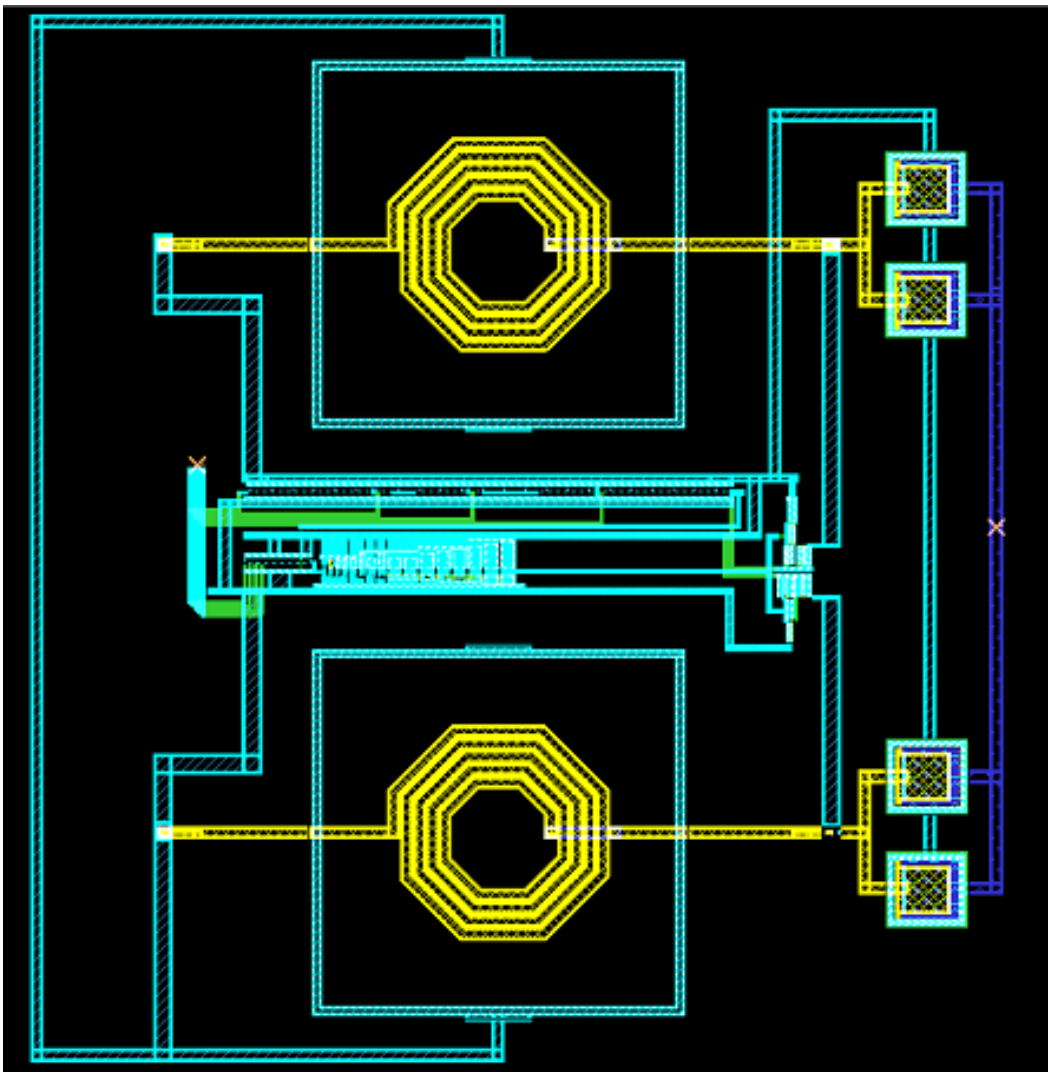

Figure 4.1 Gaussian pulse generator Layout.

The total area is 600x650µm, including two Gaussian pulse generator. The Gaussian pulses obtained in post layout simulation are shown in figure 4.2.

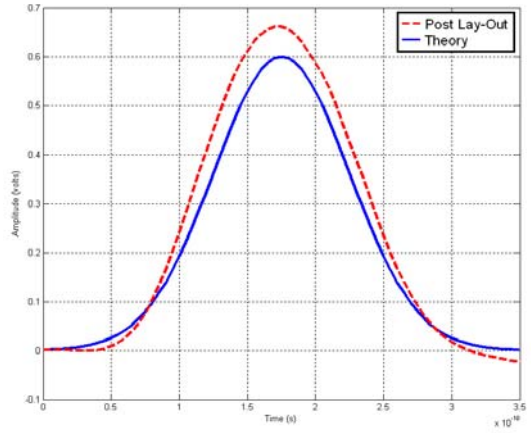

(a)

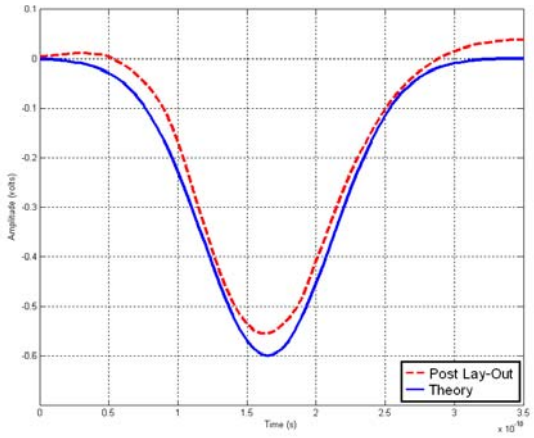

(b)

Figure 4.2 (a) Positive and (b) Negative Gaussian pulses Theory and post layout simulation results.

The Gaussian pulses are compared with respect to theoretically obtained results in Matlab. The Relative Error is obtained by the equation 4.1 and the percentage error from 4.2.

$$\delta x = \frac{x_o - x}{x} \tag{4.1}$$

$$\%error = \delta_x \text{x}100\% \tag{4.2}$$

where x is the projected value, x_o is the real value. The similitude percent obtained for the positive Gaussian pulse is 90.2% and 89.7% for the negative Gaussian pulse. Table 4.2 makes a comparison with different generator architecture.

Reference	Basic Modulation Adaptability	Pulse Shape	Width Pulse	Center Frequency
[62]a	PPM|OOK|PIM|BPSK	Gaussian	280 ps	3.6 GHz
[62]b	PPM|OOK|PIM|BPSK	Gaussian	280 ps	3.6 GHz
[63]	PPM|OOK|PIM	Gaussian	300 ps	3.3 GHz
[64]	PPM|OOK|PIM	Mono cycle	270 ps	3.6 GHz
[65]	PPM|OOK|PSM| BPSK|PAM	Mono cycle and Gaussian	160 & 153 ps	6 & 6.5 GHz
[88]	PPM|OOK|PIM|BPSK	Doublet Gaussian	3.36 ns	0.92 GHz
Proposal	PPM|OOK|PIM|BPSK| PSM	Mono cycle and Gaussian	297 ps	3.3 GHz

Table 4.2 UWB generator comparison.

Using the modulation scheme proposed in this thesis the obtained PSD is depicted in figure 4.3. This figure shows that the PSD has idle tones that can be reduced if the TH technique is used, as shown in the figure 4.4 where the PSD is smoother than in figure 4.3. Therefore if a good PSD is needed, then it is necessary to use more bits and get a smoother PSD. The figure 4.5 shows the PSD using four bits. Depending on the word size of TH generator, the PSD will be smoothed.

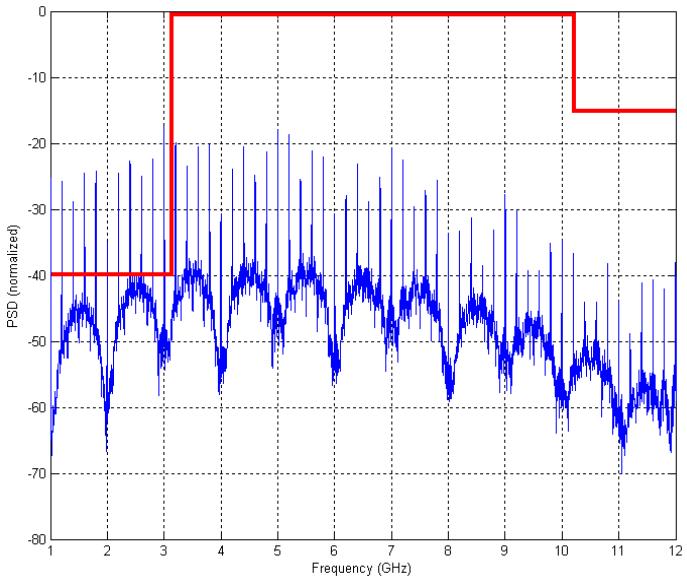

Figure 4.3 Power Spectrum Density of the proposed modulation scheme.

It is clear that the PSD in the figure 4.3 violates the FCC mask from 1-3 GHz. On the other hand, if TH technique is used in the data transmission, it barely complies with their respective spectral mask but at expense of very low spectrum utilization, as is depicted in figures 4.4 and 4.5. As a result, the Gaussian monocycle could not be a good option in some UWB system applications.

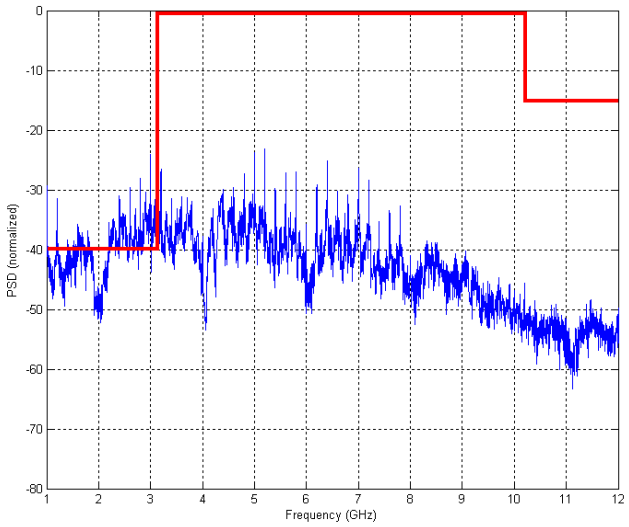

Figure 4.4 Power spectrum of the proposed modulation scheme using TH technique.

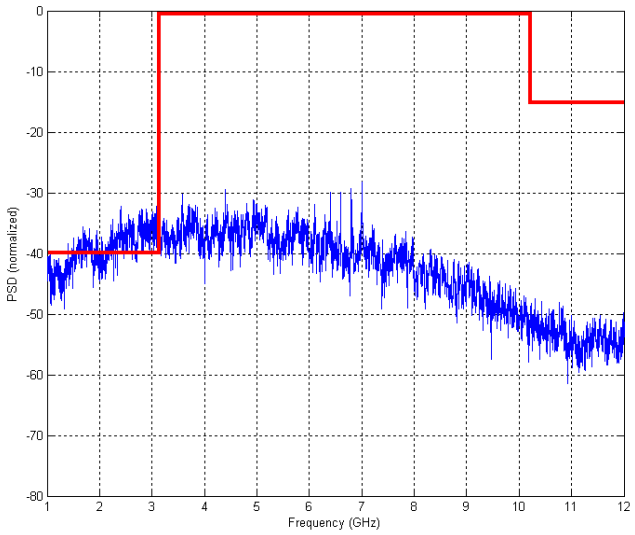

Figure 4.5 Power spectrum of the proposed modulation scheme using TH technique with four bits.

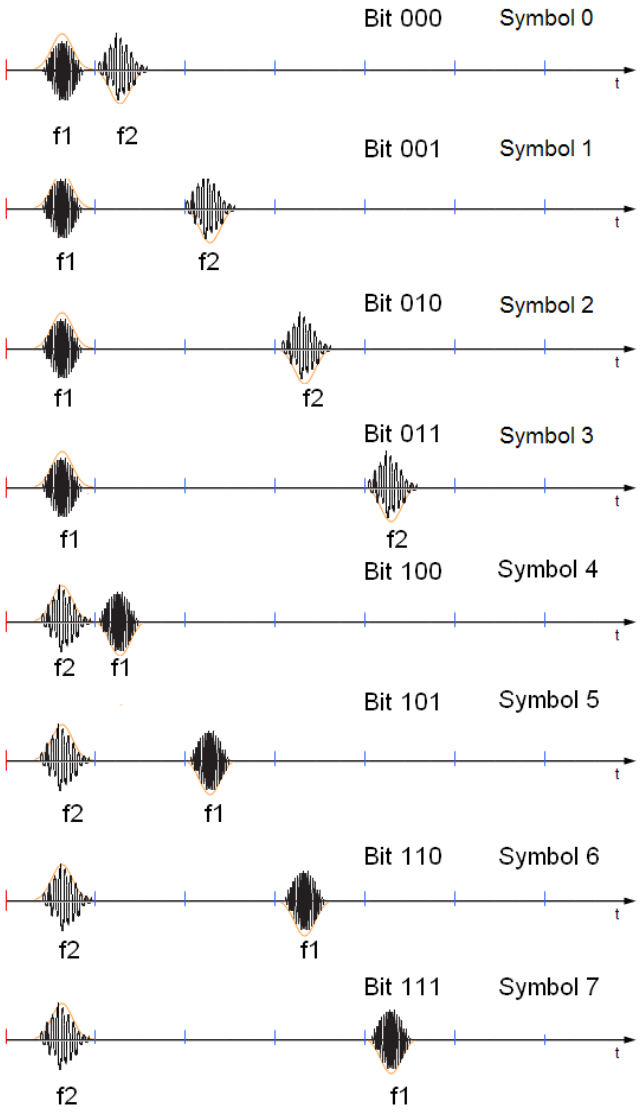

Figure 4.6 Symbols interpretation using MB modulation technique.

The implementation of the TH technique increases the hardware in the circuit design in the processing of the data. However, the hardware used for TH implementation can be toward another technique, for example MB, which has been proposed for wireless personal area network under IEEE.15.

An advantage of the proposed modulation scheme offers is that it can be easily implemented by using MB technique. The MB technique is directly related to the size

of the word, but at expense of hardware increasing, and depending on the number of frequencies will be the size of the word. In this thesis, is a modulation scheme proposed that uses only two frequencies f1=7GHz and f2=7.5GHz as shown in figure 4.6.

The functions in time domain are expressed by the equation:

$$w_1(t) = \pm A_0 e^{-(t/d)^2} \sin(2\pi f_1 t) \tag{4.3}$$

$$w_2(t) = \pm A_0 e^{-(t/d)^2} \sin(2\pi f_2 t) \tag{4.4}$$

where w_1 is f1 modulated by the Gaussian pulse and w_2 is f2 modulated by the Gaussian pulse.

The figure 4.6 shows that depending on the word to transmit, f1 or f2 will be transmitted in first or second place. When the first positive Gaussian pulse is modulated by f1, the most significant bit will be 0. When f2 modulates the first positive Gaussian pulse the most significant bit will be 1. The last two bits will be determined by the correlation between Gaussian pulses; therefore, the size of the word is three bits.

On the other hand, when f1 is turned on, the f2 is turned off and, conversely, when f2 is turn on, f1 will be turned off, but the frequencies will not work at the same time. These conditions allow the obtained PSD to be very smooth and very similar to modulation BPSK, as shown in figure 4.7. In fact, the random is carried out by modulation it self, therefore it is not necessary to increase the hardware in the random technique implementation. It is clear that the PSD in figure 4.7 complies with its respective spectral mask and it has high spectrum utilization.

In MB case, it is necessary to use mixers to carry out the modulation. In this thesis, they are only simulated at behavioral level.

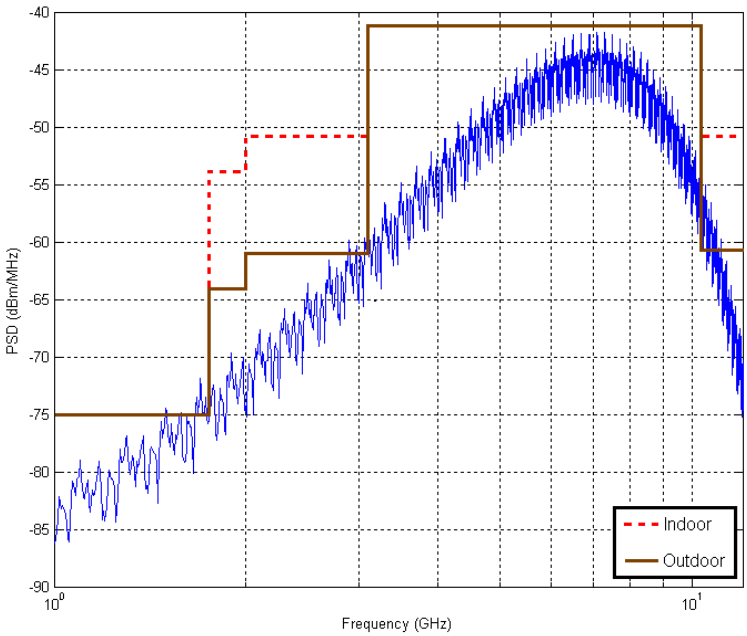

(a)

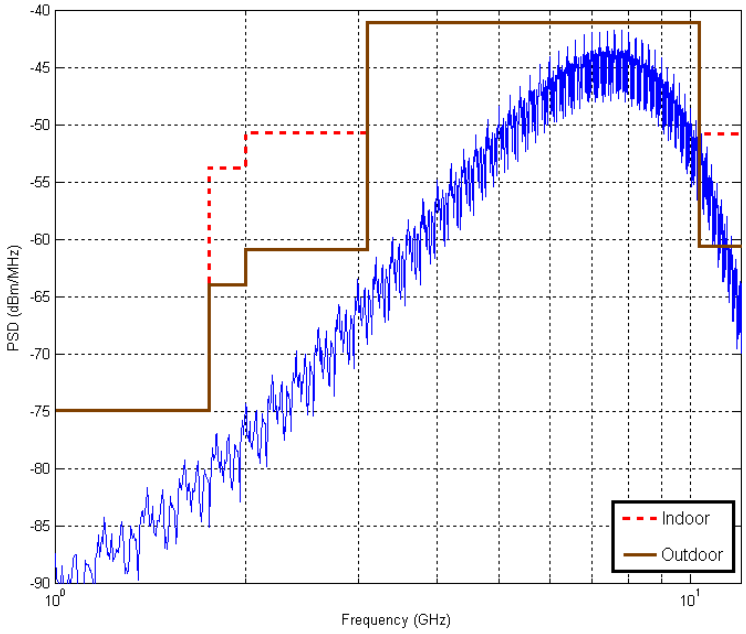

(b)

Figure 4.7 PSD result using MB technique with (a) f1 and (b) f2.

The Gaussian pulse generator can be easily implemented in other kind of modulation scheme such as BPSK modulation. The BPSK modulation is the most popular

application in UWB systems because it has a smooth PSD. The BPSK modulation is carried out as is depicted in the figure 4.8. The hardware used in this implementation has low complexity and uses the same architecture that in the proposed modulation scheme.

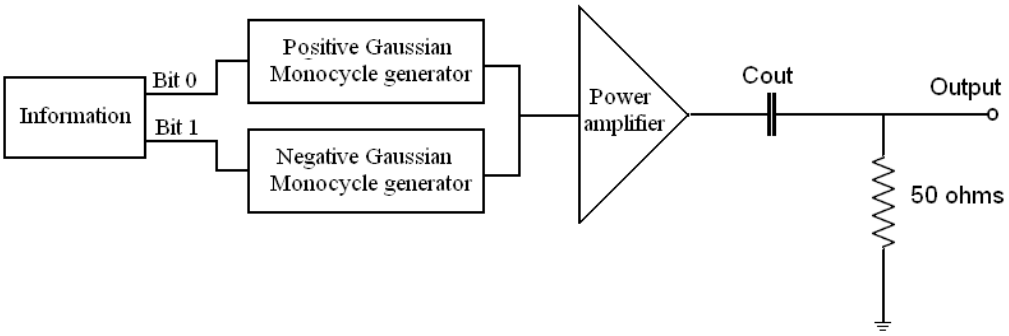

Figure 4.8 BPSK modulator based monocycle Gaussian pulse generator.

From figure 4.9 is clear that the spectrum in BPSK modulation is not complying with the spectral Mask, but it can be improved if it is complemented with MB technique and thus fulfill with the mask spectral as it was demonstrated in the proposed modulation scheme.

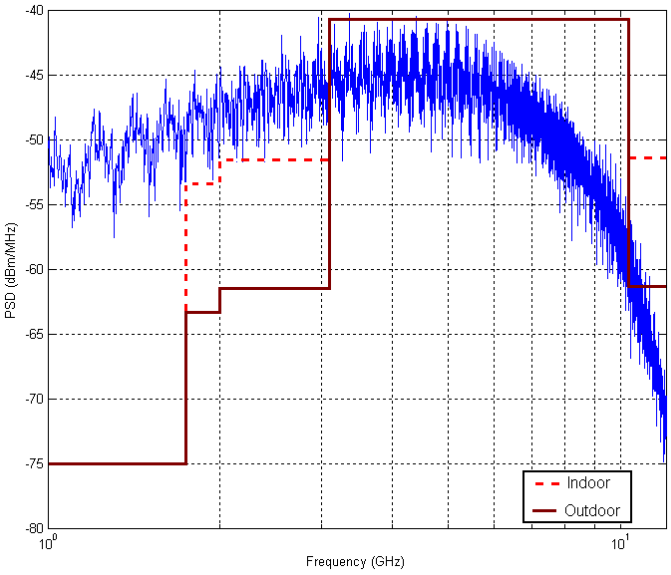

Figure 4.9 BPSK modulation PSD.

The Gaussian pulse generator is not restricted for BPSK application and can be used in other modulation applications such as PPM, OOK, PIM, etc.

The Gaussian monocycle pulse generator is an option with high potential depending on the requirements of the design, can be used as a monocycle generator or as a Gaussian generator. The table 4.3 shows some characteristics of the proposal with respect to other base band modulations.

Modulation	M-ary	Carry-modulation	Multiple Access	Random technique
BPSK	No	Yes	Yes	No
PPM	No	Yes	Yes	Yes
OOK	No	Yes	Yes	Yes
PAM	Yes	Yes	Yes	Yes
PSM	Yes	Yes	Yes	Yes
QPSK	Yes	Yes	Yes	Yes
Proposal	Yes	Yes	Yes	No

Table 4.3 Basic modulation comparison.

The proposal offer some advantages as a M-ary modulation and can work without a random technique.

4.3 Demodulator

In general, a coherent receiver requires several parameters concerning with the received signal, radio channel, and interferences characteristics. Multipath delays, channel coefficients for each multipath components and distortion of the pulse need to be estimated for optimal coherent reception.

On the other hand, noncoherent receiver designs in UWB relax the amount of information that needs to be estimated accurately for detection of the transmitted bits.

In other words, the synchronization, channel estimation and pulse shape estimation is not as stringent as in the coherent receivers. The last case is the kind of receiver proposed in this thesis and its performance is evaluated in this section.

As mentioned before, the circuit outputs of h_1 and h_2 are normally near to V_{SS} or V_{DD} respectively. This condition allows h_1 and h_2 to have a great dynamic range to amplify the input signal where h_1 will only amplify the positive Gaussian pulse and the negative will be attenuated and h_2 will only amplify the negative Gaussian pulse and the positive will be attenuated.

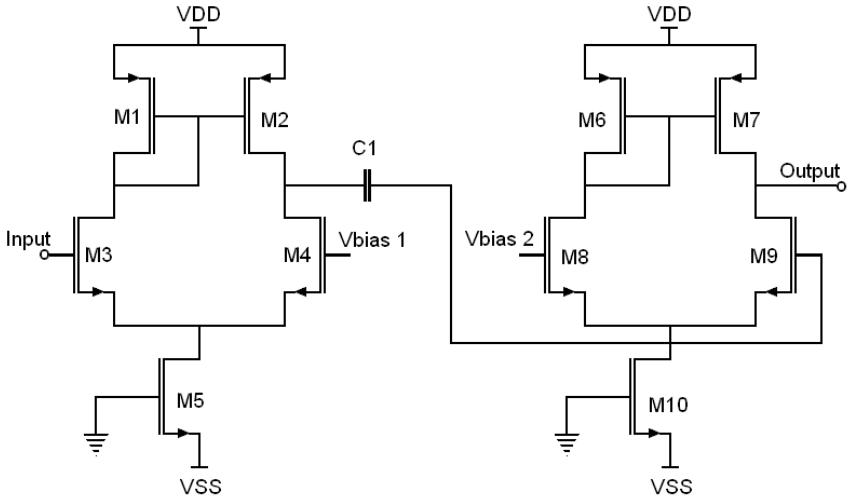

Figure 4.10 Differential amplifier.

The transistor dimensions for h_1 and h_2 have been calculated with respect to the Gaussian pulse waveform. The first differential amplifier is shown in the figure 4.10; the upper 3 dB frequency is given by:

$$f_{out} = \frac{1}{2\pi\tau_{out}} \tag{4.5}$$

where the constant at the output is given by:

$$\tau_{out} = (r_{o2} \parallel r_{o4})C_L \tag{4.6}$$

Assuming that the load capacitance is large compared with the output capacitance of the differential amplifier; the slew rate is given by

$$\frac{dV}{dt} = \frac{I_d}{C_L} \tag{4.7}$$

The final dimension of the transistor are computed in table 4.4

Transistor	W(µm)	L(µm)
M1=M2=M6=M7	2	0.18
M3=M4=M8=M9	5	0.18
M5=M10	10	0.18

Table 4.4 Transistors dimension of differential pairs.

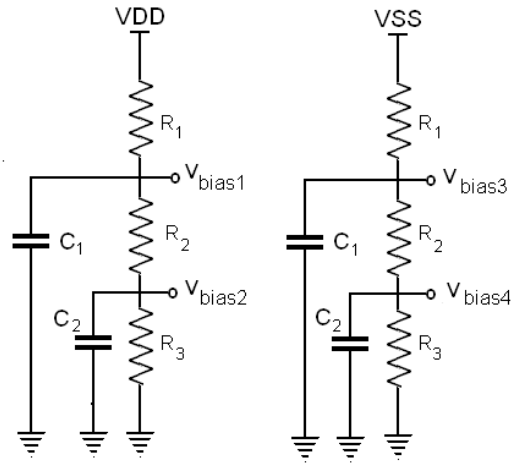

Figure 4.11 V_{bias} circuit network.

All the V_{bias} voltages are obtained by the two network resistances as is shown in the figure 4.11. V_{bias1}, V_{bias2}, V_{bias3} and V_{bias4} are voltages that keep unbalanced the currents of the differential pairs and the voltage values are computed in the table 4.5.

The V_{bias2} is calculated considering the minimal V_{DS8} so that the differential pair 2 works in the saturation region.

V_{bias1}	V_{bias2}	V_{bias3}	V_{bias4}
0.1v	0.05v	-0.1v	-0.05v

Table 4.5 V_{bias} voltages used in the differential pairs.

$$V_{DS} = V_{GS} - V_T = \sqrt{\frac{2I_D L}{K_n W}} \tag{4.8}$$

On the other hand, V_{bias1} is twice V_{bias2} value, with the objective that its output voltage be near to V_{SS}. Therefore, only positive Gaussian pulses are amplified and the negative almost are attenuated, in other words the M4 is in the liner region.

The resistances and capacitances values are computed in table 4.6. The capacitances keep the level of the noise voltage that is generated at the input of the differential pairs low.

R_1	R_2	R_3	C_1	C_2
16000Ω	1000Ω	1000Ω	500pf	500pf

Table 4.6 Resistances and capacitances values.

The resulting lay-out is shown in the figure 4.12 where the area is 580x150µm

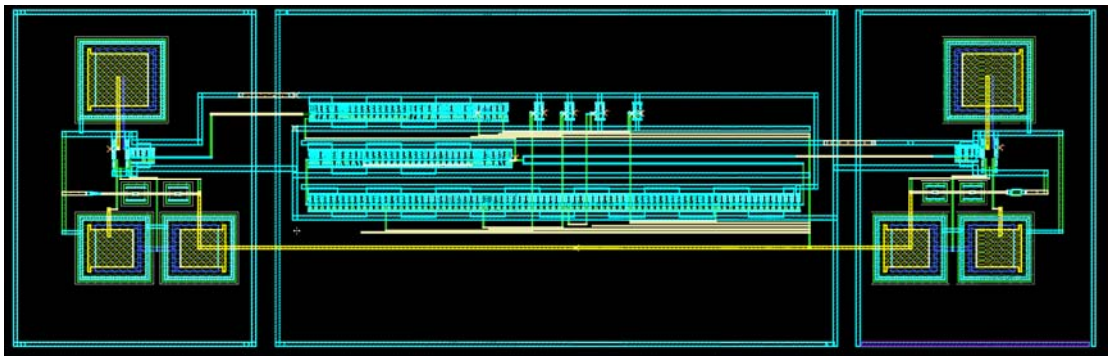

Figure 4.12 Demodulator lay-out design.

The performance of the modulation schemes can be affected differently in practical scenarios. Due to reflection, diffraction, and scattering effects, the transmitted signal arrives to the receiver through multiple paths with different delays. The propagation of UWB signals in indoor environments is an important issue with significant impacts on the future directions.

In this thesis, AWGN and multipath channel model IEEE.802.15.3a are considered. The interference from other communication systems is ignored. The location of the transmitter is limited by a circumference of 4m radius. The receiver is tested under the proposed modulation scheme for two bits and the system used in the evaluation is shown in figure 4.13.

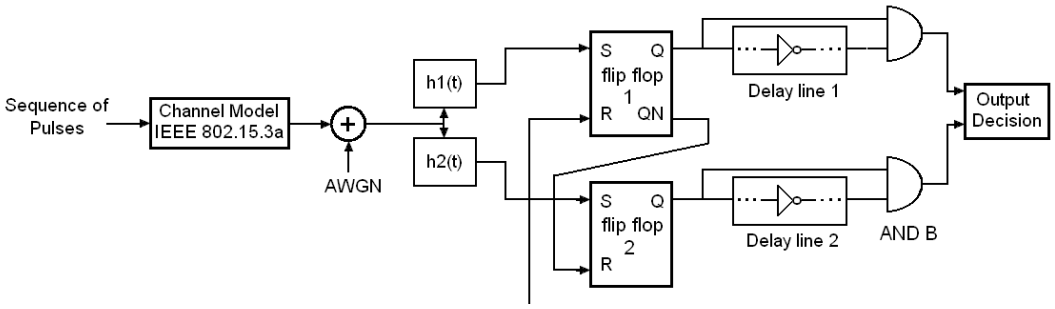

Figure 4.13 System model tester used in the BER estimation.

The impact of the channel IEEE 802.15.3a and AWGN in the BER is depicted in figure 4.14, where the channel model CM1 of [76] is used. The simulation results are based on 100 realizations of 1000 information bits. Computer simulations are performed to observe the data modulation and interference effects in the proposed modulation. Figure 4.14 depicts the simulation results and shows a comparison with [8]. An ARake receiver and SRake receiver proposed in [83] with 1, 3, and 10 finger are employed in BPSK and PPM modulation schemes and they are compared with the proposal. In these references, the channel model CM1 is used, 50000 realizations of the channel are generated, the channel impulse responses are truncated into 60 ns and the BER is evaluated.

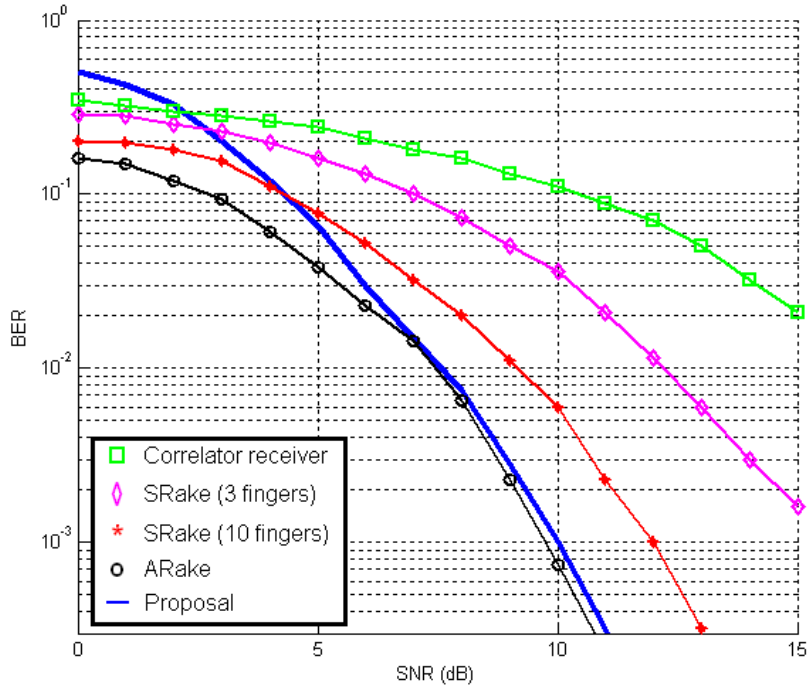

(a)

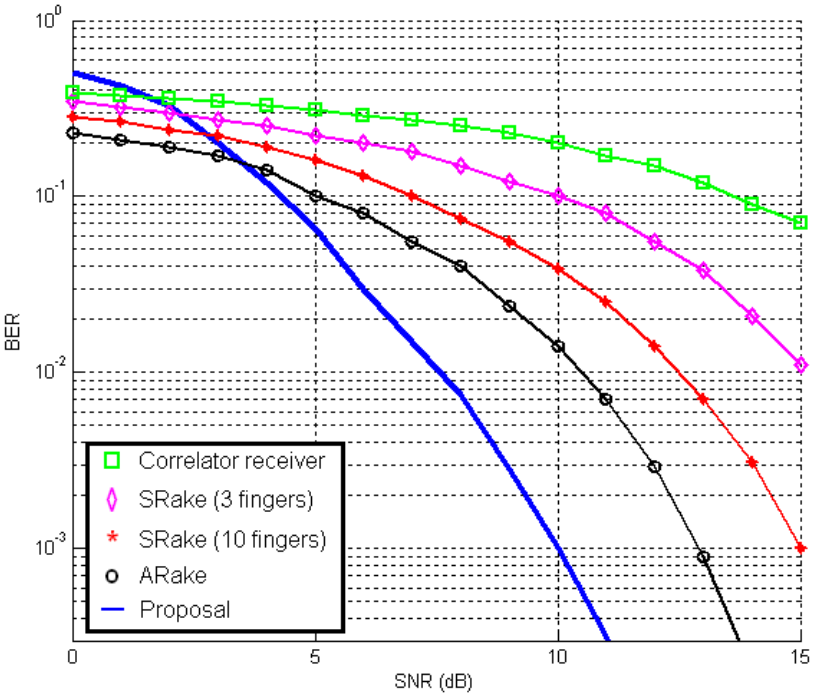

(b)

Figure 4.14 (a) Performance of proposal and BPSK in CM1 channel and (b) performance of the proposal and PPM in CM1 channel.

The figure 4.15 depicts the BER of the proposal and it is compared with [84, 85, 86, and 87].

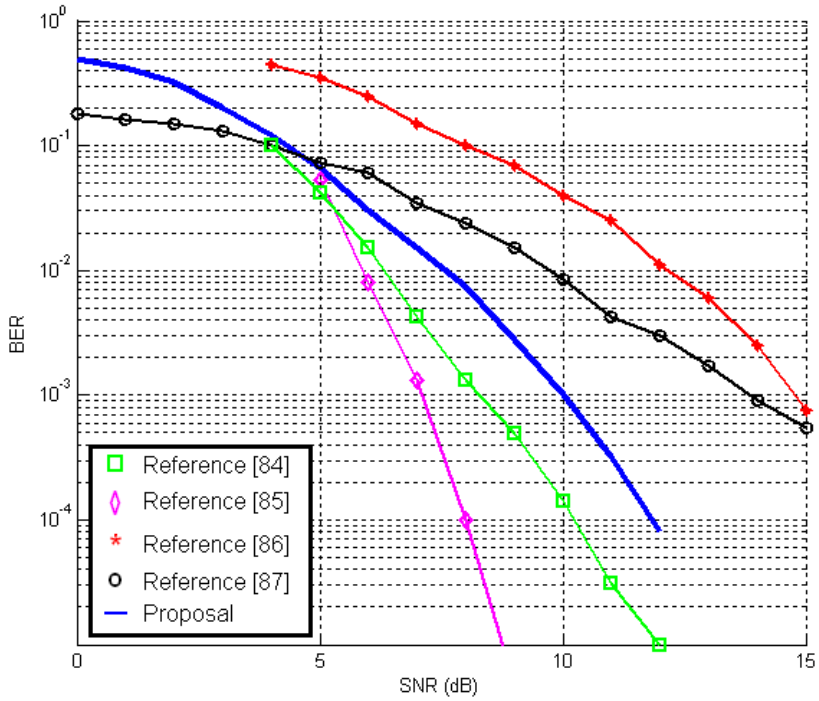

Figure 4.15 Performance of the proposal and [84, 85, 86 and 87] references in CM1 channel model.

Reference	Characteristic channel	RF Technique	Multiple Access technique	Band base modulation
[87]	CM1	Wavelet	OFMD	FTH-PPM
[86]	CM1	Carrier	OFMD	BS-OFMD
[85]	CM1	Wavelet	OFMD	QPSK
[84]	CM1	Carrier	OFMD	QPSK
[83]a	CM1	Wavelet	-	BPSK
[83]b	CM1	Wavelet	-	PPM
Proposal	CM1	Wavelet	CDMA & OFMD	BPSK/PPM

(a)

Reference	Energy Collection	Band Protection	Synchronization	Mbps
[87]	rake	No	Algorithm	250
[86]	rake	No	Algorithm	-
[85]	A-Correlator	No	Algorithm	-
[84]	A-Correlator	No	Algorithm	307
[83]a	-	-	Algorithm	312
[83]b	-	-	Algorithm	312
Proposal	D-Correlator	Yes	Auto synchrony	200

(b)

Table 4.6 UWB Demodulator comparison.

In the figures 4.15 and 4.16, is clear that the proposal has poor fitting in highly noisy channel but has a good performance when the SNR increases. The table 4.6 compares different systems with respect to the proposal presented in this thesis. It is clear that the advantages of the proposal are digital domain correlation; the system is auto synchronous and the protection band with respect to references.

4.4 Process Voltage and Temperature (PVT) Variations

Although a UWB modulator and demodulator have been designed to meet design specs, the response of the circuit can change over process, supply voltage and temperature (PVT) variations. Therefore, Corner models and Monte Carlo simulations have been carried out in modulator and demodulator circuits.

As mentioned before, the UWB pulse generator is a key element of the transmitter block. The main issue is to keep the UWB pulse shape. Figures 4.16 and 4.17 show the post layout simulation results when the generator is tested with process variation using corner models and Monte Carlo.

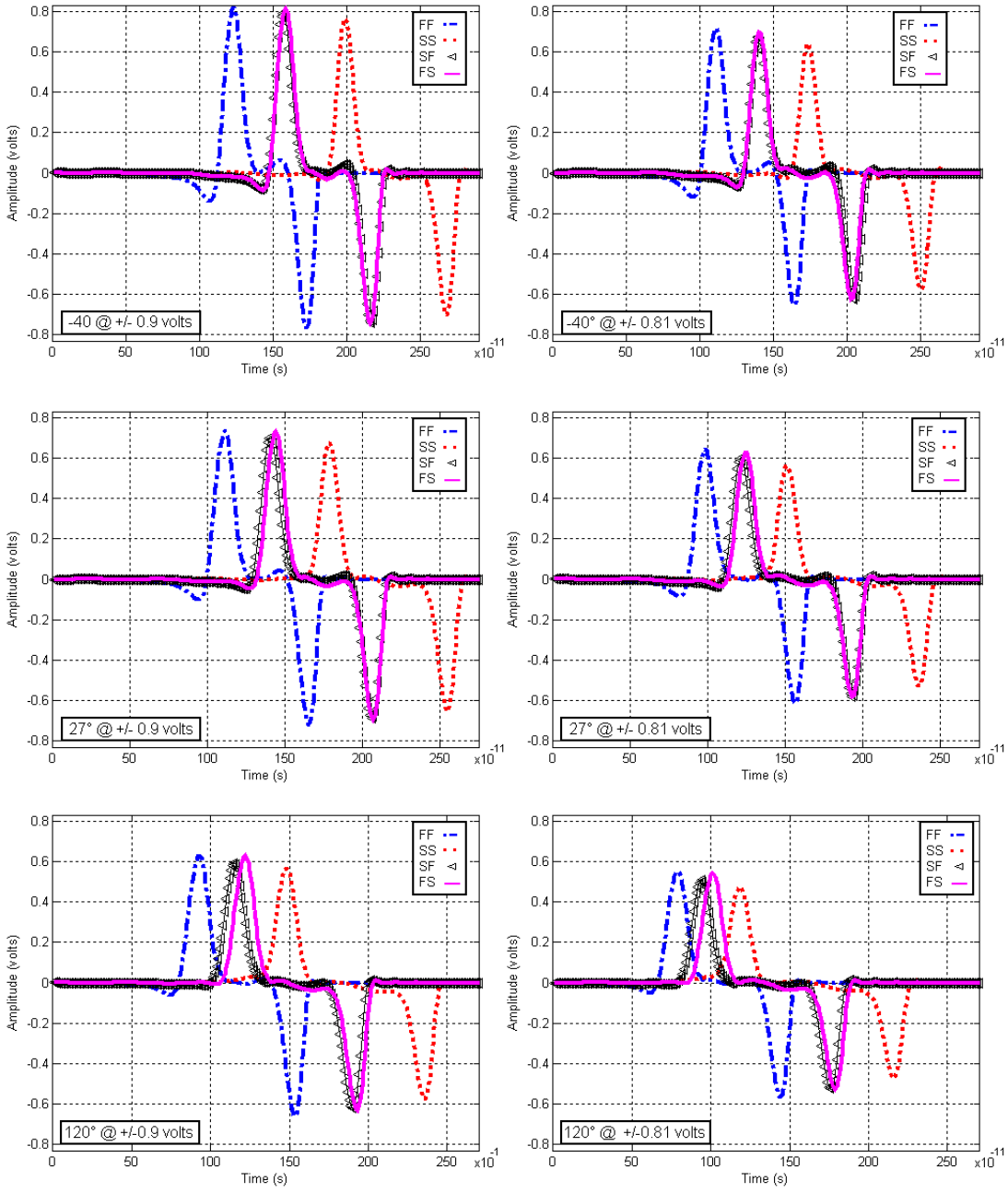

Figure 4.16. PVT variations using corner models

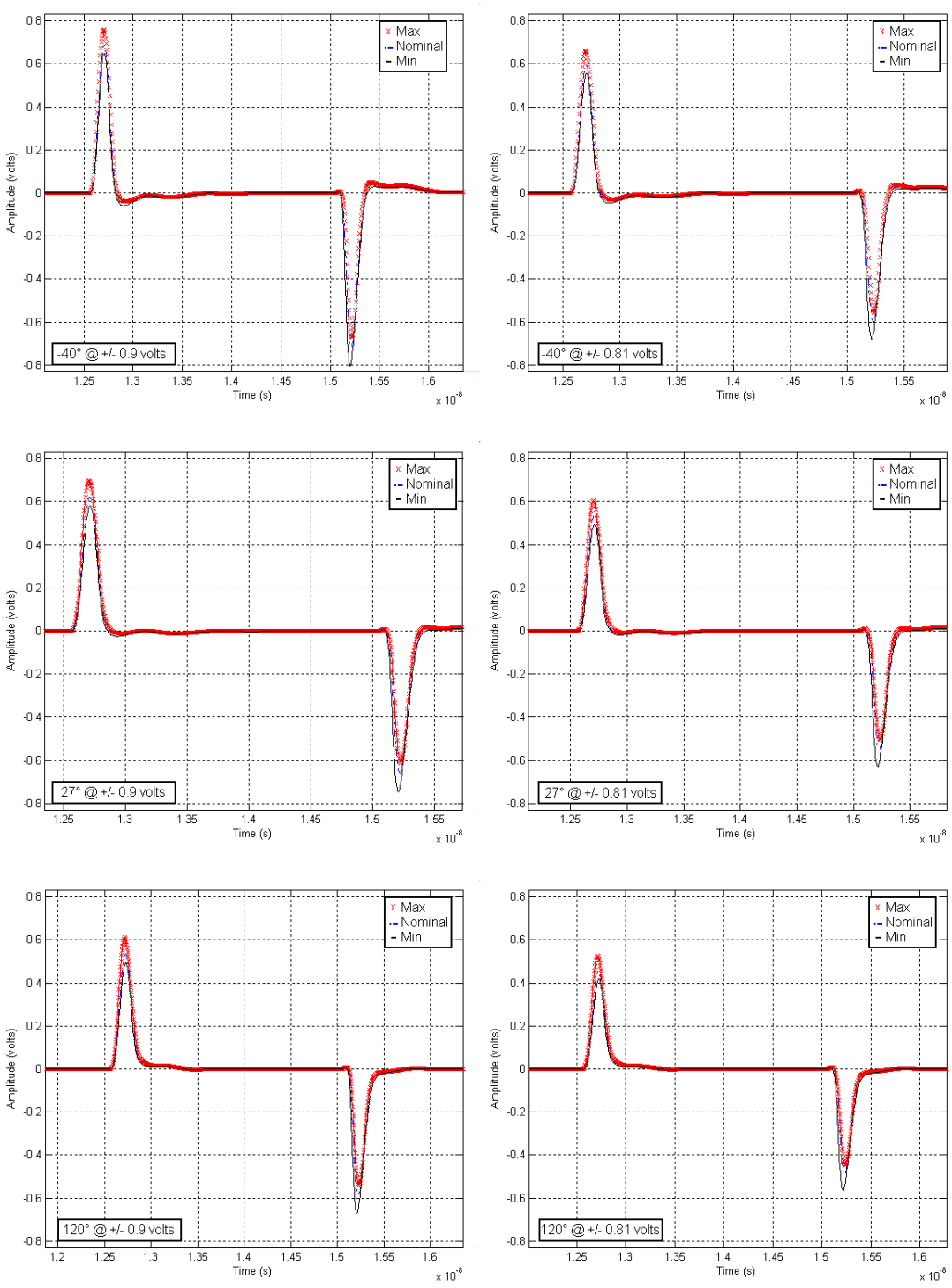

Figure 4.17. PVT using Monte Carlo variations.

In the figures, it is possible to observe that the circuits are robust to such variations sine the differences in the delay time between pulses do not affect the performance of both modulator and demodulator. A symbol critical in this scheme modulation is the 00. Therefore, it is used as a test pulse in the simulation results of figure 4.16. The reason is because the pulses (positive and negative) could be overlapped or the delay between pulses could varies and thus be could have loss the information as is shown in the figure 4.17 where the symbol 11 is used as testing and assured that the maximal delaying pulses in PVT variation. In fact neither overlap nor excess delays are present in the PVT variations.

On the other hand, the critical part in the demodulator is the process of digital correlation. The digital pulses must have a tolerance to signal delay and process variations.

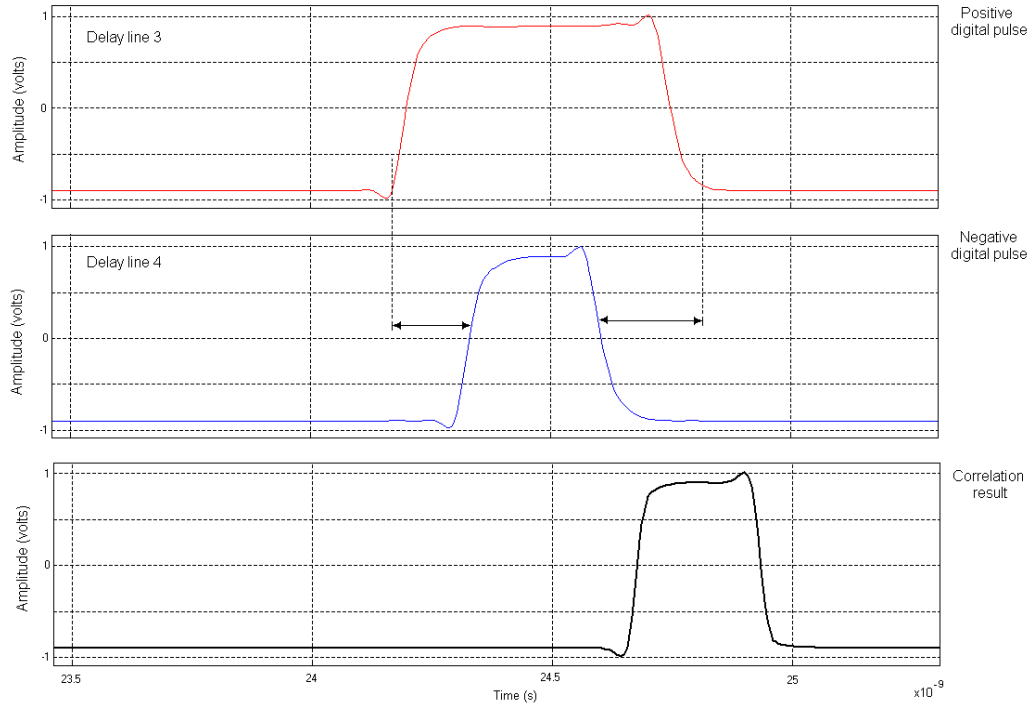

Figure 4.18 The different characteristics between PD1 and PD2 pulses.

Other very important point is to consider is that the pulses are not overlapped in time. In other words, when a pulse that corresponds to delay line 3 (PD1) is present, the rest of the pulses are absent. This is the reason why the delay in the line 1 is bigger than the delay in line 2 and consequently, PD1 pulse is wider than PD2, as shown in figure 4.18.

This characteristic allows the demodulator to center the PD2 with respect to PD1. Thus, the pulses can move with certain tolerance without correlation affectation. When the correlation is achieved, the result is processed and one bit is estimated. In part, good bit estimation will depend on a well performance of correlation process. The objective in this part of the design is to have a system robust to process variations as shown in figure 4.19, where the circuit response has a well performance to process variations.

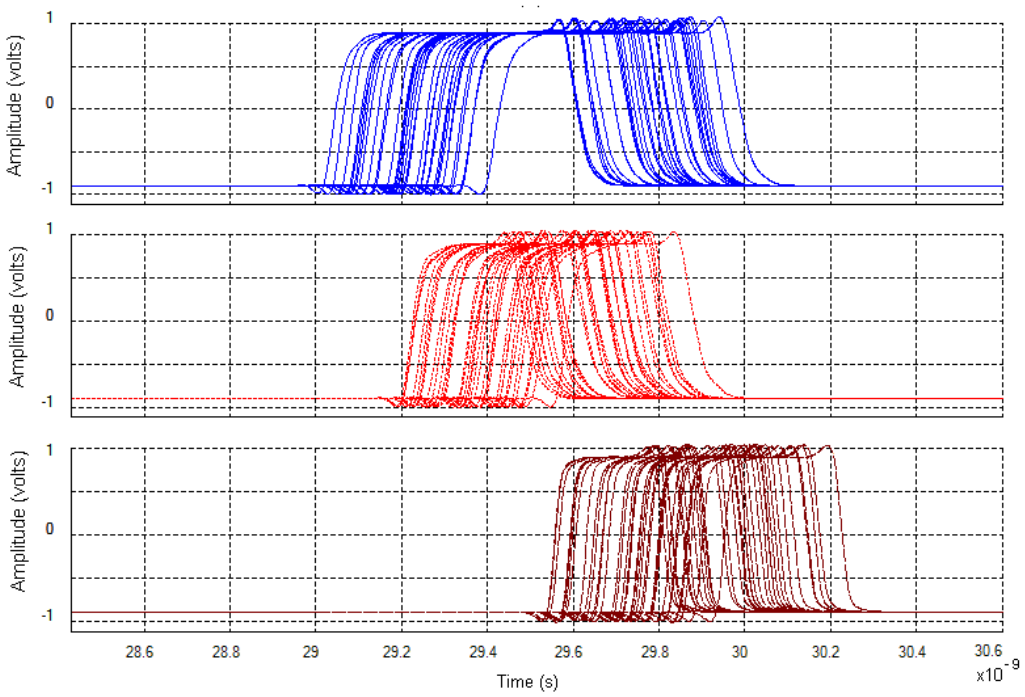

Figure 4.19 Correlation between PD1 and PD2 with variations process.

The last stage of the process is to assign the detected symbol its corresponding binary code. The next stages are digital blocks that convert the correlation result to binary

code. In this case the size of the word is two bits. The figure 4.20 shows a Mentor Graphic post layout simulation in order to illustrate that the circuit design is robust to Process, Temperature and Voltage (PVT) variations (V=+/-0.9V and T=100ºC).

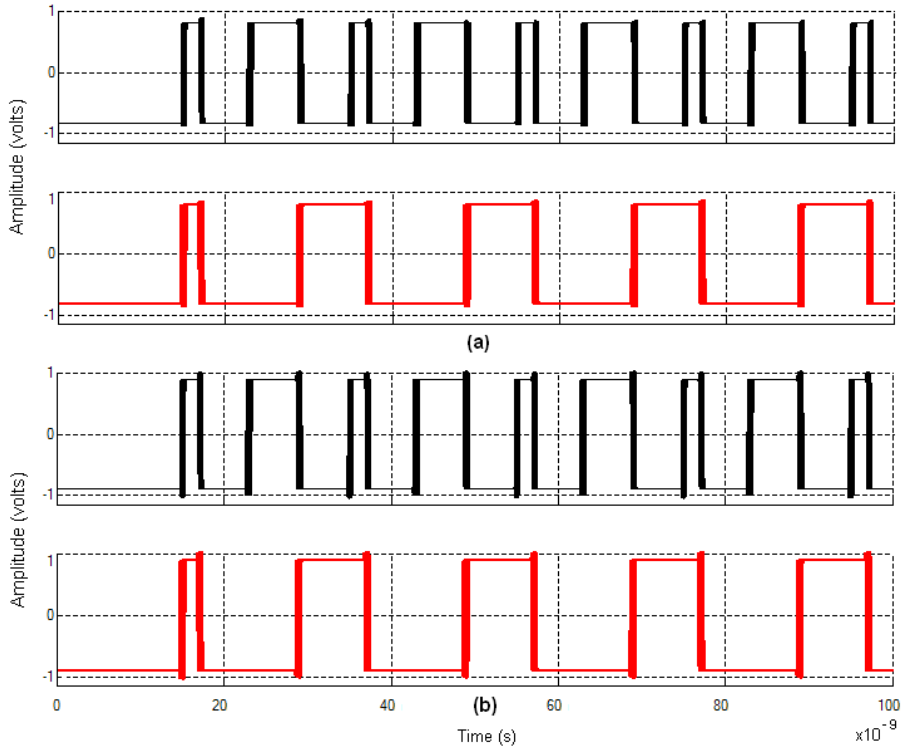

Figure 4.20 Demodulator variation process response (a) +/-0.9v and (b) +/-0.81v @ 110°C.

In general the circuit designs have an acceptable performance when a Monte Carlo process variation analysis is performed. This result is because lay out techniques are used in the layout implementation and the design points proposed in the chapter 3 are considered. The same shape and size, minimum distance, same orientation, interdigitize are some techniques used in the design circuit.

Chapter 5

Conclusions

This thesis has been focused on improving the main drawbacks of the state-of-the-art UWB communications systems using integrated circuits. The main contributions of this work can be divided into three parts: Data modulation technique, design of Modulator and Demodulator circuits for wireless personal area network CM1. Therefore, in this thesis a novel data modulation technique and circuit designs that support such modulation technique have been presented.

5.1 Modulation Scheme

The data modulation technique presented in this thesis allows less string sat constraint of several parameters concerned to the received signal, radio channel, and interferences characteristics at the same time. This modulation does not allow the hardware and computational complexity to be increased because of all these parameters, as synchronization, channel estimation and pulse shape estimation are not necessary. The way that the data are modulated by this technique has two functions: (a) the auto synchronization and (b) to represent the data in symbols.

The auto synchronization is achieved by the opposite polarity characteristic, where the pulses sequence indicates when a duty cycle ends and other cycle begins. The delay between positive and negative pulses gives the information so that a word is estimated in a duty cycle.

In conclusion, the pulses polarity, the sequence, and the delay of the Gaussian pulse are characteristics that need to be known by the receiver in order to achieve the auto-synchronization. Also the modulation technique allows the timing estimation to be easier which permits the receiver performance to be more immune to timing mismatch. The results are a modulator and demodulator implementation with low complexity, as shown in this thesis.

The modulation scheme is applied to IR modulation and two bits, but it can be implemented for M-ary scheme, where the PSD can be adapted to the restriction established by FCC. However the PSD is carried out at expense to extremely low power. This condition limits the applications using IR technique, therefore depending on the requirements of the design it will determine its use.

On the other hand, it has been demonstrated that the modulation technique can be implemented easily to MB modulation technique. In this application, the frequencies are used to increase the size of the word and to get a better PSD with respect to IR technique. The principle of the demodulation is the same that the IR case. The difference between IR and MB is that now the frequencies have assigned a bit or bits.

The MB systems allow flexibility in efficiently “filling up” the spectral mask, and facilitate co existence with legacy systems and worldwide deployment by enabling some band to be turned off in order to avoid interference and accomplish with different regulatory requirements as, demonstrated in section 4.2.

5.2 Modulator and Demodulator

A novel pulse generator has been presented as a UWB signal source which can generate two kind of pulses: Gaussian pulses or Monocycle Gaussian pulses. The use will depend on application.

The Gaussian pulse generator can be easily adapted to other modulation schemes, for example PPM, BPSK, OOK, PIM, PAM, and PSM. The reason why is that the generator input is completely digital; therefore, only the falling or rising edge ere necessary to generate the Gaussian pulses. Thus, the generator does not require a complex signal processing as has been demonstrated in the chapter 4, where the generator is applied to BPSK modulation.

The minimal length of the Gaussian pulses is acceptable for application in UWB and may be adjusted by changing the rising or falling edge time. The shape of the pulse is nearly Gaussian, mathematically; the generated pulse is not equal to Gaussian pulse. However the waveform may be considered as a reasonable approximation to the Gaussian pulse.

Performance results demonstrate that the generator is a good option in UWB modulator application. In addition, the generator has minimal RF components and the architecture is low complexity.

In the demodulator part, the correlation process is carried out in the digital domain; in other words, the analog mixers are not used in this process. The representation of the Gaussian pulses with digital pulses allows the modulator to correlates the digital pulses using a AND gates and carry out the correlation.

The correlation process provides the estimation of the bits, so, the estimation stage is not used in this modulator. In fact, only the conversion from thermometer code to

binary code is necessary as demonstrated in chapter 3. This is another advantage that the modulator presents.

The separations of the Gaussian pulses in positive and negative is a technique that allows to the input circuits to process only half the received signal. This condition relaxes the processing part because of modulator process the pulses using interleaving process.

Other advantage that offers the demodulator is that the processing is divided into two stages: (1) the detection of the pulses and (2) detection of the symbol, it is to say, when a symbol is being estimated in bits, on the other side, other symbol is processed. These two processes are carried out at the same time. The result is a demodulator faster than if this technique was not implemented.

The basic architectures proposed in this thesis can be used as a basic block, if MB modulation is used. The number of blocks will depend on the number of frequencies used in the modulation. The modulation scheme proposed in this thesis will not change. In this case analog mixers will be used in the signal processing.

The circuit design architectures are simple, low complexity, practical, and are fully integrated in CMOS technology, assuring that the occupied areas are small and low cost in RF components as it has been shown in the layout proposed in the chapter 4. The process variations shows the robustness of the circuits design, the behavior does not affect to modulation and demodulation systems

5.3 Future Work

The manufacturing of the circuits design needs to be implemented and carry out the characterization at silicon level arise out. The MB and SB techniques must be compared with respect to results shown in this thesis.

On the other hand, the coupling with antenna and BPF are step that must be contemplated to complement the transceiver system and establish the systems behavior in different scenario.

Resumen en Extenso en Español

Capítulo 1

En las últimas décadas, las comunicaciones inalámbricas han tenido una gran evolución, que cada vez más productos que salen al mercado utilizan esta tecnología para comunicarse entre ellos. Este hecho implica, que más usuarios utilicen un determinado espectro y por lo tanto este se vea saturado; por lo que es necesario, emplear técnicas que hagan un uso eficiente del espectro para asegurar el servicio de comunicación sin que halle interferencia entre usuarios.

Una de las características que resaltan en los productos que utilizan la comunicación inalámbrica, es la velocidad de transmisión de bits. A medida que la tecnología avanza, también la velocidad de transmisión lo hace. La saturación del espectro así como la velocidad de transmisión, hace que las comunicaciones inalámbricas sean redirigidas hacia otros espectros que no se encuentran saturados por otras aplicaciones.

Banda ultra ancha o UWB (por sus siglas en ingles Ultra Wide Band) es una banda que recientemente fue abierta para el consumo comercial, específicamente en febrero del 2002 por la FCC (por sus siglas en ingles Federal Communication Commission). Esta tecnología en realidad no es nueva, históricamente los sistemas en UWB fueron

desarrollados principalmente para aplicarse a los sistemas de radares desde 1974 y su uso era exclusivo para aplicaciones militares.

La FCC define a los sistemas de comunicación en UWB como sistemas de comunicación inalámbricos que usan un gran ancho de banda en comparación con los sistemas de comunicación de banda angosta.

UWB por su gran ancho de banda tiene características únicas que dan ventajas con respecto a los sistemas de banda angosta. Tales características como: Baja densidad espectral de potencia que la hace atractiva para aplicaciones militares, debido a que es muy difícil de que los pulsos sean detectados. Robustez a múltiples trayectorias; es decir que los sistemas en UWB pueden hacer distinción entre cada una de las trayectorias que llegan al receptor. La característica de penetración que esta ligada a la longitud de onda de la señal de la siguiente manera: Cuando la señal transmitida es de frecuencia su longitud de onda es más grande con respecto a los objetos que atraviesa por lo tanto puede pasar sin problemas. Debido a que la señal que se transmite en UWB tiene un gran de componentes desde baja hasta alta frecuencia esta puede atravesar paredes sin problemas.

Debido a su baja densidad espectral de potencia, los sistemas de UWB tienen un gran potencial en aplicaciones de corto alcance, es decir no más de 10 metros. Con respecto a otras tecnologías en el mercado los sistemas UWB ofrecen una razón transmisión de datos mucho más grande. En conclusión los Sistema en UWB tiene un gran potencial en aplicaciones de corto alcance.

Capítulo 2

Una de las principales desventajas que aún tienen los sistemas en UWB es llevar a cabo la sincronización. Se han hecho intentos para lograr que tanto el transmisor como el receptor estén alineados en tiempo, desarrollando algoritmos que modelen el

comportamiento de transmisión a través del medio. Lo anterior permite que el receptor procese el pulso correcto y por lo tanto que la señal transmitida sea interpretada correctamente en bits. No obstante, dichos algoritmos aumentan la complejidad del sistema de recepción que casi se vuelven imprácticos por el momento. Sin embargo se han hecho esfuerzos para desarrollar algoritmos más simples y que no aumenten las arquitecturas ni la complejidad del sistema.

Los sistemas en UWB, tienen la ventaja de ser menos complejos con respecto a los sistemas de banda angosta, ya que en UWB se pueden realzar la transmisión de la señal en banda base, por lo que no es tan necesario que halla una etapa de corrimiento de la señal hacia altas frecuencias. Los esquemas de modulación como PPM, BPM, OOK, entre otras de banda base, son prácticamente realizable en sistemas de comunicación en UWB.

Existen diversas formas en que la señal transmitida es recibida, sin embargo, esta puede dividirse en dos grandes categorías, en receptores coherentes y no coherentes. Los receptores basados en la coherencia, necesitan de una gran cantidad de parámetros relacionados con la transmisión de los que destacan: modelos de canal, señal de sincronía y que deben ser considerados en el diseño de los receptores. Lo anterior repercute directamente en la cantidad de circuitos que se necesitan par a llevar a cabo la detección coherente. Por otra parte, están los receptores no coherentes, que relajan las especificaciones de diseño del receptor, ya que no necesitan de la información de canal ni de la señal de sincronía, sin embargo, estos tipos de receptores con susceptibles a canales altamente ruidosos ya que todo el tiempo están procesando la señal de entrada esto implica que algunas muestras sean ruido y otras símbolos.

Existe diversidad de formas de pulsos para utilizarlos en la transmisión, muchas de ellas son muy complejas para poder generarlas que aún no son de uso práctico. Sin embargo una de las formas de pulso que son relativamente fáciles de realizar son las

formas Gaussianas, la cual se presentan sus expresiones matemáticas y su espectro en frecuencia.

En general, el tomar en cuenta los conceptos básicos aplicables a sistemas en UWB, ha permitido el desarrollo del esquema de modulación y de los circuitos presentados.

Capítulo 3

En esta tesis es propuesto un esquema de modulación que permite la auto sincronización en el receptor a través de la señal transmitida. Para logra la auto sincronización, la señal transmitida debe cumplir con dos funciones: la primera es la de sincronización y la segunda es representar en forma de símbolo a los bits.

El esquema de modulación, permite realizar un sistema de recepción que comparte características de los receptores coherentes, por que existe un tiempo de integración de pulso que es característica de los receptores coherentes, sin embargo, no requiere información del canal, ni de una señal de sincronía para ser ajustado. Lo anterior define al receptor propuesto como receptor ligeramente coherente

El esquema de modulación así como los circuitos, pueden ser utilizados dentro de las dos grandes categorías de los sistemas en UWB. Es decir que pueden ser utilizados usando la técnica de radio impulsos o usando multi-bandas. En ambos casos, se tienen buenos resultados que son comparados con otros sistemas.

Una de las ventajas del diseño, esta en el proceso de correlación, el cual es realizado de manera digital, lo que permite que el uso de componentes analógicos sea menor. Esto implica el utilizar menor área como se muestra en el capitulo 4

El uso de transistores en el modulador y demodulador es menor en comparación con otras propuestas presentadas en la tesis. Por parte de transmisor, los circuitos no están

limitados a esta aplicación sino que también pueden ser adaptados fácilmente a otros esquemas de modulación, ya que no necesitan de un procesamiento extra para acoplarlos a otros sistemas como se demuestra en esta tesis.

Capítulo 4

Este capítulo este enfocado a la caracterización del los diseños propuestos así como usar los conceptos básicos planteados para darle interpretación a los resultados obtenidos. Los patrones geométricos de los circuitos son realizados usando la herramienta Mentor Graphic y la tecnología TSMC 0.18μm MMRF CMOS y una polarización de +/- 0.9v. Los patrones geométricos son presentados en la tesis, y a los cuales se realizaron simulaciones post patrones geométricos.

La similitud de los pulsos Gaussianos generados con respecto a la función Gaussiana ha sido de un 89% y 90% con anchos de 292 y 297 ps. negativo y positivo respectivamente. Se han realizado comparaciones con otras referencias que obtienen anchos de pulsos más angostos, sin embargo los generadores empleados utilizan mas transistores con respecto a la propuesta presentada.

La densidad espectral de potencia obtenida por el esquema de modulación empleando sólo radio impulsos, no cumple con la normas especificadas por la FCC, sin embargo, si se emplean técnicas de aleatoriedad, la forma de la densidad espectral obtenida, son satisfactorias según el reglamento establecido por la FCC.

Por otra parte si se utiliza la técnica de multi-bandas, la densidad espectral de potencia sin utilizar técnica de aleatoriedad, cumple con las especificaciones establecidas. En conclusión el esquema de modulación puede ser empleado como sistema de radio impulso o multi-bandas. Lo anterior de ventajas sobre otros esquemas de modulación que no pueden o no son fáciles para adaptarse a estos cambios sin que tengan que llevar a cabo la aleatoriedad de la señal transmitida.

Los diseños son probados bajo variaciones de procesos, voltaje y temperatura, usando los modelos de esquinas y Monte Carlo. La respuesta en general ha sido satisfactoria, los circuitos muestra robustez a dichas variaciones que el procesamiento de modulación y demodulación no se ven afectados.

Capítulo 5

La contribución principal de esta tesis es dividida en tres partes principales. La técnica de modulación, el circuito modulador y el demodulador.

El esquema de modulación propuesto es novedoso que compite con los esquemas de modulación propuestos en la literatura, como ha quedado demostrado en las comparaciones realizadas en el capítulo 4. El esquema permite desarrollar circuitos que modulan y demodulan muy simples y que son fácilmente integrables en la tecnología CMOS. Como todo sistema de comunicación las ventajas y desventajas pero en general se muestra un sistema con un alto potencial de aplicación según como ha quedado demostrado en el capitulo 4 en donde se ha caracterizado y comparado la propuesta.

La fabricación así como el acoplamiento a un el filtro pasa-banda y una antena son pasos para un trabajo futuro.

List of figures

List of tables

Abbreviations

C_{gd}	Gate to drain capacitance
C_{gs}	Gate to source capacitance
f_c	Centre frequency
f_H	Upper frequency
f_L	Lower frequency
g_{ds}	Drain to source conductance
gm	Transconductance small signal
I_{D1}, I_{D2}	Drain currents of transistor M1, M2…
V_{bias}	Bias voltage
V_{GS}	Gate to source voltage
V_T	Threshold voltage of a MOS transistor
γ	Ray decay factor
Γ	Cluster decay factor
λ	Ray arrival rate
Λ	Cluster arrival rate
Ω	Mean energy of the first path of the fist cluster
σ	Standard deviation
σ_1	Standard deviation for cluster lognormal fading
σ_2	Standard deviation for ray lognormal fading

σ_x	Standard deviation for lognormal shadowing
$\tau_{k,l}$	Delays for the *k*th multipath component
A-rake	All rake receiver
AWGN	Additive White Gaussian Noise
BER	Bit Error Rate
CDMA	Code Division Multiple Access
CFOS	Complex First Order Systems
DS	Direct Sequence
FCC	Federal Communication Commission
IR	Impulse radio
LNA	Low Noise Amplifier
LOS	Line of sight
MB	Multiband
OOK	On Off Keying
OFMD	Ortogal Frequency Modulation Division
PAM	Pulse Amplitude Modulation
PN	Pseudo Random Noise
PPM	Pulse Position Modulation
P-rake	Partial rake receiver
PSD	Power Spectral Density
PSM	Pulse Shape Modulation
PVT	Process, power supply Voltage, Temperature
RF	Radio Frequency
SS	Spread Spectrum
SV	Saleh-Valenzuela channel model
TD	Time Domain
TDMA	Time Domain Multiple Access
TH	Time Hopping
UWB	Ultra Wideband

References

[1] Gerald F. Ross, Transmission and Reception System for Generating and Receiving Base-band Duration Pulse Signals without Distortion for Short Base band Pulse Communication System, United States Patent, No. 3, pp. 728-632, april 1973. www.freepatentsonline.com

[2] Terence W. Barret, "History of Ultra Wideband (UWB) Radar & Communications: Pioneers and Innovators", Progress in Electromagnetic Symposium 2000, Cambridge, MA, july 2000. www.fcc.gov/oet/dockets /et98-155

[3] FCC, "Revision of Part 15 of the Commission's Rules Regarding Ultra-Wideband Transmission Systems," First Report and Order, ET Docket 98-153, february 2002. www.fcc.gov/Document_inaxes/Engineering_Technology/2002_index_OET_order.html.

[4] Ian Oppermann, Matti Hämäläinen and Jari Linatti, "UWB Theory and Applications", John Wiley & Sons, Ltd, 2005.

[5] Matti Hämäläinen, Jari Linatti, V. Hovinen and M. Latva-aho, "In band interference of three Kind of UWB signal in GPS LI band and GSM9000 oulink band

personal", 12 th IEEE Int. Symposium on Indoor and Mobile Radio Comm., vol. 1, pp 78-80, september 2001.

[6] M. L. Welborn, "System considerations for ultra-wide bandwidth signals in dense multipath environments", IEEE Communications Letter, vol 2. pp. 245-247, september 1998.

[7] J. Williams, " The IEEE 802.11b security problem, Part 1", IT Professional, IEEE computer society, vol. 3 no. 6 pp. 91–96, november 2001.

[8] Richard Yao, Grace Gao, Zhengqi Chen, Wenwu Zhu, "UWB Multipath Channel Model Based on Time Domain UTD Technique", IEEE Global Telecommunications Conference, Globecom 03, vol. 3 pp.1205-1210, december 2003.

[9] New ultra-wideband technology, white paper, prepared by Discrete Time Communications, pp. 1–8, 2002. info@discretetime.com

[10] H. Kikuchi, "UWB arrives in Japan. Nikkei Electronics", pages 95–122, february 2003. www.internetnews.com/wireless/articule.php/1370251

[11] R. Mark, "Xtreme Spectrum rolls out first UWB chipset", Internet News Website, june 2002.

[12] X. Gao, R. Yao, and Z. Feng, "Multi-band UWB System with Hadamard Coding," IEEE Conference on Vehicular Technology, Orlando, FL, vol. 2, pp. 1288–1292, october. 2003.

[13] Burlacu Mihai, "Ultra wideband Technologies", Helsinki University of technology, Telecommunications software and multimedia laboratory, 2003. www.tml.tkk.fi/studies/t-110.557/2002/papers/burlacu_mihai.pdf

[14] M. Ghavami, L. B. Mivhael, and R. Kohno, “Ultra Wideband signals and systems in communication engineering”, second edition, John Wiley & Sons, Ltd, 2007.

[15] Ryuji Kohno, “CRL-UWB Consortium’s soft-spectrum adaptation (SSA) UWB PHY proposal for IEEE 802.15.3a”, Yokohama University, july 2003. http://mentor.ieee.org/802.15/dcn/03

[16] Honggang Zhang, Kamya Y. Yazdandoost, Karen Li, Ryuji Kohno,“SSA-UWB and cognitive radio a suggestion for global harmonization and compromise in IEEE 802.15.3a”, National institute of information and communications, february 2004.

[17] 14. FCC regulations, 47CFR Section 15.5 (d). http://ftp.fcc.gov, 1998.

[18] R. A. Scholtz, “Multiple Access whit time hopping impulse modulation”, IEEE MILCOM93, vol. 2, pp447-450, october 1993.

[19] J. T. Conroy, J. L. LoCicero, and D. R. Ucci, “Communication techniques using monopulse waveform”, IEEE MILCOM99, vol. 2, november 1999.

[20] M. Ghavemi, L. B. Michael, S. Haruyama, and R. Kohmo, “A novel UWB pulse shape modulation system”, Kluwer Wireless Personal Communications Journal, 23, pp 105-120, 2002.

[21] J. McCorkle, “Why such uproar over ultrawideband? Communication Systems”, Design Website, March 2002. http://www.commsdesign.com/csdmag /sections/feature_article/OEG20020301S0021.

[22] S. Kolenchery, J. Keith Townsend, and A. Freebersyser, “A novel impulse radio networks tactical military wireless communications”, IEEE MILCOM, vol.1, pp. 59-65, 1998.

[23] M. Iacobucci and M: G. Benedetto, “Multiple access design for impulse radio communication systems”, in Proc. IEEE int. conf. communications, vol. 2, pp. 817-820, april 2000.

[24] M. Z. Win, “A unified spectral analysis of generalized time hopping spread-spectrum signals in presence of timing jitter”, IEEE J. selec. areas commun. Vol. 20 no. 9 pp. 36-38, 1998.

[25] Guvenc, I., Arslan, H. and Gezici, S., “Adaptation of multiple access parameters in time hopping UWB cluster based wireless sensor networks”, In: Proceedings of the IEEE Mobile and Ad hoc Sensor Systems (MASS), Fort Lauderdale, FL, pp. 235-244, 2004.

[26] Guvenc, I. and Arslan, H., TH sequence construction for centralized UWB-IR systems in dispersive channels. IEEE Electron. Lett., vol. 40 pp. 491-492, 2004.

[27] J. R. Foerster, "The performance of a direct-sequence spread ultrawideband system in the presence of multipath, narrowband interference, and multiuser interference," in Proc. IEEE Conference on Ultra Wideband Systems and Technologies (UWBST'02), pp. 87-91, Baltimore, Md, USA, may 2002.

[28] V. S. Somayazulu, "Multiple access performance in UWB systems using time hopping vs. direct sequence spreading," in Proc. IEEE Wireless Communications and Networking Conference (WCNC'02), vol. 2, pp. 522-525, Orlando, Fla, USA, march 2002.

[29] **J.** Foerster, "Ultra-wideband technology enables low-power, high-rate connectivity." in Proc. IEEE Workshop Wireless Commun. Network, september 2002. http://swarm.caltech.edu/cas/full/foerester.pdf

[30] Withington, R. Reinhardt, and R. Stanley, "Preliminary results from ultra wideband scanning receivers", Proceedings of the IEEE Military Communication Conference, pp 1186-1190, 1999.

[31] Iyappan Ramachandran, Sumit Roy, "Acquisition of Direct Sequence Ultra-Wideband Signals", Department of Electrical Engineering University of Washington Seattle, 2005. www.ee.washintong.edu/research/funlab/publications/2005/dsuwb_ acq.pdf

[32] Fred S. Lee, Anathaun P. Chandrakasan, "A 2.5 nJ/b 3 to 5 GHz Sub banded UWB Receiver in 90nm CMOS". IEEE Solid State Circuits Conference, pp 116-117, 2007.

[33] J. Ryckaert, M. Badaroglu, V. De Heyn, "A 16 mA UWB 3 to 5 GHz 20Mpulses/s Quadrature Analog correlation Receiver in 0.18μm CMOS", International Solid State Circuits Conference, pp. 114-115, 2006.

[34] Sthephane Ciolio, Mohammad Ghavami, Hamid Aghvami, "On the Use of Wavelet Packets in Ultra Wideband Pulse Shape Modulation Systems", IEICE Trans. Fundamentals, vol. E88-A, No 9, 2005.

[35] Chia-Hsiang Yang, Yu-Hsuan Lin, Shih-Chun Lin, Tzi-Dar Chiuch, "Design of Low-Complexity for Impulse-Radio Ultra-Wideband Communicatios Systems", ISCAS, pp.IV-125-IV-127, 2004.

[36] Chaiyaporn Khemapatapan, Watit Nenjapolakul and Kiyomichi Araki, “QPSK Impulse Signal Transmission for Ultra Wide Band Communication Systems in Multipath channel Environments”, IEICE Trans. Fundamentals, vol. E88-A, No. 11, november . 2005.

[37] J. D. Choi and W. E. Stark, “Performance of ultra wideband communications with sub optimal receivers in multipath channel”, IEEE Journal of selected Areas in Communications, vol.20, no. 9, pp 1754-1766, 2002.

[38] S. Franz and U. Mitra, “Integration interval optimization and performance and analysis for UWB transmitted reference systems”, Procc. IEEE Ultra Wideband System Technology, pp 26-30, 2004.

[39] M. H. Chung and R. A. Scholtz, “Comparison of transmitted and store reference systems for ultra wideband communications”, Procc. IEEE Military Communication Conf, vol. 1, pp.521-527, 2004.

[40] Thomas Zasowski, Frank Althaus, and Armin Wittneben “An Energy Efficient Transmitted-Reference Scheme for Ultra Wideband Communications”, in proc. Of 2004 UWBST, Kyoto, Japan , may 2004.

[41] Liuqing Yang, Georgios B. Giannakis, “Optimal Pilot Waveform Assisted Modulation for Ultra-Wideband Communications”, IEEE Transactions On Wireless Communications, vol. 3no. 4, pp. 1236-1249, 2003.

[42] Franz, S. Mitra, U., “On optimal data detection for UWB transmitted reference systems”, in GLOCOM, vol. 2 pp. 744-748, december 2003.

[43] M. Pausini and G. Janssen, “Analysis and comparison of autocorrelation receivers for IR UWB signals based on differential detection”, Procc. IEEE Int. Conf. on Acoustic, Speech, and Signal Processing, pp. 1520-, 2004.

[44] Y. L. Chao and R. A. Scholtz, “Optimal and suboptimal receivers for ultra wideband transmitted reference systems”, Procc. IEEE Global Telecomunications Conf., pp. 759-763, 2003.

[45] M. Ho, V. S. Somayazulu, J. R. Foerster, and S.Roy, “ A differential detector for an Ultra Wideband communications systems”, Procc. IEEE Vehicular Technology Conf. vol.4, pp. 1896-1900, 2002.

[46] S. Paquelet, L. M. Aubert, and B. Uguen, “ An impulse radio asynchronous transceiver for high data rates”, Procc. IEEE Ultra wideband Systems Technology, pp. 1-5, 2004.

[47] A. Rabbachin and I. Oppermann, “Synchronization analysis for UWB systems whit a low complexity energy collection receiver”, Procc. IEEE Ultra wideband Systems Technology, pp. 288-292, 2004.

[48] Ian Oppermann, Matti Hämäläinen and Jari Linatti, “UWB Theory and Applications”, John Wiley & Son, Ltd. pp. 40-47.

[49] H. Kanada, N. Aoshima, “Analog Gabor Transform Filter with Complex First Order System”, In proc. SICE, pp. 995-930, 1997.

[50] Xiaomin Chen, Sayfe Kiaei, “Monocycle Shapes for Ultra Wideband systems”, IEEE International Sysmposium on Circuits and Systems, vol. 1 pp. 26 29, 2002.

[51] Matti Hämäläinen, V. Hovinen , Jari Linatti, and M. Latva-aho, “In band interference Power Caused by different kinds of UWB signal at UMTS/WCDMA frequency bands”, IEEE conf. on Radio and Wireless, RAW CON, pp 97-100, 2001.

[52] Stephane Ciolino, Mohammad Ghavami, and Hamid Aghvam, “On the use of wavelate Packets in Ultra Wideband Pulse Shape Modulations Systems”, IEICE trans. Fundamentals, vol E88-A No. 9, pp. 2310-2316, 2005.

[53] Bernd-Peter Paris, .Gaussian Pulses,. mar. 3, 1998, http://thalia.spec.gmu.edu/~pparis/classes/coll_460_4/node4.html.

[54] L. W. Fullerton, .Reopening the Electromagnetic Spectrum with Ultra-wideband Radio for Aerospace,. IEEE Aerospace conference, Vol. 1, pp. 201-201, march 2000.

[55] M. Z. Win and R. A. Scholtz, “Ultra wide bandwidth time hopping spread spectrum impulse radio for wireless multiple access communication”, IEEE Transaction on Communications, pp. 679-691, 2000.

[56] Parkay P.,”Ultra wideband data transmission systems and method”, Word Intellectual Property Organization WO01/39451 A1., 2001 www.freepatentsonline.com/6690741.pdf

[57] McCorcle J. W., “Ultra wideband communication system, method, and device whit low noise pulse formation”, Word Intellectual Property Organization WO 01/93520 A2, 2001. www.freepatentsonline.com/6735238.pdf

[58] Morgan M., “Ultra wideband scattering measurement”, IEEE Transaction on Antennas and Propagation, vol. 42 pp. 840-846, 1994.

[59] Jeong Soo Lee, Cam Nguyen, and Tom Scullion, .New Uniplanar Sub nanosecond Monocycle Pulse Generator and Transformer for Time-Domain

Microwave Applications,. IEEE Transactions on Microwave Theory and Techniques, vol. 49, No. 6, pp. 1126-1129, june 2001.

[60] J. S. Lee and C. Nguyen, “Novel Low-Cost Ultra-Wideband, Ultra-Short-Pulse Transmitter with MESFET Impulse-Shaping Circuitry for Reduced Distortion and Improved Pulse Repetition Rate”,. IEEE Microwave and Wireless Components Letters., vol. 11, no. 5, pp. 208-210, may 2001.

[61] Tiuraniemi S., “Method and arrangement for generating cyclic pulses”, United Sates patent Aplications, 10/304915, 2002. www.freepatentsonline.com/6693470.pdf

[62] Daniels J. D., “digital design from zero to one”, John Wiley & Sons, Inc. 1996.

[63] Sumit Bagga, Giuseppe de Vita, Sandro Haddad, Wouter Serdijn and R. Long, “A PPM Gaussian pulse generator for ultra wideband communications”, IEEE , pp. 109-112, ISCAS 2004.

[64] Youngkyun Jenong, Sungyong Jung and Jin Liu, “A CMOS impulse generator for UWB wireless communication systems”, IEEE ISCAS, pp 129-132, 2004.

[65] Razavi, Behzad, “Design of Analog CMOS Integrated Circuits”, New York, NY, McGraw-Hill, pp. 47-58, 2001.

[66] Kevin Mariden., “A Study of a Versatile Low-Power CMOS Pulse Generator for Ultra Wideband Systems”. Thesis submitted to the faculty of the Virginia Polytechnic Institute and State University, december 2003.

[67] A. Batra, “Multiband OFMD physical layer proposal IEEE 802.15 Task Group 3a”, IEEE P802.15 Working group for wireless Personal Area Network (WPANs) publications document: IEEE P802.15-03/268r3, march 2004.

[68] Hüseyin Arslan, Zhi Ning Chen and Maria-Gabriella Di Benedetto, "Ultra Wideband Wireless Communications", John Wiley & Sons, Inc., Publications, 2006.

[69] Tevfiv, Yüucek, "Self-interference Handling in OFDM Based Wireless Communication Systems", Thesis submitted in partial fulfilment of the requirements for the degree of Master of Science in Electrical Engineering, Department of Electrical Engineering College of Engineering University of South Florida, november 2003

[70] L. Yang, Z. Tian, and G. Giannakis, "Non-data aided timing acquisition of ultra wideband transmission using cycle stationary", in Proc. ICASSP, pp. 121-124, april 2003.

[71] M. Z. Win and R. A. Scholtz, "Characterization of ultra wide bandwidth wireless indoor communication channel: a communication theoretic view", IEEE J. Selected Areas in Communications, volt. 20, pp. 1613-1627, december 2002.

[72] S. E. Bensley and B. Aazheng, "Subspace-base channel estimation for code division multiple access communication systems", IEEE Transaction on Communications, vol. 44, no. 8, pp. 1009-1020, august 1996.

[73] R. J. Cramer, R. A. Scholtz and M. Z. Win, "Evaluation of an ultra wideband propagation channel", IEEE transaction on Antennas and Propagation, vol. 50, no. 5, pp. 561-570, may 2002.

[74] Z. Tian and G. Giannakis, "Data aide ML timing acquisition in ultra wideband radios", in Proc. Conf. on Ultra Wideband Systems and Technologies, pp. 142-146, Reston VA, 2003.

[75] L. Yang and G. Giannakis, “Blind UWB timing with a dirty template”, Proceedings of GLOBECOM conference, pp 769-773, december 2003.

[76] A. Saleh and R. A. Valenzuela, “A statistical model for indoor multipath propagation”, IEEE Journal of Selected Areas in Communications, pp. 128–137, 1987.

[77] J.R. Foerster, M. Pendergrass and A.F. Molisch, "A Channel Model for Ultra wideband Indoor Communications", November 2003. http://www.mathworks.com/matlabcentral/fileexchange/6697

[78] K. Pahlavan and A. Levesque. Wireless Information Networks. John Wiley & Sons, Inc., 1995.

[79] H. Hashemi. “Impulse response modeling of indoor radio propagation channels”, IEEE Journal on Selected Areas in Communications, pp. 967–978, 1993.

[80] J. Proakis, Digital Communications, 4th edition, McGraw-Hill, 2000.

[81] R. C. Qiu and C. Zhou, “Physics-Based Pulse Distortion for Ultra-Wideband signals,” IEEE Trans. Veh.Technol., vol. 54, No. 5, invited paper, september. 2005.

[82] M. B. Pursley, Introduction to Digital Communications, Prentice-Hall, 2004.

[83] D. Cassioli, M. Z. Win, F. Vatalaro, and A. F. Molisch, “ Performance of low complexity rake reception in a realistic UWB channel”, in Proc. IEEE Int. Conf. Commun. (ICC), vol. 2, New York, pp. 321-234, april 2002.

[84] Emeric Guéguen, Nadia Madacui, and Jean-Francois herald, “Combination of OFMD and CDMA for high data rate UWB”, Comptes Rendus-Physique, vol. 7, pp.774-784, 2006.

[85] Chris Snow, Lute Lampe, Robert Schober, “Error rate analysis for code multicarrier systems over Quasi statics fading Channels”, IEEE Globeccom, vol. 5 pp. 1736-1740, september 2007.

[86] I. S. Raad, X. Huang, D. Lowe, “Higher order rotation spreading matrix for block spread OFMD”, in Proceedings of the 2007 IEEE conference on telecommunications, may 2007.

[87] G. S. Biradar, S. N. Merchant, U. B. Desai, “Frequency and time hopping PPM UWB multiple access communications scheme”, in Journal of communication, vol. 4, no. 1 february. 2009.